ABSORPTION SPECTROSCOPY OF FLAMES

A thesis submitted for the Degree of
Doctor of Philosophy in the faculty
of Science, University of London

by

PETER FRIEDRICH JESSEN, B.Sc., A.R.C.S.

Department of Chemical Engineering
& Chemical Technology,
Imperial College of Science & Technology,
London, S.W.7.

August 1968

TO LEE

ABSTRACT.

Absorption spectra of the radicals C_2, C_3 and CH have been studied quantitatively in acetylene-oxygen flames burning at atmospheric pressure. The effective light path through the flame was increased by using a new design of multiple reflection system. This focuses the light into the flame, gives better spatial resolution and is less affected by schlieren-type deflections of the light beam than in the normal parallel-beam system.

There is little evidence for thermal disequilibrium in the luminous mantle of fuel-rich flames. Concentrations of C_2 and C_3, about 2×10^{14} and 1×10^{15} molecules cm^{-3}, are consistent with values calculated for equilibrium with solid carbon, but the concentrations of C_2 and CH are much higher in the reaction zone. Measurements of C_2 rotational and vibrational temperature support a chemiluminescent mechanism of formation.

It is concluded that C_3 is formed from evaporation of incipient carbon particles but the possibility of C_2 radicals being important in the formation of carbon 'nuclei' cannot be ruled out.

ACKNOWLEDGEMENTS.

The author wishes to thank Professor A.R.Ubbelohde, F.R.S., Head of the Department of Chemical Engineering, for the use of departmental facilities.

He would particularly like to thank Professor A.G.Gaydon, F.R.S., under whose supervision this work was carried out. Professor Gaydon has made many helpful suggestions and his unfailing encouragement is acknowledged with gratitude.

The co-operation of Mr.L.Moulder, the departmental photographer, and Mr.G.Barrett of the student workshop was gratefully appreciated. Miss Lee Spencer ably assisted in the preparation of the manuscript and Mr.L.Cripps was responsible for the expert typing of this thesis.

The author is indebted to the Gas Council, without whose financial support this project could not have been undertaken.

I N D E X.

		Page
	Abstract.	3
	Acknowledgements.	4
	Index.	5
	CHAPTER ONE. Introduction.	
1.1.	Spectroscopic approach to combustion research.	8
1.2.	Limitations of emission spectroscopy and advantages of absorption spectroscopy.	10
1.3.	Difficulties in detecting absorption spectra of flames.	12
1.4.	Summary of experimental techniques.	14
1.5.	Nature of the investigation; detection of carbon radicals in fuel-rich flames.	18
1.6.	Carbon formation in premixed flames.	22
1.7.	Role of C_1, C_2 and C_3 in carbon formation.	29
	CHAPTER TWO. Theoretical considerations.	
2.1.	Absorption coefficient k_ν, peak absorption k_o, and spectral line-width $\Delta\nu$.	32
2.2.	Integrated absorption; absorption-concentration relationship.	35
2.3.	Measurement of integrated absorption; effect of spectral slit-width.	38
2.4.	Relationship between integrated absorption and measured peak absorption.	39
2.5.	Limits of detection in theory and practice.	41

Page

CHAPTER THREE. Qualitative absorption measurements using flashtube and photographic detection.

3.1. Introduction. 46

3.2. Experimental. 47

3.3. Results. 58

3.4. Discussion. 67

CHAPTER FOUR. Quantitative absorption measurements using photo-electric detection.

4.1. Introduction. 69

4.2. Apparatus. 70

4.3. Linearity of response. 88

4.4. Absorption spectra. 89

4.5. General observations on the luminous mantle. 95

CHAPTER FIVE. Determination of effective temperatures and concentrations from C_2, C_3 and CH spectral data.

5.1. C_2 temperature measurements. 102

5.2. Concentration measurements. 121

CHAPTER SIX. Equilibrium calculations of carbon radicals and discussion of carbon formation in oxy-acetylene flames.

6.1. Equilibrium calculations. 132

6.2. Comparison with actual carbon radical concentrations. 136

6.3. Discussion. 137

Page

6.4. Equilibrium in the reaction zone and luminous mantle. 139

6.5. Connection between C_2, C_3 and carbon formation. 142

6.6. Conclusions. 148

6.7. Suggestions for future work. 149

REFERENCES. 152

APPENDIX ONE. Rotational line strengths of C_2 Swan bands. 156

APPENDIX TWO. Data for determination of rotational and vibrational temperatures of C_2. 161

CHAPTER ONE. INTRODUCTION.

1.1. Spectroscopic approach to combustion research.

Spectroscopy is an obvious and powerful tool for studying the physical and chemical processes involved in combustion because the emission of radiation is a property common to all combustion systems.

Most of the radiation is emitted in the infra-red spectral region and is due to vibrational and rotational transitions in the molecules H_2O and CO_2 which generally make up the bulk of the burnt gas. Being stable equilibrium products, they can be studied relatively easily by conventional sampling techniques.

The remainder occurs in the visible and u.v. region and is emitted most strongly in the reaction zone where the main combustion reactions are taking place. A great number of intermediate oxidation products are formed in this zone which, with the exception of the hydroxyl radical, do not generally survive in the burnt gas. Having a relatively short chemical lifetime, they cannot be studied by ordinary chemical sampling. The insertion of probes is hindered by the high temperatures encountered and may cause local disturbances so the spectroscopic approach is particularly valuable. One of the main achievements has been to identify intermediate transient species whose

presence in combustion processes had been hitherto unsuspected, and it has had a great influence on the development of chain reaction mechanisms and chemical kinetics in general.

The study of flame spectra can not only be used to identify some of the intermediate species present in combustion, but may also give information about the methods by which they are formed, removed, and give up their energy. There is very often insufficient time for the heat released in the reaction zone to be equipartitioned among the various internal energy modes of a molecule, and marked departures from thermal equilibrium can thus occur. The population among the rotational, vibrational and electronic energy levels can be determined from measurements on the band spectra and are usually expressed as effective temperatures. If the spectroscopic transition probabilities of the molecule are known, the absolute concentrations in the ground and excited states may be determined from absorption and emission measurements, respectively.

Gaydon (1957) has given an extensive account of emission spectra of flames. It is only in the last ten years that notable progress has been made in the detection of absorption spectra, the reason being that more elaborate experimental techniques are required than for emission spectroscopy.

1.2. Limitations of emission spectroscopy and advantages of absorption spectroscopy.

A study of flames by emission spectroscopy will tend to throw undue emphasis on a small number of electronically excited molecules and some important species may not be detected because they do not possess suitable emission spectra. There may be insufficient energy available to excite these species because their resonance transitions lie in the vacuum u.v., or their concentrations may be so low that their spectra are too weak to be observed.

The light emission accompanying the high temperature combustion of hydrocarbons consists mainly of the characteristic band spectra of the diatomic radicals OH, CH and C_2 but only OH is brought into the ordinary combustion equations.

Spectroscopy has so far given only limited information about the chemical kinetics of combustion. There is, in general, a lack of knowledge of the concentrations and reactions of the free radicals observed spectroscopically, the reason being that the spectra are observed almost exclusively in emission. In such cases, the intensity of a band system is determined by the temperature and conditions of chemiluminescent excitation as much as by the concentration of the radical itself. It

is, moreover, a summation over different stages of the reaction, because, owing to the narrowness of the reaction zone, it is virtually impossible to differentiate between spectra at the beginning and end of a reaction. The development of low pressure burners has enabled the reaction zone to be studied with much better spatial resolution, but the need for absolute concentration profiles is still as great as ever.

If complete thermodynamic equilibrium existed, there would be no particular advantage in measuring band intensities in absorption unless the temperature was so low as to make the emission intensity too weak to be readily detected. Molecules which do not radiate appreciably may be detected by their absorption spectra if a bright background source is employed. Methyl and ethyl radicals are examples of species which were detected in flames for the first time by this method (Gaydon et al., 1960).

The main advantage of absorption spectroscopy lies in the ease (in theory at least) with which concentration measurements can be made. It is inherently more suitable than emission spectroscopy for determining concentrations, because it concerns ground-state molecules, whose number exceeds those in all excited electronic states by several orders of magnitude at temperatures below 5000°K. The

ground-state population is insensitive to small temperature variations, whereas the emission intensity has an exponential temperature dependence and is strongly influenced by disequilibrium processes.

1.3. Difficulties in detecting absorption spectra of flames.

The only species to have been extensively studied by absorption spectroscopy is the hydroxyl radical, which has a relatively high equilibrium concentration and is found in both the inner and outer cones of premixed flames. Generally the radicals of most interest have low concentrations and are confined to the reaction zone. This is normally very thin and often curved. Even when a flat flame is used, it is difficult to obtain an appreciable pathlength through the zone, because the usable solid angle is very small and the light beam tends to be deflected out of the region by refractive index gradients.

Some radicals have abnormally high excitation temperatures as a result of their formation by chemiluminescent reactions. In order to detect their absorption spectra by photographic methods, it is necessary to use a background source having a brightness temperature higher than the excitation temperature in the flame. Bleekrode (1966) has reported electronic temperatures of CH in low-pressure oxy-acetylene flames in excess of 5000°K.

Of all the light sources commonly employed, only high-pressure xenon and mercury arc lamps have brightness temperatures of this order.

An added difficulty is that it is necessary to use a spectrograph of high resolving power in order to detect individual rotational lines in absorption. Such instruments tend to be expensive and bulky. The situation is quite different for emission lines, where opening the slit of the spectrograph, or using a low-resolution instrument, can improve the chances of observation of a weak line. However, in detecting a line in absorption, one is observing the continuum radiation from the background source, less the energy absorbed by the line. A line in the rotational fine structure of a band spectrum has a natural width of the order of 0.1 cm^{-1}, whereas the spectral slit width of an instrument is commonly an order of magnitude higher than this.

The immediate practical effect of looking at the line with a spectrograph of modest resolving power is a reduction in the peak absorption (see fig.2) because light of slightly longer and shorter wavelengths present in the background source will spread across the absorption line and render its observation more difficult. The implications regarding the quantitative interpretation of the measured absorption are discussed in section 2.3.

1.4. Summary of experimental techniques.

In this section, we give a brief review of experimental methods that have been employed to overcome some of the difficulties discussed above. The methods are conveniently divided into (a) photographic techniques, and (b) photoelectric techniques; both can be used in conjunction with (c) multiple reflection mirror systems.

(a) Photographic detection.

In its basic form it is essentially the well-known line-reversal method of temperature measurement (Gaydon and Wolfhard, 1960). The main advantages of photographic detection are that the whole absorption spectrum may be recorded simultaneously, and the background source does not have to be particularly stable. Its disadvantages are the need for using a large dispersion instrument and a very bright background source.

(b) Photoelectric detection.

A photomultiplier has a linear response and is much more sensitive to small changes in light intensity than a photographic emulsion. It may therefore be expected to be more suitable for quantitative absorption measurements. The main disadvantages are that the spectrum has to be scanned relatively slowly, and a very steady background source is required because fluctuations in light intensity are not

integrated as is the case with a photographic plate. However, it is not necessary to use a source with a higher brightness temperature than the excitation temperature of the absorbing species in the flame, because it is possible to discriminate between light from the background source and the flame. A light chopper is placed between the source and flame, which chops the source beam at a fixed frequency. The modulated light is received by the photomultiplier, together with the d.c. flame emission, but only the a.c. component of the output signal is amplified and recorded. If the flame emission is required, the light chopper is positioned immediately in front of the spectrometer slit and the background source is switched off. The technique was first employed by Silverman (1949) to study absorption spectra of carbon dioxide bands in the infrared region.

The problem of inadequate spectral resolution can be conveniently overcome by the use of a background source emitting the same lines as are absorbed by the flame. In this case, a spectrometer of lower resolution is adequate, because it is necessary only to separate neighbouring lines, without resolving the true line profiles. Kaskan (1958) was able in this way to study the decay of OH radicals in flat oxy-hydrogen flames by absorption spectroscopy, using a low pressure discharge of water vapour as a background source. The OH lines emitted by the discharge correspond to an

effective rotational temperature of about 300°K, and, therefore, are much narrower than those emitted by the hot flame. The fractional loss of intensity of the background light after passing through the flame is proportional to the peak absorption coefficient and gives a measure of the concentration of absorbing molecules.

So far, the discrete line source method has been restricted to the OH spectrum, but the principle is commonly employed by workers in the field of atomic absorption spectroscopy (Walsh, 1955).

(c) Multiple reflection systems.

Because the concentrations of transient species in the flame are always relatively low, their absorption spectra are subsequently very weak and difficult to detect. It is difficult to measure absorption of under 1% with a photomultiplier unless the background source is unusually stable, and photographic detection is useful only for absorption greater than about 5%.

The absorption can be increased by designing a burner to give a long optical pathlength, but practical complications limit the size of the flame that can be conveniently burnt. A more rewarding approach is to increase the absorbing pathlength by passing the light beam through the flame several times before it enters the slit of

the spectrograph. This can be achieved with a system of mirrors which reflect the beam back and forth through the flame a set number of times. In this way it is possible to obtain, without difficulty, a ten-fold increase in absorption, and to render observable several species which cannot normally be detected with a single traversal of the beam through the flame.

Using a mirror system designed by White (1942), Spokes (1959) was able, for the first time, to detect weak absorption spectra of C_2 and CH radicals in the reaction zone of stationary flames. He recorded the spectra photographically, using a flash-tube as background source. The flashtube gives a continuous spectrum throughout the visible and ultraviolet regions corresponding to a brightness temperature of 20,000 - 30,000^{o}K. Owing to reflection losses at each mirror surface, the emergent light intensity after several traversals is much reduced and will be insufficient to reverse the spectral lines if conventional light sources are used.

Recently, Bleekrode and Nieuwpoort (1965) incorporated a White multiple reflection system with a photoelectric method of detection, to study C_2 and CH absorption in low-pressure oxy-acetylene flames. They were able to use a high-pressure mercury lamp (brightness

temperature 4,500 - 5,500°K) as background source, because the light was chopped and selectively amplified. The absorption was sufficiently strong after 20 to 30 passes through the reaction zone to enable them to make quantitative concentration measurements.

We have designed a new type of multiple-reflection system which has certain important advantages over the White system and is more suited for the work described in this thesis. A full description and comparison of the two systems is given in Chapter 3.

1.5. Nature of work undertaken: Detection of carbon radicals in fuel-rich flames.

The equilibrium concentrations of C_2 and CH are extremely low and in general, no emission from carbon-containing radicals is observed downstream of the reaction zone of near-stoichiometric hydrocarbon flames.

However, as the mixture strength is increased to a C:O atom ratio* of about unity or greater, there is insufficient oxygen available to oxidise all the intermediate hydrocarbon fragments formed in the reaction zone, and an appreciable fraction survives into the burnt gas. Under these conditions, the radical concentrations are much higher and small carbon particles are rapidly formed downstream of the oxidation zone.

* $\frac{\text{Number of carbon atoms in one fuel molecule}}{\text{Number of oxygen atoms in one oxygen molecule}} \times \text{Mole ratio } C_2H_2 : O_2$

F I G U R E 1.

Diagram of a fuel-rich acetylene-oxygen flame showing the luminous mantle above the inner cone.

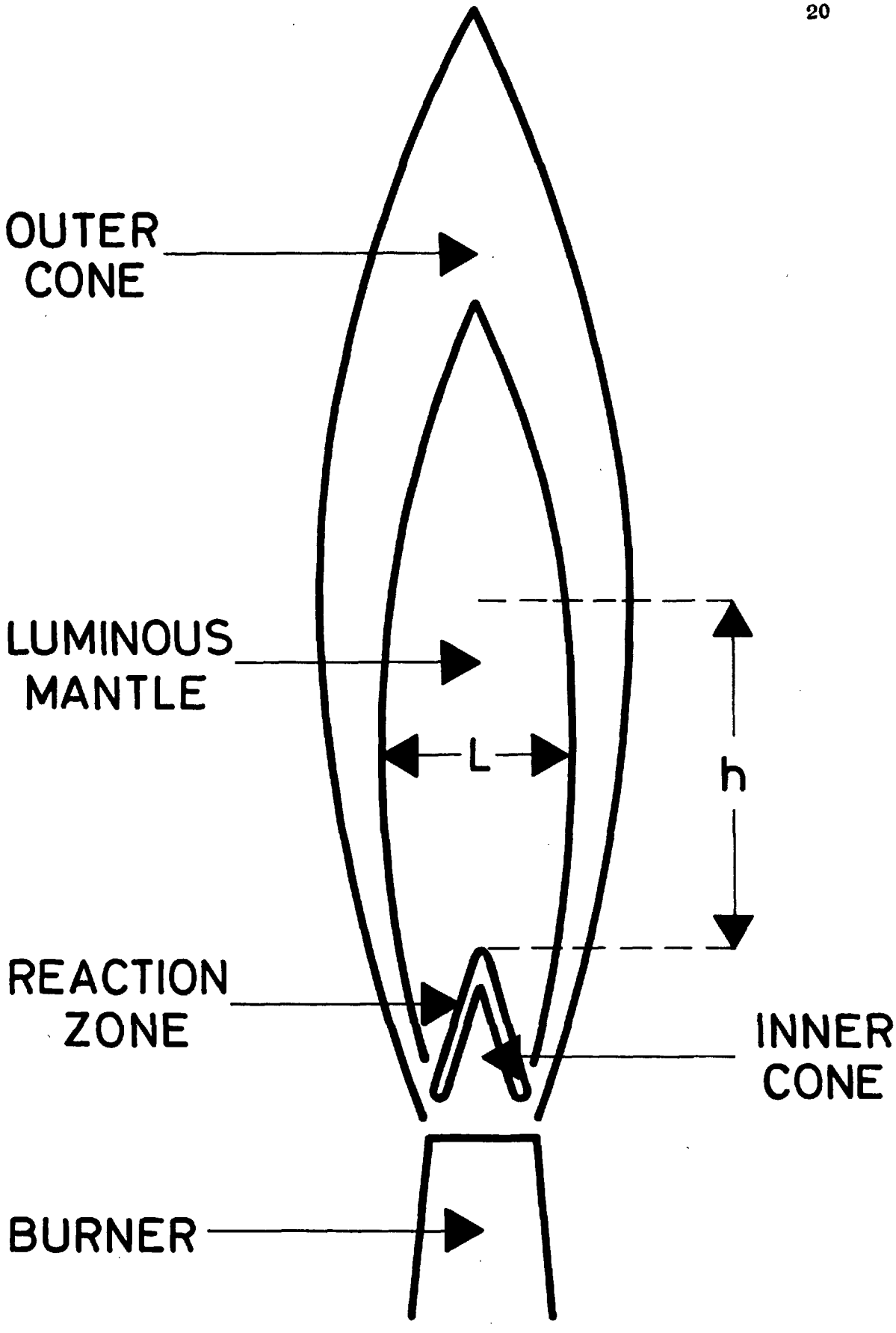
OUTER CONE
LUMINOUS MANTLE
L
h
REACTION ZONE
INNER CONE
BURNER

This process can be observed spectroscopically by studying the luminous extension around the inner cone of hot hydrocarbon-oxygen flames, which shows the band spectra of C_2 and CH, as well as the 4050 Å Comet-Head bands of C_3. Figure 1 shows the region of this mantle or 'feather', as it is sometimes known, in a fuel-rich oxy-acetylene flame. The mantle appears abruptly at a C:O ratio of about unity and extends further up the flame as the fuel content is increased. Correspondingly, the colour changes from a pale greyish-white to a more intense white and finally into the characteristic yellow luminosity indicative of a flame containing solid carbon. Emission studies (Marr,1957) have indicated that departures from thermal equilibrium may occur, although they are small compared to those occurring in the reaction zone.

The connection between the carbon radical concentrations and solid carbon is not clear. There is considerable interest in the mechanism of carbon formation in flames and the subject is discussed in sections 1.6 and 1.7.

Because of the extensive nature of the luminous mantle in oxy-acetylene flames, it is particularly suited for spectroscopic observations without recourse to the low ambient pressures required for detailed studies of the reaction zone. This thesis describes a versatile apparatus

to observe the absorption spectra of flames, and has been used to measure the concentrations of C_2, C_3, and CH radicals in the mantle of fuel-rich flames.

1.6. Carbon formation in premixed flames.

Besides being of obvious theoretical interest, the formation of carbon in flames is of great practical importance. Although a wealth of experimental data has been collected over many years, most of it is of a purely qualitative nature, with the result that the various theories that have been proposed are necessarily rather vague and lack detail. Good discussions are given by Street and Thomas (1955) and in Chapter 8 of the book by Gaydon and Wolfhard (1960). In the following section, are outlined some experimental results of previous workers which, in the author's view, are considered to be significant.

The nature of solid carbon particles formed from all hydrocarbon fuels is remarkably similar, no matter whether they are produced by pyrolysis, in diffusion flames, or in premixed flames. When examined by electron-microscopy, soot consists of a network of cross-linked chains of approximately spherical particles, each of the order of some hundred Angstrom units in diameter. Each particle contains about 10^5 to 10^6 carbon atoms and a surprisingly large number of bonded hydrogen atoms - up to 50% on an atomic basis. Thus,

it is not strictly correct to refer to soot as carbon, it is a hydrocarbon of sorts with an empirical formula usually ranging between C_2H and C_8H. The single particles are made up of a large number, about 10^3 to 10^4, of crystallites. X-ray measurements indicate that these crystallites consist of 5 to 20 sheets of carbon atoms, of the basic type existing in graphite, having a length and breadth of 20 to 30 Å. The larger planes are parallel to each other, but they are randomly stacked relative to one another and the interlayer spacing is about 3 to 5% larger than in pure graphite.

The fundamental problem is to explain how simple fuel molecules containing only a few carbon atoms are converted so rapidly into these huge aggregates. Dehydrogenation and polymerisation must obviously occur. Theories of carbon formation differ in the route and order in which these two processes take place.

The presence of oxygen in premixed flames is important not only in opposing the growth of incipient soot particles, but also in breaking up the original fuel molecules, and thereby aiding the formation of precursors to soot. Carbon would not be expected to be formed from mixtures in which there was more than sufficient oxygen to convert the carbon to carbon oxides, but, in practice, carbon formation is frequently observed with mixtures having a C:O ratio considerably less than one. Street and Thomas (1955)

determined critical C:O ratios at which many fuel-air mixtures would just form a luminous carbon zone in bunsen-type flames at atmospheric pressure. Their results showed a variation in these critical mixtures from C/O = 0.83 for acetylene to 0.45 for C_2 and C_4 paraffins.

While these results demonstrate the lack of equilibrium and show the influence of molecular structure of fuels on their tendency to form soot, they do not provide direct information on the chemical reactions involved because the original fuel molecules are generally decomposed in the reaction zone of the flame. It is the conditions pertaining in the oxidation zone and downstream of it that they are really relevant.

Considerable progress has been made over the past ten years in identifying hydrocarbon fragments in the oxidation zone and following their recombination further downstream. Isotopic tracer studies have shown that there must be an initial break-up of the C-C bonds in the fuel during its passage through the reaction zone. Ferguson's experiments (1957) with $H_3C-{}^{13}CH_2-CH_3$ explosion flames gave evidence that carbon was not formed directly by polymerisation of intact $^{13}C^{12}C$ molecules, but resulted in a random distribution of ^{13}C in the soot, corresponding to its concentration in the fuel. Furthermore, the radiating C_2

radicals in acetylene-oxygen flames (Ferguson, 1955), and in the pyrolysis of acetylene in shock waves (Fairbairn,1962), are not formed by stripping off hydrogen atoms from individual acetylene molecules.

More direct evidence was obtained by Homann and Wagner (1963, 1965). Using a mass spectrometer with a molecular-beam inlet system, they measured concentration profiles in various low-pressure flat flames. They observed the simultaneous formation of C_3 and C_4 unsaturated hydrocarbons at an early stage in the oxidation zone of flames with C_2 fuels. The concentration profiles in these stationary flames illustrate that the C-C bond breaking starts early in the oxidation zone before any carbon is formed.

It is now fairly well established that the mechanism of carbon formation in premixed flames involves a nucleation process, followed by a rapid growth and a slower aggregation of particles into larger units. Differences between nucleation and growth are evident in several experiments. Tesner (1959) stressed the difference in temperature required for growth of a carbon deposit and for nucleation of soot. The latter temperature is always substantially higher than the former. Gaydon and Fairbairn (1955) found that the after-glow of carbon monoxide in a

discharge tube contained C_2 and probably atomic carbon, and that this gas, when mixed with acetylene, was able to produce solid carbon deposits on the walls. They interpreted this in terms of C_2 playing a role in the nucleation of carbon in flames, and suggested that the reactions were

$$C_2 + C_2H_2 \longrightarrow C_4 + H_2$$

$$C_4 + C_2H_2 \longrightarrow C_6 + H_2 \text{ , etc.}$$

Although these reactions are energetically possible, there is as yet no direct proof that they do actually occur.

Evidence that poly-unsaturated hydrocarbon species are important was obtained by Bradley and Kistiakowsky (1961). Powerful arguments have been presented by Homann, Wagner, and co-workers (1965, 1967) to show that the species are polyacetylenic compounds. These workers have made an extensive study of carbon formation in low-pressure premixed flames and some of their more important results may be summarised as follows. In the reaction zone of stoichiometric and lean flames of the lower aliphatic hydrocarbons, a small amount of fuel loses hydrogen and forms unsaturated hydrocarbons having the same or a smaller number of carbon atoms. The concentrations of these intermediates rise steadily with increasing input of fuel. In addition, there appear hydrocarbons with a greater number of carbon atoms than the original fuel. At the end of the reaction

zone, where the oxygen concentration becomes immeasurably small, the dominant hydrocarbon species present are acetylene and polyacetylenes ($C_{2n}H_2$) up to $C_{12}H_2$. When carbon formation commences, concentrations of all acetylenic compounds decrease, and when carbon formation has virtually ceased, the concentrations level off. Close behind the oxidation zone, a large number of other hydrocarbons of molecular weight greater than 200 can be observed. Similar hydrocarbons can be evaporated from very 'young' soot particles sampled from the same region of the flame. These hydrocarbons which appear in the region of carbon nucleation are considered to be important intermediates or nuclei for carbon formation. They are thought to be formed by reactions between polyacetylenes and other radicals, such as C_2H, producing branched-chain radicals which can rapidly add further polyacetylene radicals and acetylene, without losing their radical character.

Place and Weinberg (1967) suggested that positive ions could act as nuclei for carbon formation. During the past few years, Weinberg and collaborators have studied the effects of electric fields on carbon formation in diffusion flames. They have been able to show that carbon particles become charged (mostly positive) very early in their life and as a result can be readily manipulated by applied electric fields. Weinberg pointed out that the effects observed in

the presence of deliberately applied fields may also be important in their absence. Owing to the different mobilities and rates of diffusion of positive ions and electrons, there is some charge separation in the flame and small electric fields are set up. Ion concentrations are abnormally high in the reaction zone of premixed hydrocarbon flames and a great variety of hydrocarbon positive ions have been detected with molecular weights up to a hundred.

Although it appears likely that positive ions can act as carbon nuclei in diffusion flames, where their residence time in the pyrolysis zone is relatively long, it if improbable that they form the predominant nuclei in premixed flames. Addition of an alkali metal, which easily forms ions in the flame, has no effect on the formation of carbon.

The account of carbon formation given by Homann and Wagner (1967) gives the best description of the processes occurring in premixed flames having temperatures in the range 1000 - 2000°K. However, there are many details still to be filled in before the theory can become even semi-quantitative.

At temperatures above 2,500°K, other reactions may become important and carbon formation could occur by different mechanisms e.g. those involving the carbon radicals, C_1, C_2 and C_3.

1.7. Role of C_1, C_2 and C_3 radicals in carbon formation.

It has been suggested that atomic carbon and the species C_2 and C_3 could be precursors to carbon formation in hot flames. The close association of C_2 production in premixed flames with solid carbon formation appears to be more than coincidental and a number of theories linking the two have been proposed. Smith (1940) observed that green premixed flames changed to yellow on increase either of mixture strength or pressure, and suggested that C_2 formed in the flame polymerises to solid carbon, the critical fuel-oxygen ratio marking the point at which the rate of association of C_2 molecules (responsible for the green emission) exceeded that of removal of oxidation.

Given a sufficiently large concentration and long lifetime, there is no doubt that C_2 molecules would condense to carbon. It is unlikely that either of these conditions holds in the majority of soot-forming flames, but the very hot region above the reaction zone of a fuel-rich oxy-acetylene flame may be suitable for such a mechanism to occur. The condensation of C_2 and free carbon atoms has been discussed by Gaydon and Wolfhard (1960). It is difficult to estimate quantitatively how much atomic carbon is present in flames; the 2478 Å carbon line is observed in the reaction zone of hot flames, but the resonance lines lie in the

vacuum u.v. and there are no accessible lines of low excitation energy which would be suitable for spectroscopic determination of concentration.

Cabannes (1956) suggested that carbon particles are formed by the sublimation of carbon vapour resulting from the decomposition of the fuel. He compared the soot-forming flame with the luminous flame of nickel carbonyl which has a similar appearance, and in which it is probable that nickel is liberated at a temperature below that of its triple point, so that the solid particles of nickel must be formed by direct passage from the gaseous to the solid phase. At temperatures above 2000°K, C_3 is the principal constituent of carbon vapour and it is observable spectroscopically in hot fuel-rich flames. The hypothesis receives support from the work of Gay, Agnew et al. (1961) who studied conditions for the formation of solid carbon in oxy-acetylene flames and calculated equilibrium compositions as a function of mixture strength when polyatomic carbon molecules were included in the flame products.

An alternative mechanism is that atomic carbon and C_2 could act as nuclei for carbon formation from acetylene and polyunsaturated hydrocarbons. This would require lower carbon radical concentrations than the direct condensation mechanism.

On the other hand, it may be that carbon radicals are products rather than precursors of carbon particles. Thus, the C_2 and C_3 radicals detected above the reaction zone of fuel-rich flames, may constitute a vapour of gaseous carbon which is in equilibrium with the hot soot particles.

Comparison of actual carbon radical concentrations with calculated equilirium values might enable some conclusions to be drawn regarding their role in the formation of solid carbon in very hot flames. This subject is discussed in Chapter 6 in the light of the absorption studies undertaken in this thesis.

CHAPTER TWO. THEORETICAL CONSIDERATIONS.

In this chapter, some theoretical relationships are introduced which are required in order to convert experimental absorption measurements into concentrations of the absorbing molecules. The ultimate accuracy and sensitivity of absorption measurements are discussed in terms of the relevant experimental and theoretical parameters.

2.1. Absorption coefficient k_ν, peak absorption k_0, and spectral line width $\Delta\nu$.

If a parallel beam of radiation of frequency ν and intensity $I_0(\nu)$ is passed through a uniform gas of thickness **L**, the transmitted intensity, $I(\nu)$, is given by

$$I(\nu) = I_0(\nu) \exp(-k_\nu L) \qquad (2.1)$$

where $k_\nu \geq 0$ is defined as the absorption coefficient of the gas, and is independent of I_0 and L.

The dependence of k_ν on ν, i.e. the absorption line shape, is determined by the nature of the transition involved and on the physical conditions such as temperature, pressure, and electric fields to which the gas molecules may be subjected.

A typical curve of k_ν versus ν is shown in fig.2a. The maximum value of the absorption coefficient is called the peak absorption, k_0, and corresponds to a frequency ν_0.

F I G U R E 2.

(a) Variation of absorption coefficient, $k(\nu)$, with frequency, ν, of a typical spectral line.

(b) Variation of peak fractional absorption $[(I_o-I)/I_o]_{peak}$, with spectral slit-width divided by true line width, $S/\Delta\nu_{true}$, of a spectral line showing 60% true absorption.

(c) Relative absorption intensity in a line for various values of $S/\Delta\nu_{true}$. The values of $S/\Delta\nu_{true}$ are marked near the minima.

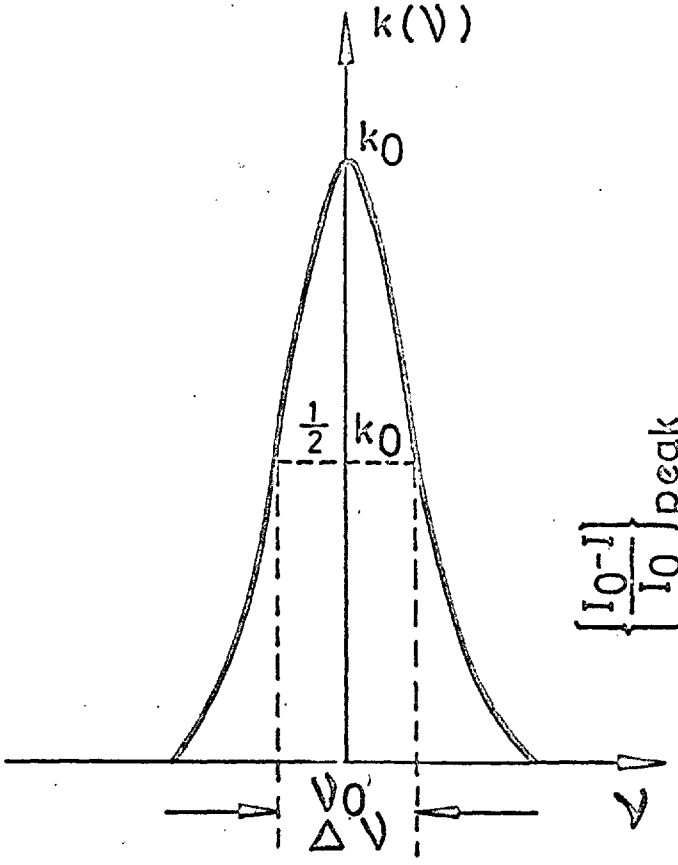
k(ν)
k0
½ k0
ν0
Δν
ν

(a)

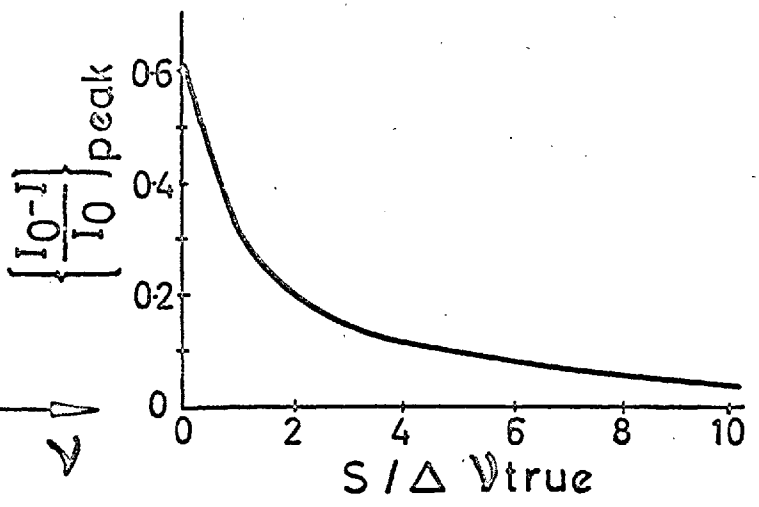
{(I0-I)/I0}peak
0·6
0·4
0·2
0
0
2
4
6
8
10
S / Δ νtrue

(b)

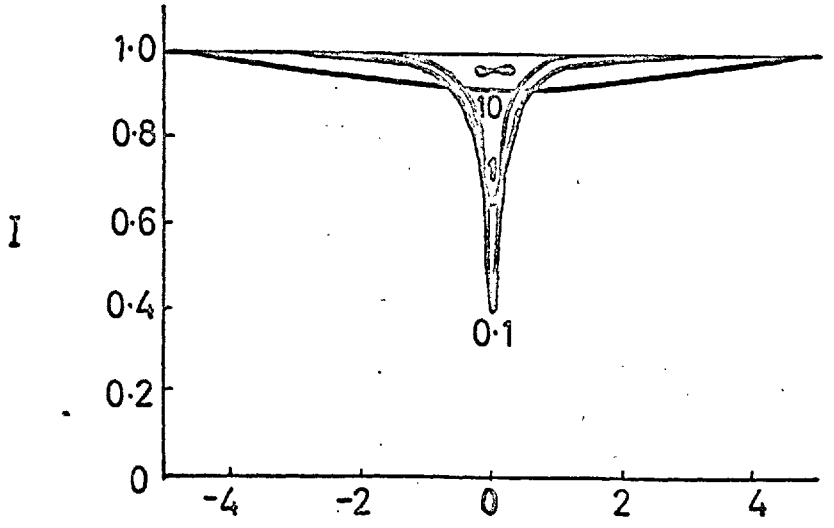
I
1·0
0·8
0·6
0·4
0·2
0
∞
10
3
1
0·1
-4
-2
0
2
4
ν-ν0
S

(c)

The distance between the two points on the curve where k has fallen to $\frac{1}{2}k_o$ is called the half-width of the absorption line, $\Delta\nu$, and is analogous to the width of the line in emission at one half its peak intensity.

2.2. Absorption-Concentration relationship.

Although it is possible to calculate exactly the shape and width of a spectral line if only one broadening parameter is effective (Penner, 1959), these expressions are of only limited use in actual combustion systems because, in general, both Doppler and Lorentz broadening are important, and the relative magnitude of each must be determined experimentally.

However, a relationship exists between the absorption coefficient and concentration of absorbing species, which is independent of the physical processes responsible for the shape of the absorption line profile. The integrated absorption $\int k_\nu d\nu$ over a single rotational line in a diatomic band system can be written in a manner similar to that of an atomic line as presented by Mitchell and Zemansky (1961):

$$\int_{\text{line}} k_\nu \, d\nu = \frac{\pi e^2}{mc^2} f_{J''J'} N_{J''} \qquad (2.2)$$

where e and m are the charge and mass of the electron respectively; c is the velocity of light in vacuo and $N_{J''}$

is the concentration of molecules in the lower rotational-vibrational state specified by the quantum numbers J", v", undergoing an electronic transition to an upper state specified by the quantum numbers J', v'. The line oscillator strength or f-number, $f_{J"J'}$, is a constant for a given transition in a particular molecule. It can be calculated in a few simple cases, but in general has to be determined experimentally and is expressed usually as a band oscillator strength, $f_{v"v'}$, which is related to $f_{J"J'}$, by the expression

$$f_{v"v'} = \frac{2J" + 1}{S_{J"J'}} f_{J"J'} \qquad (2.3)$$

$S_{J"J'}$ is called the rotational line strength and defined so that

$$\begin{aligned} \sum_{J"} S_{J"J'} &= 2J' + 1 \\ \sum_{J'} S_{J"J'} &= 2J" + 1 \end{aligned} \qquad (2.4)$$

Rotational line strengths can be calculated fairly readily (Herzberg, 1950) and are accurately known for most common diatomic flame spectra.

The total concentration of molecules in the lower electronic state may be derived from the concentration in the J" level, if the rotational and vibrational partition functions are known.

Thus the concentration of molecules in the vibrational level v" is given by

$$N_{J"} = N_{v"} \frac{2J" + 1}{Q_{rot}} \exp (- E_{J"}/k\ T_{R"}) \qquad (2.5)$$

where $Q_{rot} = \sum_{J} (2J + 1) \exp (- E_J/k\ T_{R"})$

= Rotational partition function

E_J = Rotational energy of the level J

k = Boltzmann's constant

$T_{R"}$ = Effective rotational temperature of the lower electronic state.

Similarly, the total concentration in the lower electronic state is $N_{el"}$ given by the relation

$$N_{v"} = \frac{N_{el"}}{Q_{vib}} \exp (- E_{v"}/k\ T_{v"}) \qquad (2.6)$$

where $Q_{vib} = \sum_{v} \exp (- E_v/k\ T_{v"})$

and E_v, T_v, refer to the vibrational energy and temperature respectively.

If there is more than one low-lying electronic state, the electronic partition function must also be evaluated in order to arrive at the total molecular concentration. Normally, the lower electronic state is the ground state, but in the case of the C_2 molecule, the $X^3\Pi_u$ state is 610 cm^{-1} above the $X^1\Sigma_g^+$ state (see section 5.2).

2.3. Measurement of integrated absorption: effect of spectral slit-width.

Assuming the spectroscopic constants and oscillator strengths of the relevant transitions are known, the determination of molecular concentrations is reduced to the experimental measurement of the integrated absorption of any line in the band system. As pointed out in section 1.3, in order to resolve the shape of a single rotational line using a continuous background source, a spectrograph of very high resolution is required. In practice the resolving power of any spectrograph is limited by the mechanical slit-width and properties of the dispersing element employed in the instrument.

If an infinitely narrow spectral line is viewed through a spectrograph, it appears to have a half-width of S cm^{-1}, where S is known as the spectral slit-width or band-width of the instrument and is a function of the mechanical slit-width.

If S is comparable to, or greater than, the true line-width, $\Delta\nu_{true}$, of an actual spectral line, the measured line profile will be distorted and render the line less easily visible. Fig. 2b and 2c show the effect on the measured peak fractional absorption for various values of $S/\Delta\nu_{true}$.

It is possible to make corrections to the measured

values of the integrated and peak absorption coefficients if the actual shape of the line is known and the slit function of the spectrograph can be determined (Kostkowski and Bass, 1956). For the integrated absorption the corrections are small if the absorption is weak, because to a first approximation, the area under the curve remains constant. We may then derive an expression relating the true integrated absorption with the measured peak absorption and spectral band-width of the instrument.

2.4. Relationship between integrated absorption and measured peak absorption, using a continuous background source.

The measured integrated intensity, I_o, of the background source when there is no absorption is given by

$$I_o = \int_S J_o \, d\nu = J_o S$$

where J_o is the intensity per unit frequency interval emitted by the source,

and S the spectral band-width of the spectrograph or monochromator.

When the frequency coincides with an absorption line in the flame, the observed intensity is

$$I = \int_S J_o \exp(-k_\nu L) \, d\nu$$

where k_ν is the absorption coefficient of the line, and

L the pathlength through the flame.

If $k_\nu L$ is less than 0.2 at any position in the absorbed line, we can write

$$I = \int_S J_o (1 - k_\nu L)\, d\nu$$

$$= I_o - \int_S J_o\, k_\nu L\, d\nu$$

where J_o has been assumed constant over the absorption line, i.e. the spectral band-width is much greater than the true line-width.

The error is smaller than 3% if $S/\Delta\nu_{true} > 4$.

$$\therefore \quad I = I_o - J_o L \int_S k_\nu\, d\nu$$

and $$(I_o - I)/J_o = L \int_S k_\nu\, d\nu$$

Thus, the peak absorption measured in the flame is

$$\left[\frac{I_o - I}{I_o}\right]_{peak} = \frac{L}{S_H} \int_{line} k_\nu\, d\nu \qquad (2.7)$$

Concentrations may be derived from measurements of the peak fractional absorption, using equations (2.2) and (2.7), if the spectral slit-width of the monochromator is known. This can be readily determined by measuring the apparent half-width of a very narrow emission line such as that emitted by a hollow-cathode lamp.

Thus, it is possible to use a moderate-resolution instrument to make quantitative absorption measurements, the

only criterion being that the dispersion must be sufficiently large to separate neighbouring lines. The method has an advantage over the use of a discrete line source, section 1.4, in that a single continuous background source can be used to detect absorption spectra of a large number of species.

2.5. Detection limits in theory and practice.

The minimum amount of absorption that can be detected is determined by the accuracy with which small changes in light intensity can be measured. Photoelectric methods are generally the most accurate, but an upper limit to the sensitivity is set by the random fluctuations occurring in the photomultiplier output current. These will ultimately determine the smallest concentration of species that can be detected and it is, therefore, useful to derive this quantity for a typical experimental arrangement. The following simple calculation gives a rough estimate of the optimum sensitivity obtainable under ideal conditions.

Consider radiation from a continuous background source of brightness temperature T, passing through the flame and into a monochromator with a photomultiplier detector at the exit slit.

The radiant energy falling on the P.M. per sec. is equal to

$$I_B (\lambda_o, T)\, hw\, \Omega\, t\, \Delta\lambda \qquad (2.8)$$

where $I_B(\lambda_o,T)$ = energy emitted by a black-body of temperature T , per cm^2 per sec. per steradian in a unit wavelength interval centred around λ_o; h is the height of the monochromator entrance and exit slits (assumed equal); w is the width of the slits; Ω is the angular aperture of beam falling on the P.M. (this is equal to A/F^2, where A is the effective area of the diffraction grating and F is the focal length of the collimating mirror); t is the total transmission factor of the optical set-up; and $\Delta\lambda$ is the effective width of the transmitted spectral interval.

$I_B(\lambda_o, T)$ is given by Planck's formula, and may be written as

$$I_B(\lambda_o,T) = 2hc^2 \lambda^{-5} \exp(-hc/\lambda kT) \qquad (2.9)$$

where h is Planck's constant; c is the velocity of light; and k is Boltzmann's constant.

The average number of photo-electrons emitted at the photocathode per sec. is proportional to the anode current and is given by

$$\bar{n} = I_B(\lambda_o,T)\, hw\Omega t\, \Delta\lambda\, \eta/(hc/\lambda) \qquad (2.10)$$

where η is the quantum efficiency of the photocathode surface and hc/λ is the energy of a photon of wavelength λ.

Statistical fluctuations will be superimposed on this mean value owing to the random character of the arrival of photons and the emission of photo-electrons. Assuming

a normal distribution for these events, the standard deviation from the average value is denoted by Δn and given by

$$\Delta n \simeq \bar{n}^{1/2} \qquad (2.11)$$

It is this quantity which fundamentally determines the detection limit in absorption measurements. An absorption signal that corresponds to a reduction of Δn in the emitted photo-electrons will be on the threshold of detection if

$$[\,(I_o - I)/I_o\,]_{peak} \simeq \Delta n/\bar{n}$$

i.e.
$$(\Delta I/I_o)_{min} \simeq \bar{n}^{-1/2}$$

$$\simeq [I_B(\lambda_o,T)hw\Omega t\,\eta\Delta\lambda/(hc/\lambda)]^{-1/2}$$

If the background source is a high-pressure arc lamp,

$$I_B(\lambda_o,T) \simeq 3 \times 10^{25} \text{ photons cm}^{-3}\text{sec}^{-1}\text{.sterad.}^{-1}$$

for $T = 5{,}000^{\circ}K$ and $\lambda_o = 5{,}000$ Å.
Also $h = 0.2$ cm., $w = 10^{-3}$ cm(10μ), $\Omega = A/F^2 = 10^{-2}$ sterad., $\Delta\lambda = S = 2 \times 10^{-9}$ cm. (0.2 Å), being the values applicable to the Jarrell-Ash monochromator employed in Chapter 4. Finally, $\eta \simeq 0.1$ and $t \simeq 0.1$ for a typical system.

Substituting these constants into the above equation, we obtain

$$(\Delta I/I_o)_{min} \simeq 3 \times 10^{-5}.$$

If the transmitted intensity is weak, thermal noise from the flame and Johnson noise generated in the anode

resistor will also become important. Overall, a value of $(\Delta I/I_o)_{min}$ of about 10^{-4} (i.e. 0.01% absorption) is likely to represent the ultimate sensitivity that can be obtained. For a tungsten-strip lamp having a brightness temperature of 2500°K, $(\Delta I/I_o)_{min} \simeq 5 \times 10^{-4}$, and the minimum absorption that can be measured is consequently about 0.1%.

In practice, it is difficult to measure absorption under about 1% because fluctuations caused by instabilities in the background source are generally much larger than the statistical fluctuations calculated here. The photo-electric apparatus described in Ch.4 employed a high pressure Xenon arc which produced a noise level of about 1% even under optimum measuring conditions.

Using eqs. (2.2) and (2.7), we can convert the minimum peak fractional absorption into the number of absorbing molecules per cm^3 and thereby arrive at the smallest concentration which can be measured by absorption spectroscopy.

The concentration of absorbing molecules in the rotational level J" of an electronic band system is given by

$$N_{J''} = \frac{mc^2}{\pi e^2} \frac{S}{L} \left[\frac{I_o - I}{I_o}\right]_{peak} \frac{2J'' + 1}{S_{J''J'}} \frac{1}{f_{v''v'}} \qquad (2.12)$$

where $\frac{mc^2}{\pi e^2} \simeq 1 \times 10^{12}$ cm.

Putting S = 1 cm^{-1} (corresponding to a resolving

power of 0.25 Å at 5000 Å); $2J''+1/S_{J''J'}f_{v''v'} \sim 5 \times 10^2$, for a typical line in the (0,0) band of a diatomic molecule; L = 100 cm. for a low pressure flame, using a multiple reflection system; and assuming $(\Delta I/I_o)_{min} = 10^{-4}$, we obtain

$$(N_{J''})_{min} \simeq 5 \times 10^8 \text{ molecules cm}^{-3}.$$

The total concentration of molecules in all possible energy states will be about 10^2 higher than the concentration in a single rotational level; thus

$$N_{TOTAL} \simeq 5 \times 10^{10} \text{ cm}^{-3}.$$

In practice, $(\Delta I/I_o)_{min} \simeq 10^{-2}$, and concentrations greater than 5×10^{12} cm^{-3} should be detectable using multiple-reflection techniques if the molecule has a suitable absorption spectrum. This figure may be compared with the lower limit of detection of present-day mass-spectrometric and electron spin resonance techniques applied to flames, ca. 5×10^9 ions cm^{-3} and 5×10^{13} radicals cm^{-3}, respectively.

The absolute accuracy of concentration measurements by absorption spectroscopy will depend on the accuracy with which the f values of the relevant transitions are known. Errors of 50% are not uncommon. The total error will be slightly higher still owing to uncertainties in the values of the spectral slit-width and the effective optical pathlength through the flame.

CHAPTER THREE.

QUALITATIVE ABSORPTION MEASUREMENTS USING FLASHTUBE AND PHOTOGRAPHIC DETECTION.

3.1. Introduction.

For a preliminary survey, absorption spectra were recorded photographically, using a multiple reflection system to increase the pathlength and a flashtube as background source. By such means, Spokes (1959) was able to detect weak absorption in the (0,0) bandhead of the C_2 Swan bands and the piled-up Q branch of the 3143 Å band system of CH. He studied low pressure oxy-acetylene flames and employed a multiple reflection system designed by White (1942). This consisted essentially of three spherical concave mirrors, the centres of curvature of mirrors B and C lying on the surface of mirror A. A diagram showing the method of image formation is given in Fig. 3b. Mirror A may be split into two in order to allow the initial light beam to enter centrally between the two halves. (Welsh et al., 1951).

Although very compact and moderately easy to adjust, the light traversing the flame is approximately parallel and the consequent poor spatial resolution limits the usefulness for combustion investigations. Only thick reaction zones, such as those of low-pressure flames or near-

limit flat flames can be studied, and even here the detailed flame structure cannot be resolved. The reason is that the light beam is focused on the mirror surface and a fairly wide beam actually passes through the flame. This nearly parallel beam is also very subject to schlieren-type deflections due to temperature gradients in the flame and these cause deterioration of the image formation, limiting the number of traversals which can be obtained.

In this work a multiple reflection system has been employed which focuses the light into the flame and consequently has much better spatial resolution and is less affected by refractive-index gradients than the White system. These properties made it ideally suited for studying the luminous mantle of hot oxy-acetylene flames at 1atm.

3.2. Experimental.

(a) The multiple reflection system.

Figure 3a shows the mirror system. It consists essentially of two spherical concave mirrors of equal focal length, separated by a distance equal to twice their radius of curvature. The centres of curvature of each mirror coincide at the point O. A narrow beam of light is brought to a focus at a point P which is laterally displaced from O by a small distance dependent on the number of traversals required. The beam is refocused after reflection from

F I G U R E 3.

(a) Focussing multiple reflection system set up to give 7 traversals.

(b) White multiple reflection system set up to give 16 traversals.

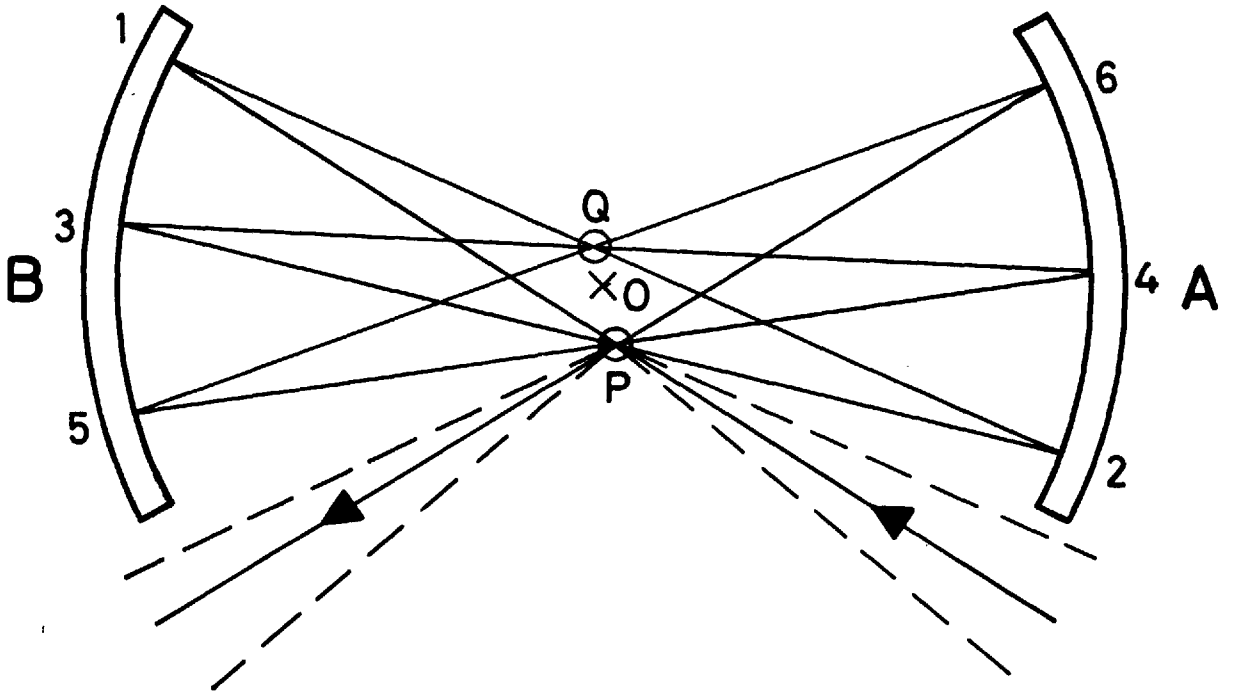

(a) Focussing System

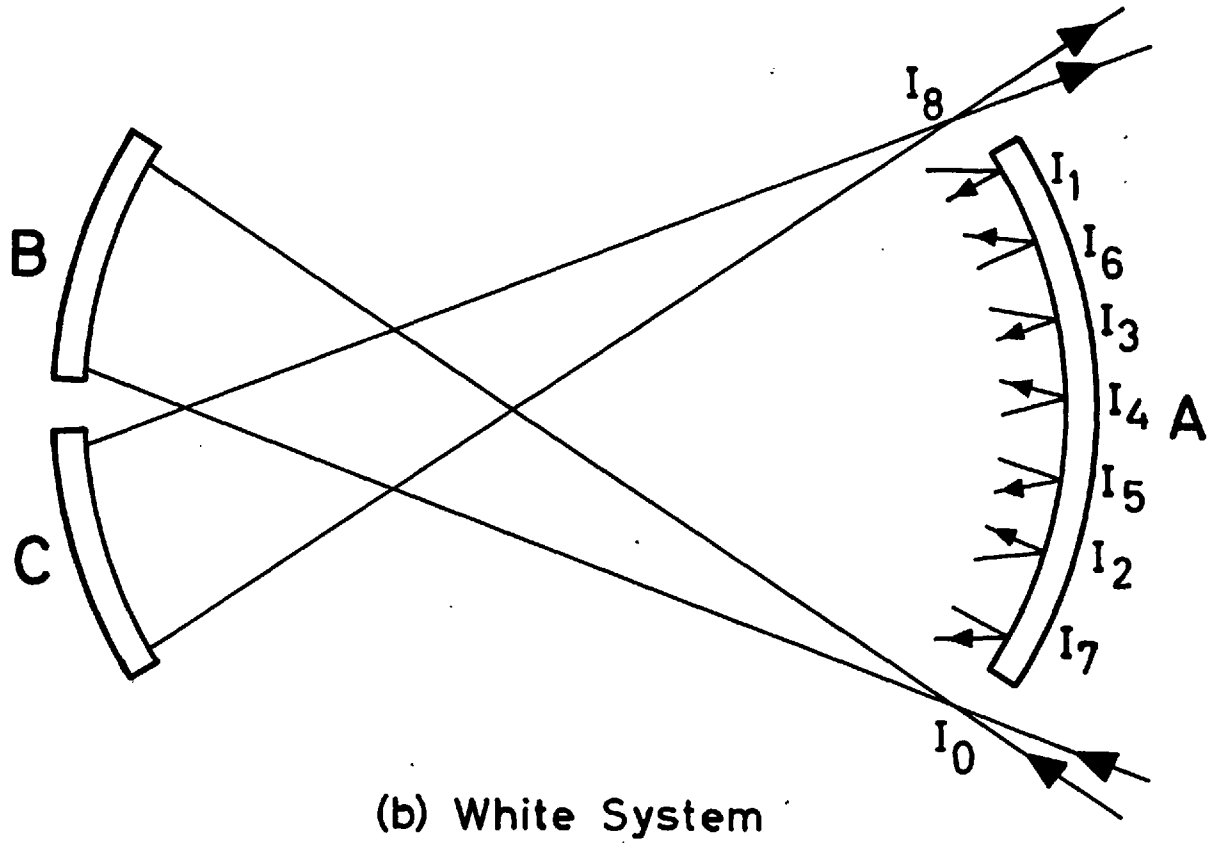

(b) White System

mirror B at a point Q on the other side of the centre of curvature an equal distance away. Further images are formed at P and Q by successive reflections from mirrors A and B, respectively; this results in the light beam moving round the arc of the circle defined by the mirrors. For a given angular aperture of the beam, the number of reflections possible is determined by the distance OP and the diameter of the mirrors. The minimum length of OP, corresponding to the maximum number of reflections, is set by the angular aperture of the beam.

Obviously, it is possible to increase the number of reflections by increasing the size, or number, of mirrors, but it should be noted that the image formation deteriorates with increasing number of traversals. Since we are working slightly off the axis of the mirrors and rays strike them obliquely, the system is subject to all the aberrations associated with spherical mirrors. Thus, after several reflections, the images will become blurred and enlarged, and the points P and Q increasingly less clearly defined. We therefore have to make a compromise between the number of traversals and the spatial resolution required when studying a particular flame.

Initially four mirrors were used, each of 6 cm. diameter and 10 cm. radius of curvature. It was found that

up to twelve reflections were possible without adversely affecting the spatial resolution. In the later work (see fig.10), the mirrors were replaced by two larger ones, and up to fifteen traversals could be employed by further reducing the angular aperture of the light beam.

It should be noted that the images formed at P and Q are inverted to one another. This prevents simultaneous study of an extended zone of the flame, but does not interfere with the step-by-step investigation of the absorption spectrum when the background lamp is effectively a point source.

(b) The burner.

To take full advantage of the increased absorbing path-length offered by the system, two flames must be used, or alternatively a single burner can be employed having a diameter greater than the distance PQ, e.g. a flat flame burner. It is impossible to run a large, flat oxy-acetylene flame other than at reduced pressure, because of the tremendous heat release and high burning velocity of the mixture. Several types of burner were tried. The water-cooled meker burner of the type extensively used by Sugden and collaborators, (see Padley and Sugden, 1958) was found unsuitable because the central area of the burner top quickly melted. Dilution of the acetylene-oxygen mixture

with an inert gas reduced the temperature sufficiently to prevent this occurring but the resulting lower gas temperature made it difficult to detect any carbon radical absorption in the flame.

The most effective burner consisted of a pair of simple slot-type burners, placed at the image points P and Q. They were built onto a modified welding torch to prevent danger from flash-back. The burners were constructed from copper tubing of about 2 mm. i.d., the end of which had been squeezed into a rectangular shape of dimensions 3 x $\frac{3}{4}$ mm.

Commercial-grade acetylene and oxygen were used without further purification (B.O.C.). Flow rates were measured with calibrated flow-meters made by the Rotameter Manufacturing Company.

(c) Flashtube and associated triggering device.

The Lyman flashtube, developed at Imperial College (Garton, 1953; Wheaton, 1964), and used in this work, gives a good continuous spectrum throughout the entire visible and u.v. regions, corresponding to a brightness temperature of 20,000 - 30,000°K. A single flash lasts only a few microseconds and, in general, several flashes are required to obtain a reasonable exposure when the flashtube is used in conjunction with a multiple reflection system and large dispersion spectrograph.

To obtain the absorption spectrum of a continuously emitting flame or gas, it is necessary to uncover the slit of the spectrograph only for the very short time interval during which the flash is operated. Garton and Rajaratnam (1957) have described a sector disc device which acts as a suitable shutter and can be synchronised to operate the flashtube. It consists of a pair of rotating discs of equal diameter, mounted on the same axis but geared to rotate at different speeds. The discs have radial slots near the periphery which come into line with each other and with the slit of the spectrograph once in every revolution of the slow disc. At about 120° to the slot in each disc is a second aperture. The flashtube is triggered by a spark from a thyratron circuit initiated by a light beam which passes through the auxiliary slits and falls onto a photocell. About 20 flashes a minute were possible without overloading the flashtube charging unit.

Spokes has given full details of the design of the flashtube and associated triggering equipment in his Ph.D. thesis (London University, 1959). Much of his original apparatus was still serviceable and could be adapted for use in the present work. Consequently a full description of this part of the apparatus is omitted.

(d) Spectrograph and optics.

Figure 4 shows the optical set-up. The

F I G U R E 4.

Schematic diagram of photographic set-up showing the light path.

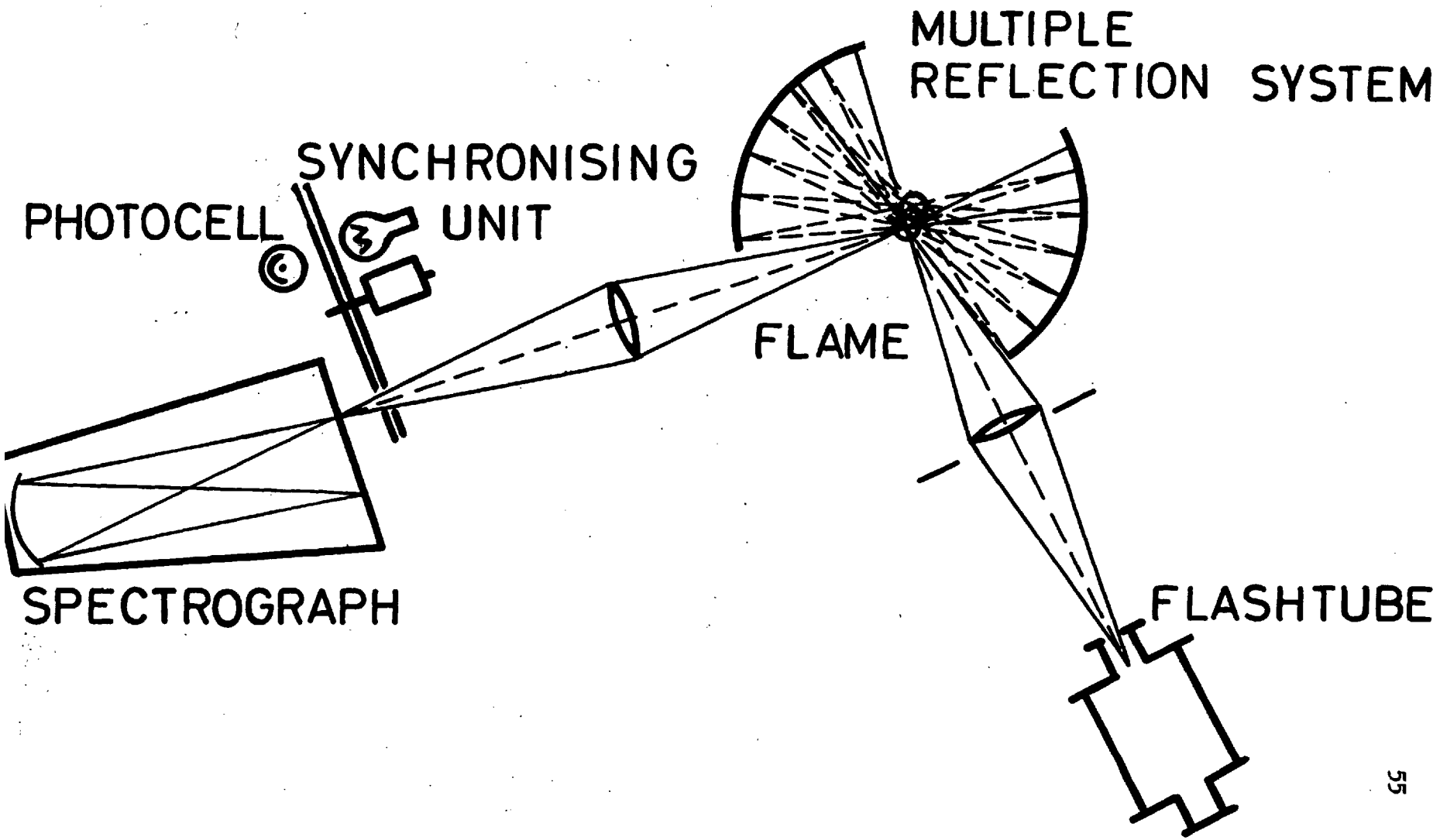
MULTIPLE
REFLECTION SYSTEM
SYNCHRONISING
UNIT
PHOTOCELL
FLAME
SPECTROGRAPH
FLASHTUBE

spectrograph is a 2 m. grating instrument designed by Dr. R.C.M.Learner. It employs a grating having 25,000 lines/inch and gives a reciprocal dispersion of 5 Å/mm. in the 1st order. A wavelength interval of 2500 Å can be photographed with a single exposure. Using a 10μ entrance slit, it was possible to resolve much of the fine-structure in the C_2 and CH band spectra. The resolving power was not measured but was estimated to be at least 0.2 Å at 5000 Å.

Achromatic lenses were used to focus the light beam into the flame and onto the slit of the spectrograph. They are necessary to ensure that the spectrum is sharply focused over the entire wavelength region covered by the photographic plate.

Alignment of the optics requires considerable care and it is important to ensure that the best use is made of the available light. The grating of the spectrograph should always be completely filled with light in order to utilise the maximum resolving power of the instrument. It is difficult to move a large, heavy spectrograph in a controlled manner and make accurate adjustments to the multiple reflection system using a flashtube light source. A common practice in such cases is to make the necessary adjustments by sending the light through the optical system in the reverse direction, using an alternative bright source.

The plate-holder was removed and a Pointolite lamp positioned in the focal plane of the spectrograph so that green light emerged from the entrance slit. By fully opening the slit, the intensity was sufficiently high to retrace the light beam back through the multiple-reflection system and through the capillary of the flashtube. In this way, it was possible to align the various optical components with relative ease; a final small adjustment, to bring the image exactly onto the spectrograph slit, could be made while the flashtube was running.

(e) Photographic plates.

Emission and absorption spectra were recorded on H.P.S., Zenith, and X.K. plates manufactured by Ilford Ltd. H.P.S. is a fairly fast panchromatic plate and was used to record the C_2 Swan spectrum. The other plates are unsensitised and were used to cover the spectral range from about 2300 Å to 4500 Å. The X.K. plate has been specially designed for flashtube work. It is extremely fast when bright, short-duration exposures are made, but the effective speed of the emulsion is reduced if longer exposures are necessary, i.e. for recording flame emission spectra.

About 20 flashes were sufficient to obtain reasonable exposures of absorption spectra using X.K. plates. Zenith and H.P.S. plates required 100-300 flashes, depending

on the wavelength region examined. Plates were developed in PQ Universal (dilution 1:4) for 4 minutes or Johnson's Contrast developer for 2 minutes.

3.3. Results.

The absorption spectra of stoichiometric and fuel-rich oxy-acetylene flames were studied in the wavelength range between 2300 - 6500 Å. Propane and ethylene flames were also briefly investigated, as well as flames of acetylene with nitrous oxide and air. The results are summarised below; they refer to acetylene-oxygen mixtures unless otherwise stated.

With five traversals through the tip of the reaction zone of stoichiometric flames, strong OH absorption was observed in the (0,0) band around 3100 Å. The absorption decreased with increasing mixture strength and was very weak in the mantle-forming flames of rich mixtures.

Weak C_2 absorption was detected in the (0,0) bandhead at 5165 Å with nine traversals through the reaction zone of rich flames. With thirteen traversals, the absorption spectrum was strong enough to show up all the more prominent bandheads and much of the rotational fine structure. Figure 5 shows lines in the (0,0) band up to about R(50). A microphotometer trace of the photographic plate is presented in Fig. 6(a). Emission spectra have been

F I G U R E 5.

C_2 absorption in a fuel-rich oxy-acetylene flame. Absorption spectrum of the (0,0) Swan band between 5165 - 5000 Å. Emission spectra have been juxtaposed for comparison.

Experimental details: 13 traverses through the tip of the reaction zone. Mixture strength C/O ~ 1.2. H.P.S. plate, 300 flashes.

60
5165Å

F I G U R E 6.

Microphotometer traces of (a) C_2 (5165 Å) and (b) CH (4315 Å) absorption spectra. Emission spectra have been included for comparison.

N.B. The C_2 emission spectrum is overexposed.

13 traversals through the tip of the reaction zone of a fuel-rich oxy-acetylene flame.

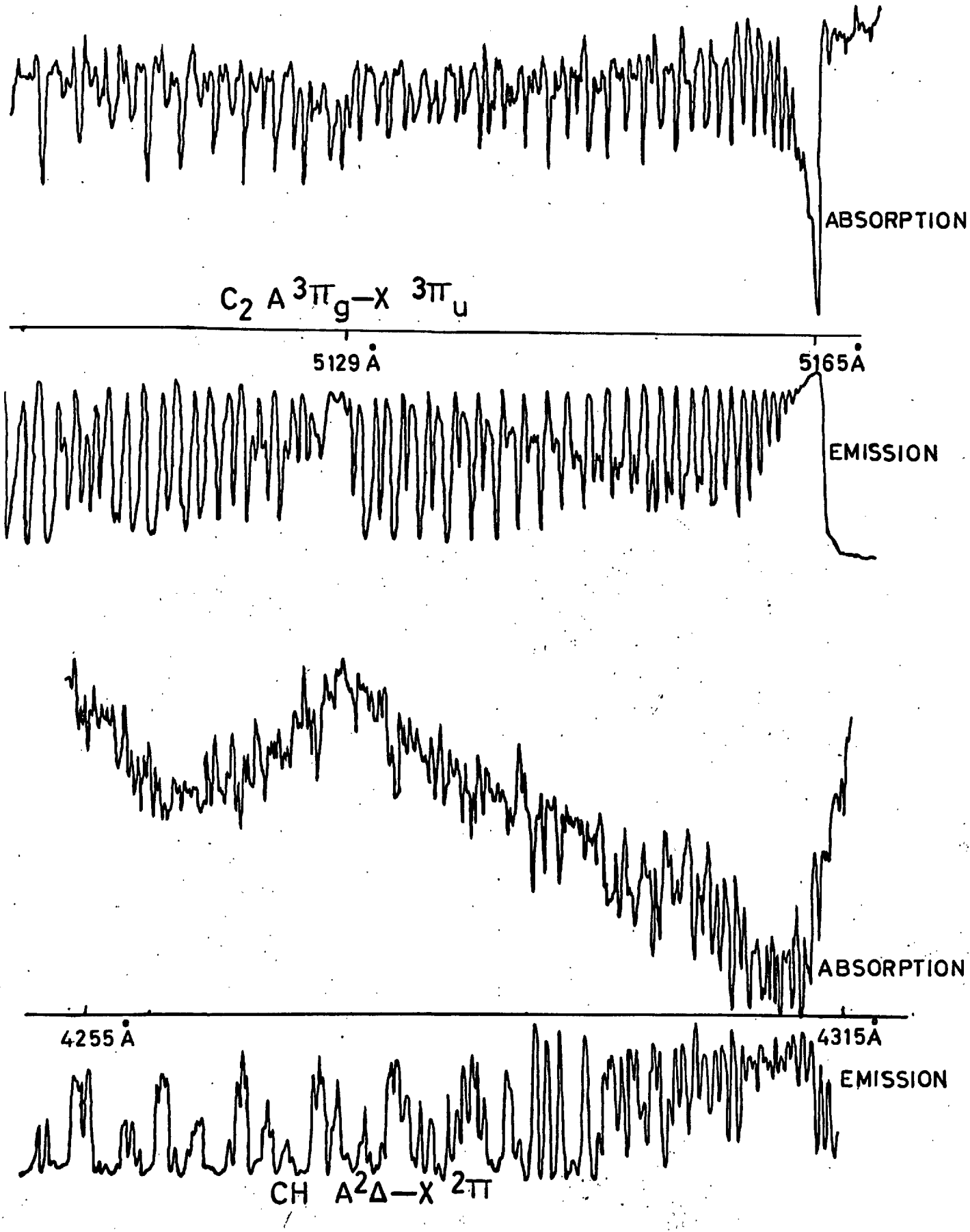
ABSORPTION
C_2 $A\,^3\Pi_g - X\,^3\Pi_u$
5129 Å
5165 Å
EMISSION
ABSORPTION
4255 Å
4315 Å
EMISSION
CH $A\,^2\Delta - X\,^2\Pi$

included for comparison. The absorption intensity was strongest in the reaction zone with mixture strengths of $C/O \sim 1.2$. It extended several millimetres above the reaction zone into the luminous mantle although with reduced intensity.

We have succeeded in detecting all three band systems of CH in absorption with thirteen traversals through the reaction zone. The piled-up Q branch of the 3143 Å band was recorded with least difficulty but weak absorption was also observed, for the first time in the 3900 Å and 4315 Å band systems. A microphotometer trace of the 4315 Å $^2\Delta - ^2\Pi$ transition is shown in Fig.6(b). The absorption is only just greater than the average background noise level, and it was not possible to obtain a clear positive from the photographic plate. Maximum absorption occurred at mixture strengths between C/O = 1.0 and 1.2; no CH absorption could be detected in the mantle above the reaction zone.

Both C_2 and CH emission spectra were much stronger in the reaction zone than in the mantle region. A diffuse band system at about 4050 Å, ascribed to the C_3 radical, was observed in richer mixtures exhibiting the mantle and appeared to be equally strong in the inner cone and luminous mantle. It was possible to detect feeble C_3 absorption just above the tip of the reaction zone for mixture strengths between three and four times the stoichiometric value, i.e. C:O = 2:5.

F I G U R E 7.

C_3 Comet-Head Band.

The line at 4051.5 $\pm$ 1 Å is prominent in emission and absorption.

N.B. The wavelength scales for the emssion and absorption traces are different.

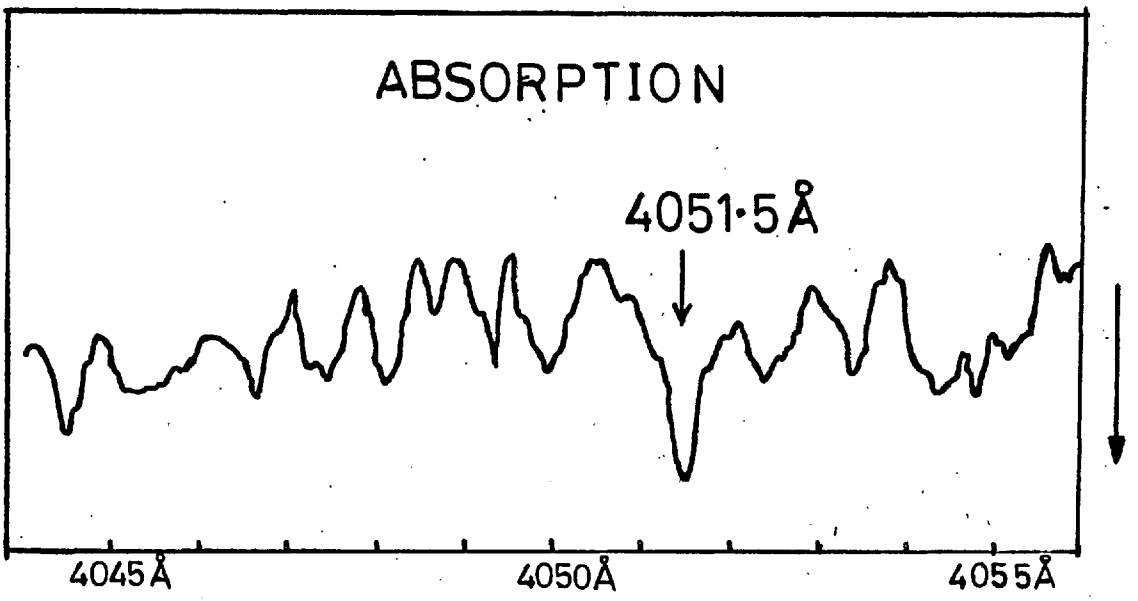

C_3 COMET-HEAD BAND

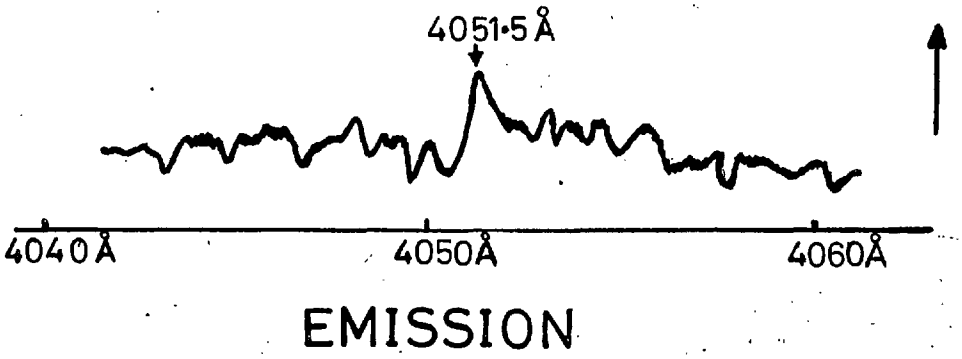

EMISSION

Fig. 7 shows a weak but reproducible peak at 4051 Å superimposed on the general background noise.

The carbon line at 2478 Å was emitted by the inner cone of slightly rich oxy-acetylene flames but there was no sign of it appearing in absorption, even with thirteen traversals through the reaction zone. The only other absorption spectrum detected was that of the CN radical, which is formed in the luminous mantle owing to entrainment of surrounding air. It was always fairly weak and its intensity varied with height above the reaction zone. The strongest absorption occurred in rich mixtures, being a maximum 2-3 cm. above the reaction zone.

If the oxygen of the unburnt mixture was replaced by nitrous oxide, the CN absorption spectrum became very intense throughout the flame and, in addition, absorption due to the NH radical was detected in the reaction zone. C_2 absorption was still observed, but it was estimated to be about an order of magnitude lower than in oxygen-acetylene flames. No CH or C_3 radicals could be detected in absorption although their emission spectra were observed. There was no indication of C_2, C_3, or CH absorption in flames of ethylene and propane with oxygen, or in acetylene-air flames. The emission intensity of the radicals in these flames was lower than in oxy-acetylene flames.

3.4. Discussion.

At the commencement of this work, there was only one previous report of C_2 and CH absorption in steady flames (Gaydon, Spokes, and van Suchtelen, 1960). The absorption was always very weak, even though an effective pathlength of over 120 cm. was employed.

Recently, Bleekrode and Nieuwpoort (1965) succeeded in detecting all three band systems of CH as well as strong C_2 absorption in low-pressure oxy-acetylene flames similar to those studied by Gaydon et al. They worked with absorbing pathlengths of up to 220 cm. and recorded the spectra photoelectrically using a high-pressure mercury lamp as background source.

There do not appear to be any previous reports of C_3 absorption in flames, but it has been observed in absorption (together with C_2 and CH) in the explosive oxidation of acetylene-oxygen mixtures by the flash photolysis of nitrogen peroxide (Norrish, Porter and Thrush, 1953). The carbon radicals were observed for C:O ratios of unity or greater. It was suggested that C_2 and CH radicals were formed as the result of pyrolysis reactions, and had appreciable equilibrium concentrations only if there were insufficient hydroxyl radicals to oxidise them. The C_3 molecules were thought to be formed from solid carbon

particles and were considered to be in equilibrium with them but no absolute concentration measurements were made.

It is not surprising that the 2478 Å carbon line is not observed in absorption. It is due to the transition $3s\,^1P - 2p^2\,^1S$, and requires an excitation energy of 7.7 eV. because the lower ^1S state is 2.7 eV above the (^3P_o) ground state. In equilibrium, only about 10^{-5} of the total carbon atom concentration is in the $2p^2\,^1S$ state at any particular time. Resonance transitions from the ground state lie in the vacuum u.v. and would not be expected to occur in ordinary flame sources.

The results obtained indicate that the focusing multiple-reflection system provides a powerful method for detection of radicals in flames at atmospheric pressure. Acetylene-oxygen mixtures give the highest carbon radical concentrations and are therefore most suitable for quantitative absorption measurements of C_2, C_3 and CH radicals.

CHAPTER 4.

QUANTITATIVE ABSORPTION MEASUREMENTS USING PHOTOELECTRIC DETECTION.

4.1. Introduction.

The photographic results given in Chapter 3 showed that appreciable concentrations of C_2, C_3, and CH radicals exist above the tip of the reaction zone of fuel-rich oxy-acetylene flames. In order to facilitate quantitative measurements, particularly of continuous absorption, it was decided to record the absorption spectra photo-electrically using modulation techniques to eliminate the flame emission signal. The main advantage of this method is that a less bright background source may be used, because it need not have a higher brightness temperature than the electronic excitation temperature of the radicals in the flame. A brief discussion of the photoelectric and photographic methods of recording was given in Section 1.4.

In this chapter, we describe the photoelectric set-up, and present typical emission and absorption spectra from which C_2, C_3, and CH concentrations in oxy-acetylene flames have been derived.

4.2. Apparatus.

Figure 8 is a schematic diagram of the experimental set-up. The flash-tube and sector-disc device have been replaced by a high-pressure Xenon arc lamp and mechanical light chopper which modulates the beam at a fixed frequency. A scanning spectrometer and photomultiplier detector was used in place of the spectrograph and photographic plate. The output signal of the P.M. was selectively amplified and fed into a pen recorder which traced out the absorption spectrum as the wavelength region was slowly scanned.

a) The light chopper.

This consisted of an 8" rotating aluminium disc driven by a small electric motor. The disc was divided into 36 equal segments and alternate ones were cut away to make 1" long radial slots around the periphery. The unit was positioned in front of the background lamp as shown in fig.8. A 'Variac' transformer was used to control the speed of rotation and it was usually set to give a chopping frequency of about 210 c/s. The frequency used could be readily determined by feeding the square-wave output signal from the photomultiplier into an oscilloscope. A second light beam from a small torch bulb was passed through the chopping wheel onto a photodiode in order to produce a reference signal.

F I G U R E 8.

Schematic Diagram of Photo-electric Detection System.

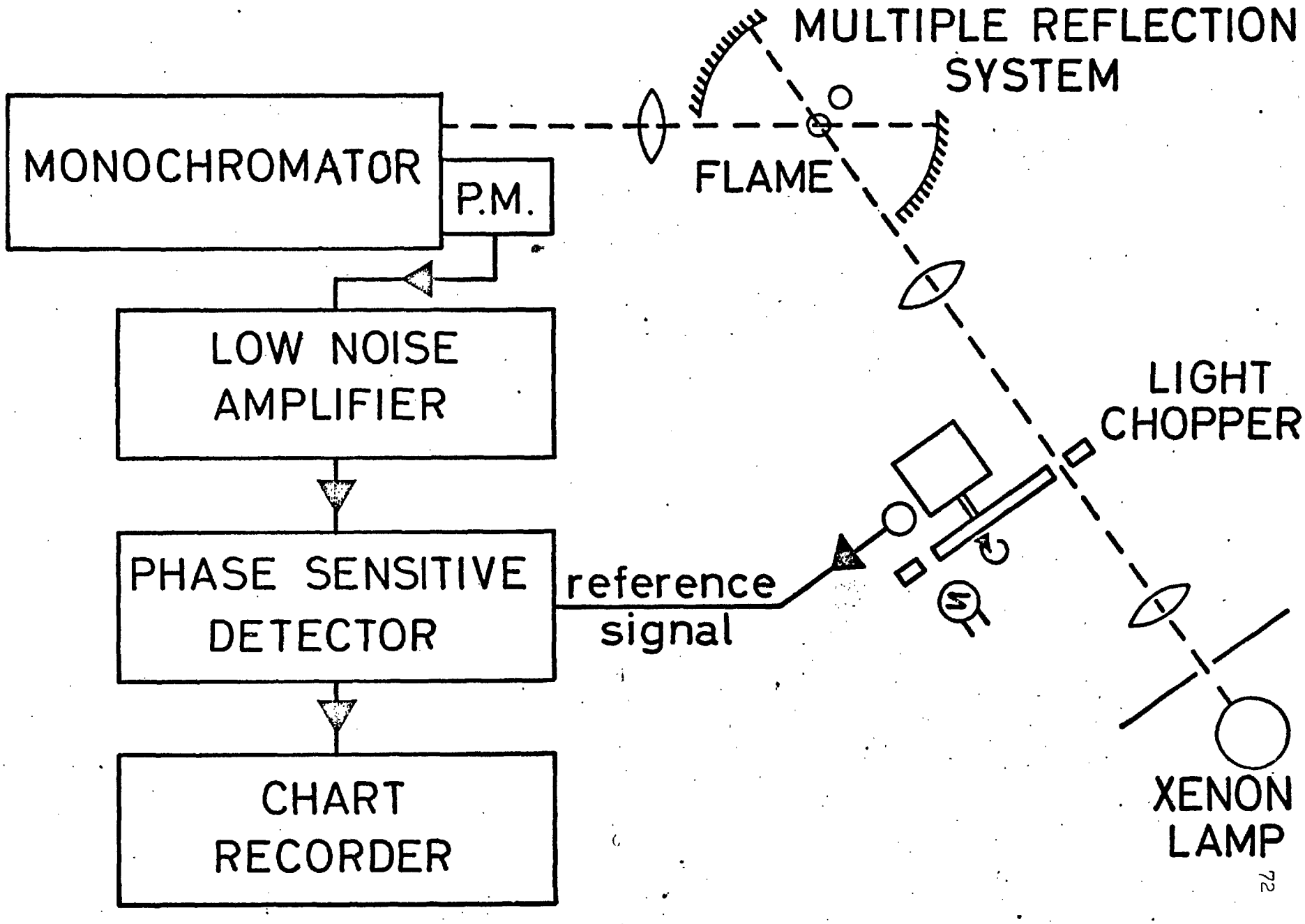
MULTIPLE REFLECTION SYSTEM
MONOCHROMATOR
P.M.
FLAME
LOW NOISE AMPLIFIER
LIGHT CHOPPER
PHASE SENSITIVE DETECTOR
reference signal
S
XENON LAMP
CHART RECORDER

b) Electronic detection.

The total P.M. output signal will contain a d.c. component and a wide range of frequencies in addition to the chopping frequency of interest. The steady flame emission produces a d.c. signal and there is also a small contribution from the photomultiplier dark current. Inherent to any photoelectric cell is a small, random a.c. signal, which is made up of so-called flicker noise, shot noise, and Johnson noise. Also, any irregular variations in the emission intensity of the flame due to slight changes in the gas flow rate, etc., will give rise to a complicated a.c. waveform.

The d.c. component of the signal can be effectively eliminated by the addition of a blocking capacitor in the output circuit. It is impossible to completely eliminate the random noise, and it will ultimately limit the sensitivity of the absorption measurements (see section 2.5).

There are two common methods of amplifying a given a.c. signal in the presence of appreciable background noise. The first employs a narrow-band amplifier, tuned to the frequency of interest. All frequencies will be rejected except those lying within the band-width of the amplifier. By making this band-width very narrow, only a small fraction of the total noise will be amplified and recorded. The

second method makes use of the principle of phase-sensitive detection to increase the signal-to-noise ratio. A phase-sensitive detector (P.S.D.) is a device which compares a reference signal and a test signal and gives a d.c. output. This d.c.output is proportional to the amplitude of that component of the test signal which is of the same frequency and phase as the reference signal. The noise on the test signal does not produce an output from the P.S.D. unless it has a component which lies within a frequency band centred on the reference frequency and is in phase with it. The width of this band is determined by the time-constant of the pen recorder which is used to measure the d.c. output; this is typically one second, which gives a band-width of 1/3 c/s. An untuned amplifier is used to amplify the signal from the photomultiplier before it is fed into the test signal input of the P.S.D.

It was decided to use the phase-sensitive detection system for a number of reasons; (i) it is difficult to achieve a band-width of only 1/3 c/s with a narrow-band amplifier; (ii) it is difficult to synchronise the chopping frequency with the tuned frequency of the amplifier; slight variations in either will cause the two frequencies to drift out of phase. The reference signal of a P.S.D. is obtained by placing a photodiode next to the chopping wheel, with a

small lamp to excite it. The photodiode is moved round the circumference of the chopping wheel until the P.S.D. output is a maximum, the test signal and reference signal being exactly in-phase. Once set, the frequency and phase of each signal will remain equal even though there may be slight variations in the chopping speed. (iii) A narrow-band amplifier can be tuned over a limited frequency range only, whereas the P.S.D. can be made to operate over an almost unlimited frequency range. The chopping frequency giving the optimum signal-to-noise ratio can therefore be determined experimentally simply by varying the speed of the electric motor. (iv) The cost of a P.S.D. plus untuned amplifier is no more than the cost of a low-noise tuned amplifier.

A phase sensitive detection unit suitable for spectroscopic work is made by Brookdeal Electronics. The output from the photomultiplier (E.M.I. type 9558 QB) was fed into a low-noise amplifier, (Brookdeal, model LA 350), and from there into the signal input of a P.S.D., (Brookdeal, model PM 322). The d.c. output was measured on a 7" chart-recorder having a 1 sec. time response.

It is necessary for the P.M. power supply to be extremely stable because small variations in the e.h.t. voltage can cause relatively large variations in the P.M. output signal. Some trouble was experienced at the outset

because a 'home-built' power pack was used which was insufficiently stable and consequently affected the accuracy of absorption measurements. For the later work, a highly stabilised d.c.power supply (Hewlett-Packard, model 6516A) was used which produced less than 5 mV. ripple and noise at the operating voltage of 1000-1100 V.

c) Background lamp.

An air-cooled high-pressure Xenon arc (B.T.H. 2 kW. type XE/D) was employed as backing source for most of the absorption measurements described in this thesis. The Xenon arc lamp is a compact, d.c. or a.c. light source which has an extremely high brightness temperature throughout the u.v., visible and near i.r. spectral regions and an approximately continuous spectrum in the wavelength range 3000-8000 Å. The brightest part of the arc is a region about one mm. in diameter just above the cathode. It corresponds to a brightness temperature of 4500-5500°K, the exact value depending on the power input to the lamp.

The arc was run from a 220 V., 55 amp. d.c. mains supply. Dropping resistors were used to limit the current to 50 amp. Stability is all-important because the spectrum is scanned at only 2Å/min for the highest resolution studies. Fluctuations in light intensity other than those produced by genuine absorption in the flame will hamper the

interpretation of the results. A ripple on the mains voltage at 50 c/s and 600 c/s proved troublesome, but was eliminated by passing the supply through a large choke and R-C filter network.

The remaining fluctuations in light intensity were due to slight wavering of the arc between the poles of the electrodes. The problem is made more acute by the need for focussing the light beam onto the spectrometer entrance slit after traversal of the long optical path through the flame. This effectively determines the minimum amount of absorption that can be determined in practice. For a well-designed lamp, these fluctuations produce a random error of about 1% in the P.M. output signal.

Low-resolution absorption spectra of the 1-0 sequence of the C_2 Swan bands were obtained using a quartz halogen tungsten lamp. The filament can be operated, for the same life, at a rather higher temperature than conventional tungsten lamps, thus making it better suited for absorption studies. It is not possible to use the Xenon arc because its spectrum exhibits broad emission peaks around 4700 Å which coincide with the C_2 absorption bands. The lamp runs very stably off a 12V car battery and the signal-to-noise ratio can be increased by using wide slits. The brightness temperature is, of course, much lower than that

of the Xenon lamp, but the loss in sensitivity is compensated for, to some extent, by the increased stability of the quartz halide lamp.

d) Spectrometer.

Emission and absorption spectra were measured with a 0.5m Ebert grating spectrometer (Jarrel-Ash, model 82-000). The resolution is claimed to be at least 0.2 Å in the first order, using a 1180 grooves/mm (30,000 lines/inch) grating and 10μ slits. Adjustment of both entrance and exit slits of the monochromator is made simultaneously by use of a single control, calibrated in 2μ units to provide slit-widths from 5 to 400μ. Spectra could be scanned electrically at eight different speeds ranging from 2 to 500 Å/min. Two gratings were employed blazed at 4000 Å and 5000 Å respectively.

In order to make quantitative measurements, it is necessary to know the spectral band-width, S, of the instrument at a given slit setting (Section 2.4). S was determined experimentally by slowly scanning the 3650.15 - 3654.83 Å lines from a low-pressure Hg discharge source and was checked between 3000-6000 Å by using emission lines from a hollow cathode Fe lamp. The spectral bandwidth is equal to the area of a narrow emission line divided by its peak height and is approximately given by the width of the line at half intensity. It was found that the reproducibility for various

slit settings was very poor, and so the slits were 'closed' to their minimum value (10μ nominal) and kept at this position throughout the high resolution measurements. The spectral bandwidth of the monochromator at this setting was determined to be 0.19 $\pm$ 0.01 Å for the 5000 Å blazed grating and 0.20 $\pm$ 0.01 Å for the 4000 Å blazed grating.

e) Multiple reflection system.

Minor modifications were made to the multiple reflection system described in Section 3.2. The four original mirrors were replaced by two larger mirrors, each of 6" focal length and 6" diameter. It was necessary to increase the focal length of the mirrors because their aluminised front surfaces became hot and caused the reflectivity to deteriorate fairly rapidly. The multiple reflection system was much easier to adjust when only two mirrors were used, although the design of suitable holders for heavy, large-diameter mirrors required careful consideration. The mounts had to support the weight of the mirrors rigidly but allow accurate, controlled movements in two dimensions. It was important the initial light beam and emergent beam passed very close to the edge of the mirror in order to utilise the full surface area of each mirror. The holder shown in fig.9 was found to be suitable. The mirrors were mounted on an optical bench and once the multiple

F I G U R E 9.

Construction of multiple reflection mirror mounts.

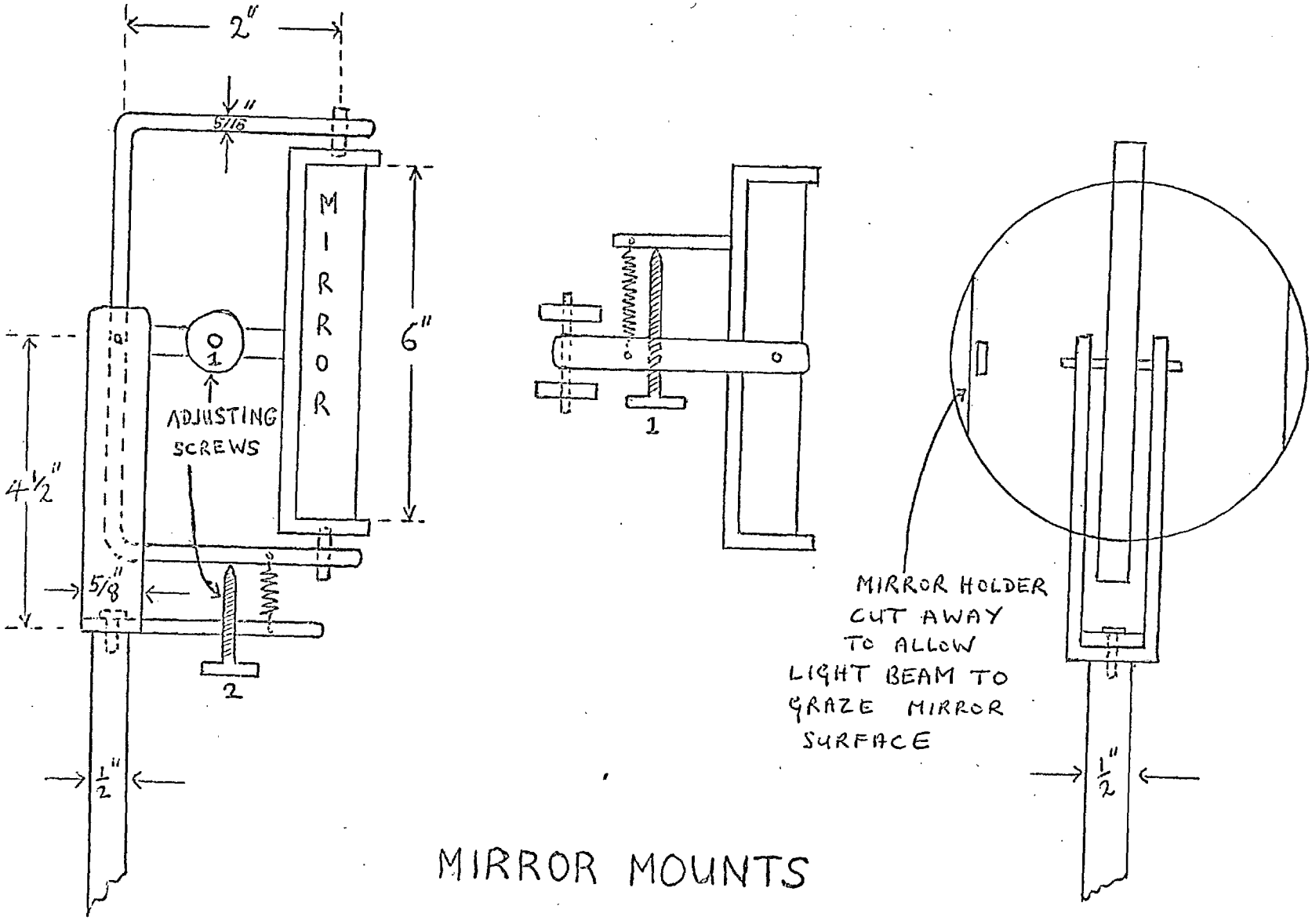

MIRROR MOUNTS

reflection system had been set up, no further adjustments were generally required. Up to 15 traversals were possible with a spatial resolution of about 1 mm. Figure 10 shows the system set up to give 7 traversals; the light beam has been made visible by blowing smoke into the space between the mirrors.

f) Burner.

A pair of burners, based on oxy-acetylene welding design, were made using nozzles of 0.9 mm. diameter (see Figure 11(a)). These gave two identical laminar flames with typical conical reaction zones and well defined luminous mantles of the type depicted in Figure 1. In this respect these burners were better suited to quantitative measurements than the slot burners described in Chapter 3, even though the peak absorption was slightly lower. They were mounted on a travelling-microscope table to allow adjustments in position and height to be made with an accuracy of at least 0.1 mm.

The burners were provided with outer jackets to supply a shielding stream of inert gas. It was found that air entrainment has a marked effect on the dimensions of the mantle surrounding the inner cone of fuel-rich flames. If secondary air was prevented from reaching the flames by shielding them with a stream of argon or nitrogen, the

F I G U R E 10.

Photograph of multiple reflection system adjusted for seven traverses. The light has been made visible by blowing smoke into the beam.

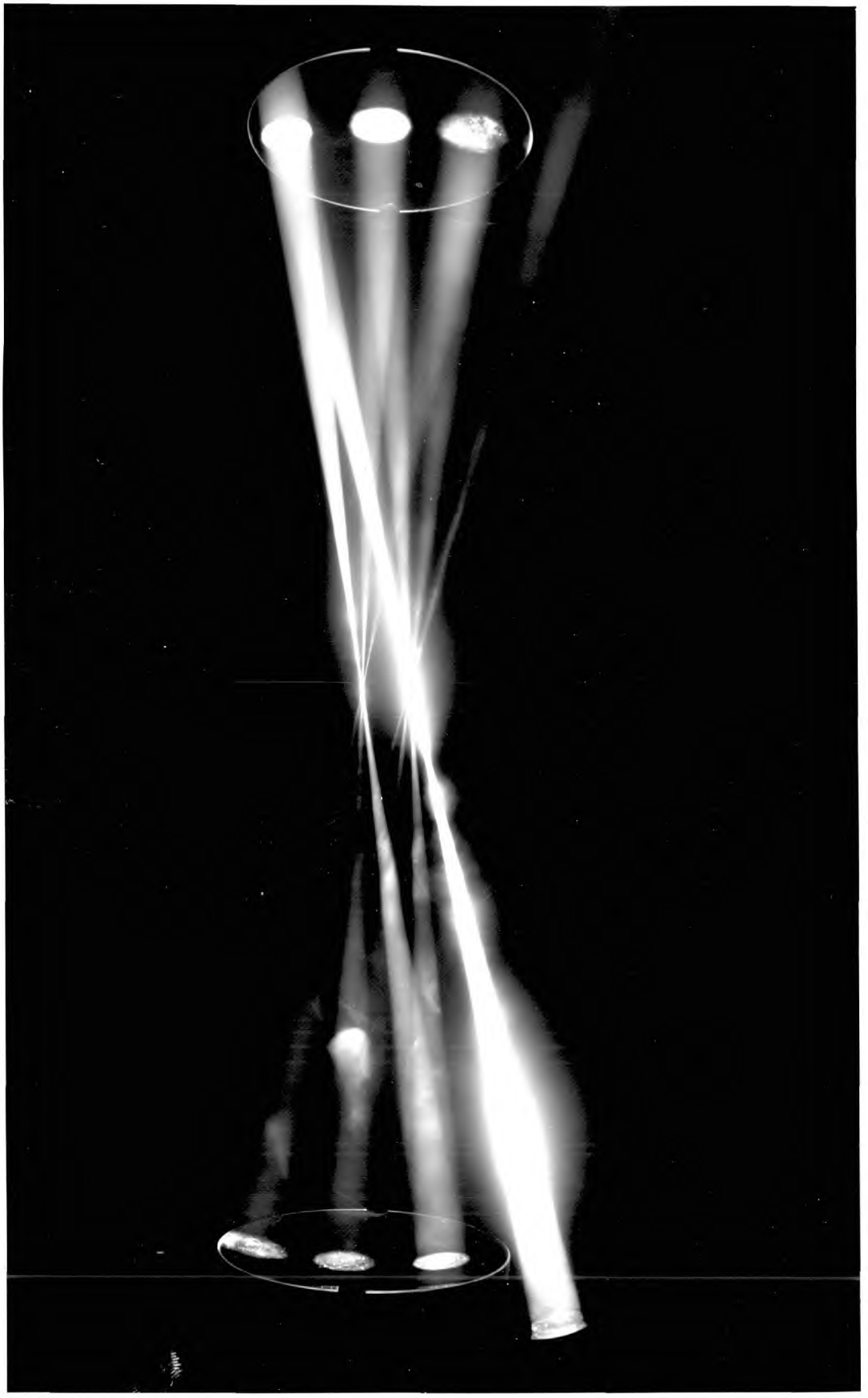

F I G U R E 11.

(a) Oxy-acetylene burner (not to scale)

(b) Schematic diagram showing relative positions of flame and neutral density wedge.

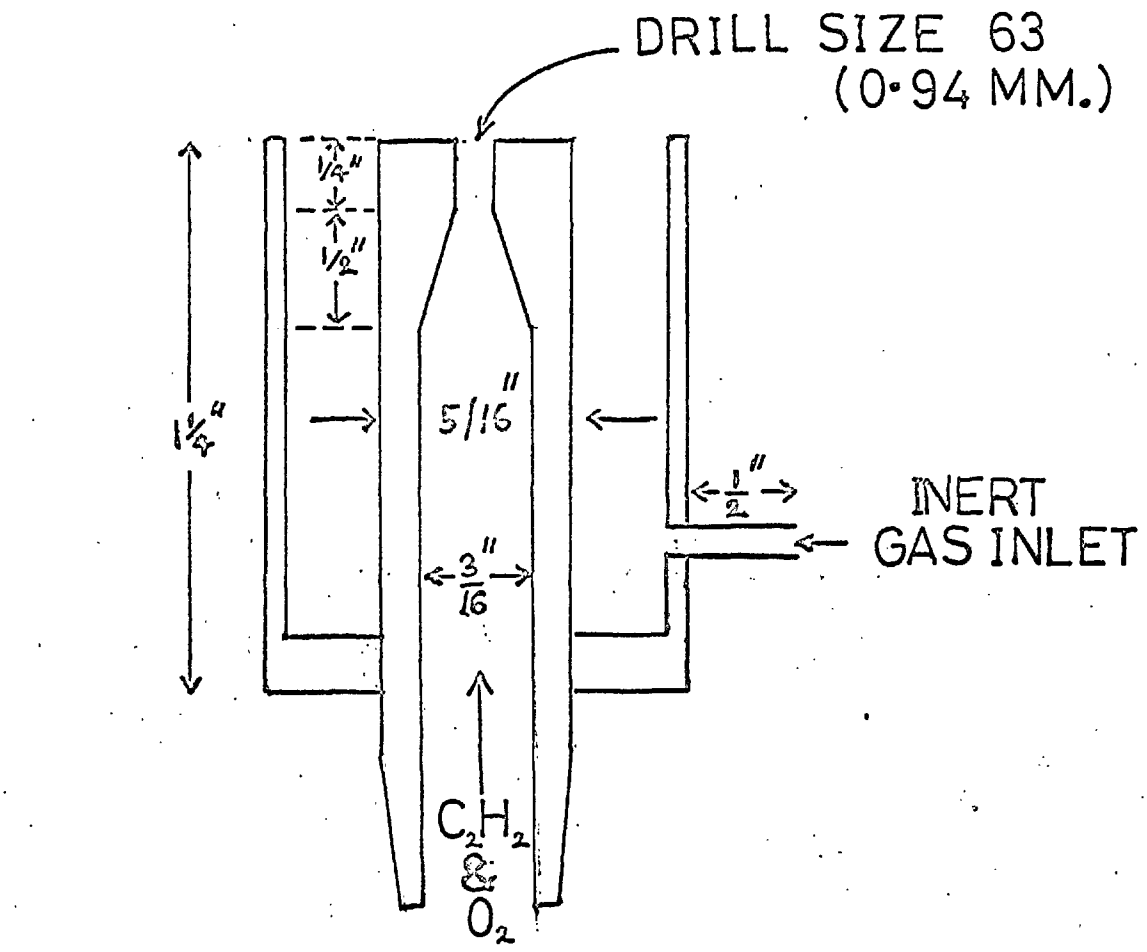
DRILL SIZE 63
(0·94 MM.)
1/4"
1/2"
1 1/4"
5/16"
1/2"
INERT
GAS INLET
3/16"
C2H2
&
O2

(a)

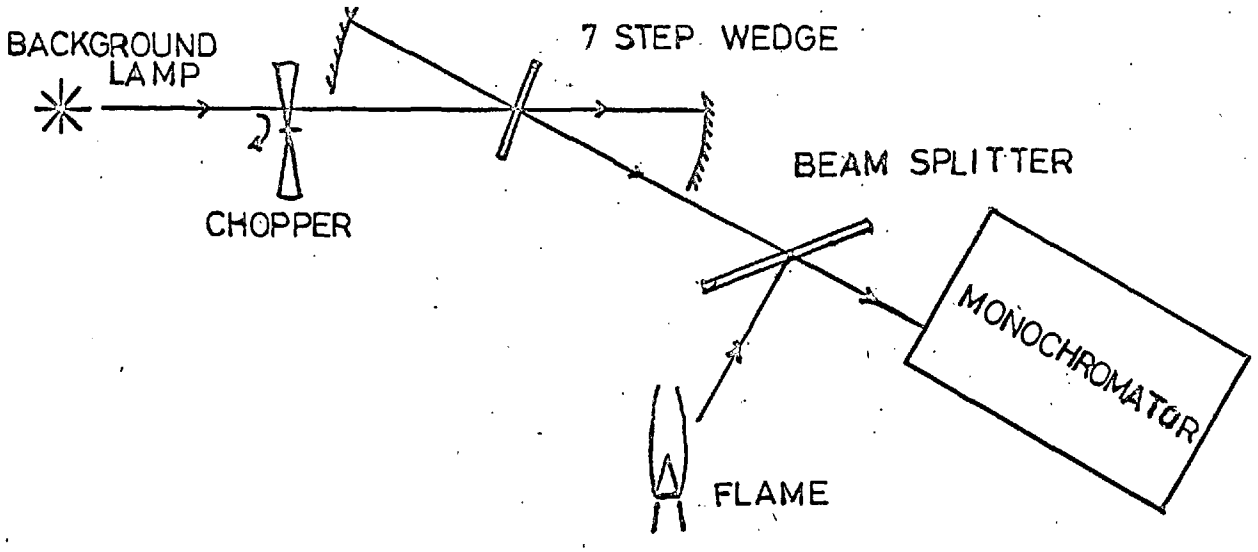
BACKGROUND
LAMP
7 STEP WEDGE
BEAM SPLITTER
CHOPPER
MONOCHROMATOR
FLAME

(b)

radical emissions extended much higher up the flame and the yellow carbon luminosity could be observed at less rich mixtures than without the shielding. The effect is illustrated in figure 15, c and d.

g) Gases and flowmeters.

Commercial grade gases were used throughout with no additional purification, except insofar as acetylene cylinders were replaced when the internal pressure dropped below 8 atmospheres. Since the acetylene is dissolved in acetone in the cylinders, the gas flowing from the cylinder contains a certain amount of acetone. As the pressure in the cylinder runs down, an increasing amount of acetone is given off which, among other things, causes a reduction in the final flame temperature. Thus a decrease in C_2 absorption was observed only if near-empty acetylene cylinders were used. Snelleman (1965) found that the acetone contamination was about 1% of the acetylene flow when the total pressure was 15 atm., increasing to about 2% for a pressure of 6 atm.

Flow rates were measured to an accuracy of $\pm$ 2% by means of calibrated Rotameter flowmeters. The flows were checked periodically with a standard gasmeter. Corrections were made for the back-pressure in the tubing leading to the burners.

4.3. Linearity of response.

A number of tests were carried out in order to check the linearity of response of the electronic detection system. Although the method chosen for the absorption measurements is, in principle, independent of the brightness temperature of the light source employed, complications may arise if the signal-to-noise ratio is very small or if one of the detection units is overloaded. An indicator lamp lit up if the phase sensitive detector was overloaded, and this would always occur before the photomultiplier saturation current was reached.

The linearity of the P.M. amplifier and P.S.D. output was checked with and without the steady flame emission contributing to the background noise. A seven-step neutral density wedge (Hilger & Watts) was positioned in the light-beam in place of the flame. The wedge was calibrated to give transmissions between 6% and 100%. Good agreement was obtained between the measured and given transmission for all signal levels up to the P.S.D. overload.

The flame itself emits light of exactly the same wavelength as it absorbs and thus contributes to the general noise level. If the flame emission intensity is much higher than the transmitted background light, the signal-to-noise ratio will be very low and spurious absorption may be

recorded. In order to investigate this, the apparatus was set up to detect the background light and spontaneous flame emission simultaneously but without actually passing the light beam through the flame. A semi-silvered glass plate was used to reflect the light from the flame onto the spectrometer slit, as shown in fig.11(b). No emission or anomalous absorption was detected even with the seven-step wedge retained in position, although the recorder trace became very noisy for the lowest transmitted intensity, (6%). This shows that the phase-sensitive detection system is a very effecient device for eliminating unwanted noise from a weak a.c. signal.

4.4. Absorption spectra.

Using 10μ slits, the background noise was about 1% of the signal at 5000 Å and, in practice, about 2% absorption could be measured. The signal-to-noise ratio decreased at lower wavelengths owing to a fall in the reflectivity of the mirrors and reduced output intensity of the Xenon lamp in the u.v. regions. About 5% absorption could be measured at 3000 Å using 30μ slits.

Figure 12 gives some indication of the improvement in the detection of the C_2 spectrum. The absorption trace is free from background noise and the intensity of absorption for individually resolved P and R branch lines can be measured

F I G U R E 12.

C_2 emission and absorption spectra in a fuel-rich oxy-acetylene flame.

Experimental details: 11 traverses; 2 mm. above the tip of the reaction zone; C/O = 1.2; 5 Å/min. scan; 10 μ slits.

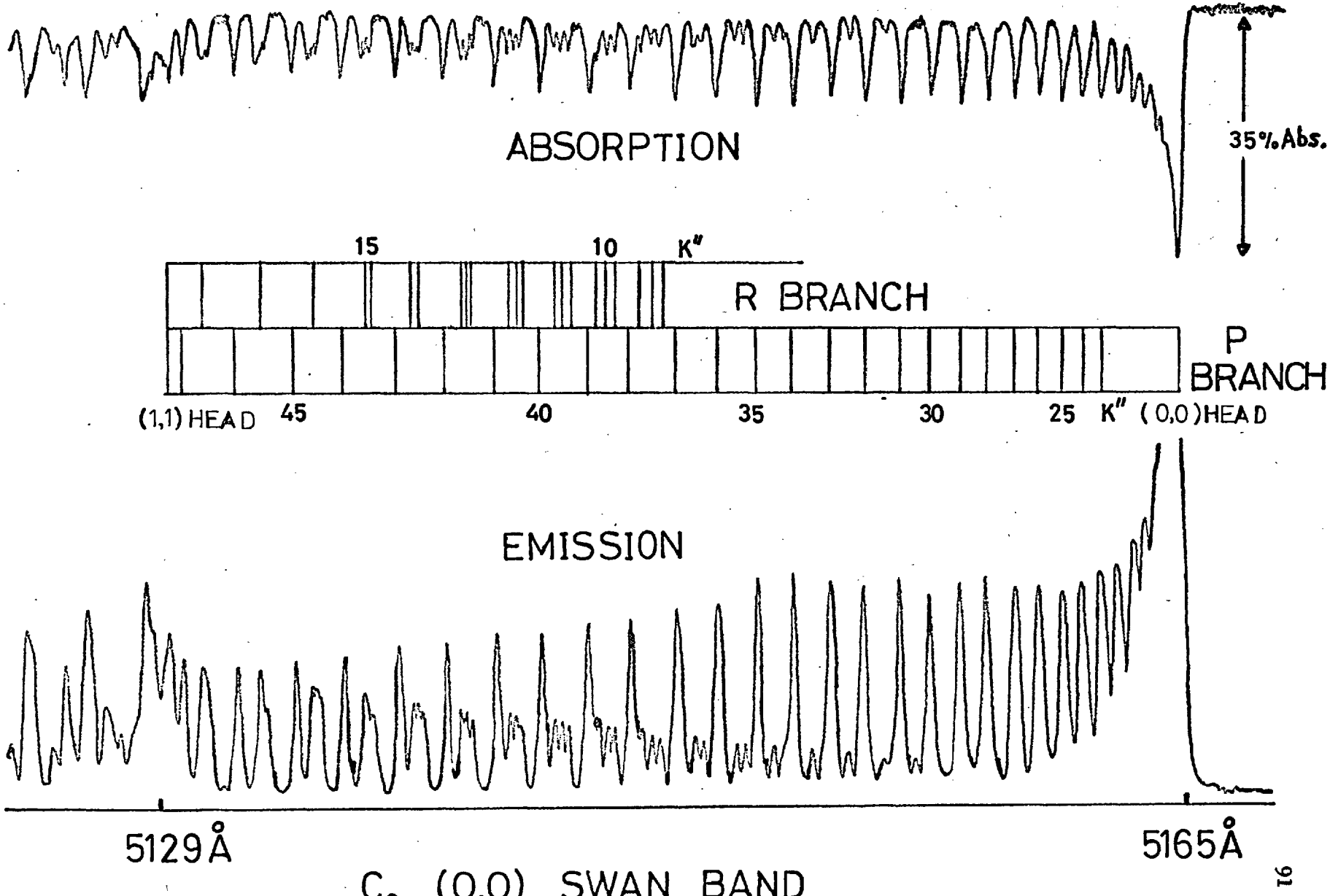

C_2 (0,0) SWAN BAND

directly. Comparison of the trace with Fig.6 illustrates the effectiveness of the photoelectric method of recording C_2 absorption compared to the photographic/flashtube method of detection.

An additional absorption spectrum was discovered that had not been obvious from the preliminary investigations. In the range 3000 - 5000 Å, a region of continuous absorption was found to be present in the mantle of rich flames. The continuum had a maximum around 3900 Å and was independent of the spectral slit-width used. Although no fine-structure was evident, there were indications of some broad band structure and a secondary smaller maximum occurred at 4300 Å. (see Figure 13).

This absorption is different from that caused by soot particles. The continuous absorption due to the presence of solid carbon particles in the flame increases uniformly with wavelength and occurs only in much richer mixtures.

It is probable that the C_3 molecule is responsible for the absorption, as an underlying emission continuum is always found accompanying the Comet-Head band in flames. The subject is discussed in greater detail in Section 5.2.

It was not possible to record absorption spectra of the 4315 Å and 3900 Å band systems of CH. The absorption

F I G U R E 13.

Absorption spectrum attributed to C_3.

11 traversals; 2 mm. above the reaction zone. The dotted lines between experimental points are extrapolated and only show the gross structure.

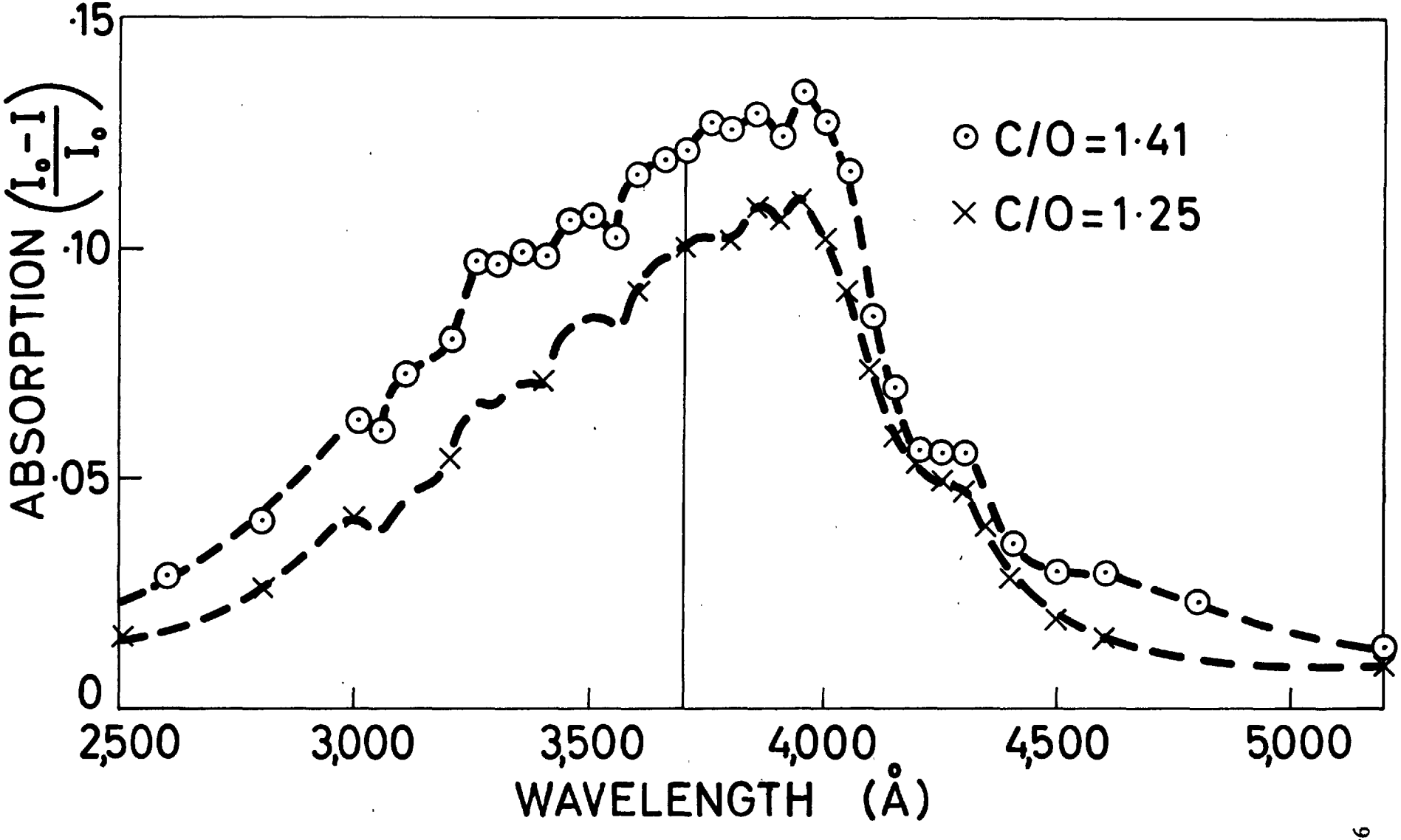
·15
·10
·05
0
ABSORPTION $\left(\frac{I_o - I}{I_o}\right)$
⊙ C/O = 1·41
× C/O = 1·25
2,500
3,000
3,500
4,000
4,500
5,000
WAVELENGTH (Å)

is always very weak and high resolution is required. Increasing the number of reflections causes a reduction in the signal-to-noise ratio. In instances where spectra are especially weak and electronic noise is high, it is likely that the photographic/flashtube method of detection offers a more effective means of separating signal from noise.

Semi-quantitative calculations of CH concentrations could be made from the 3143 Å band absorption. Here the (0,0) Q branch is piled up and the absorption was sufficiently strong to enable lower resolution to be used. An emission trace of this line-like band-head is shown in Figure 14.

No other new spectra were revealed that had not been observed previously by photographic detection. Flames of acetylene-oxygen and acetylene-nitrous oxide only were investigated.

4.5. General observations on the luminous mantle.

The onset of a mantle around the reaction zone of oxy-acetylene flames occurred for mixtures richer than $(C/O)_{unburnt} = 0.95$, and was independent of air entrainment into the flame. The yellow carbon luminosity became first noticeable for mixtures richer than $C/O \simeq 1.1$ in shielded flames, or $C/O \simeq 1.5$ in unprotected flames. In general the carbon luminosity was fairly uniformly distributed around the inner cone although yellow carbon streaks would sometimes

F I G U R E 14.

Emission spectrum of the piled-up Q branch in the 3143 Å band system of CH.

Reaction zone of an oxy-acetylene flame.
10 μ slits, 2 Å/min. scan.

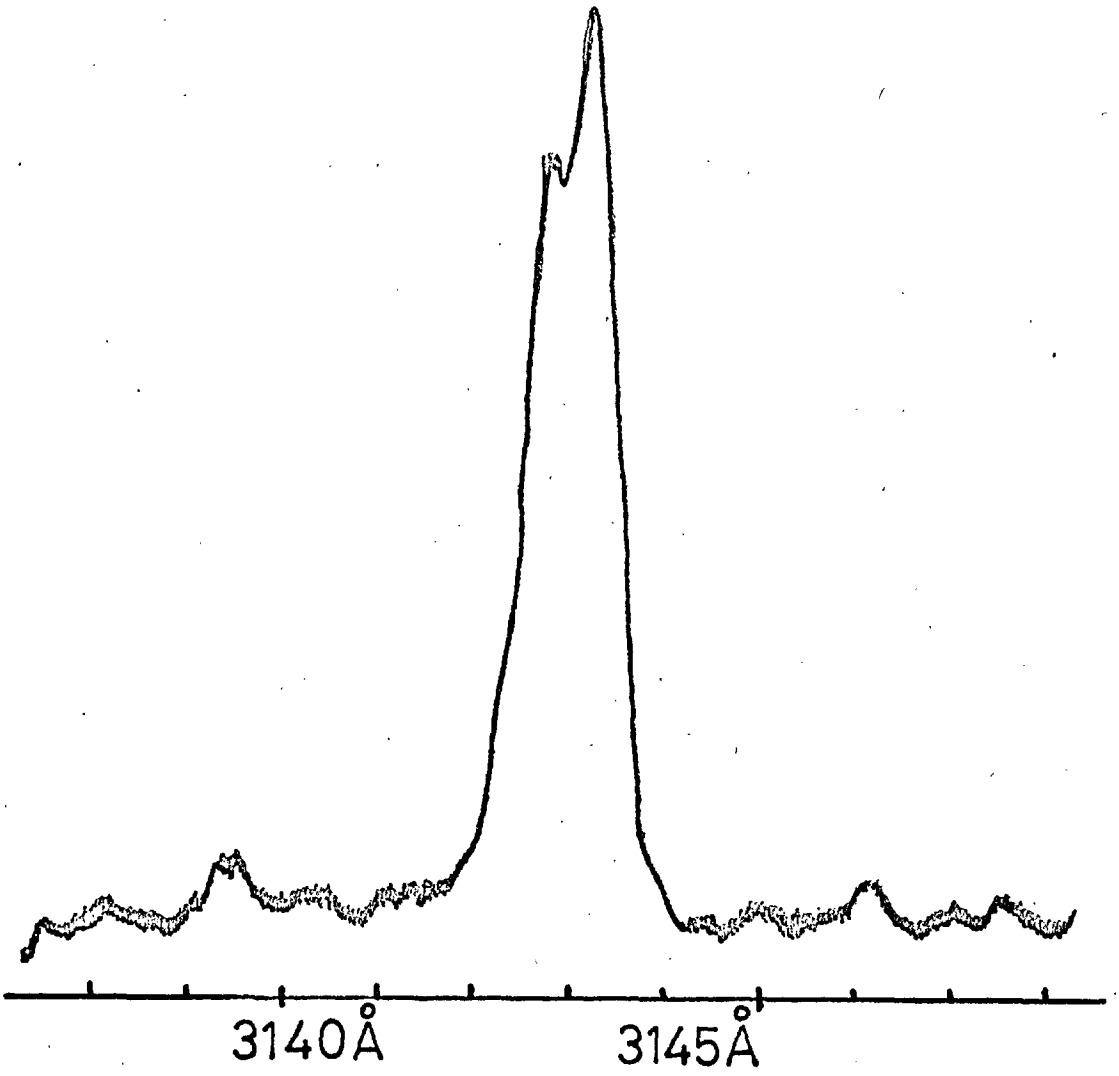

The piled-up Q branch of the $C^2\Sigma^+ - X^2\Pi$ transition of CH.

originate from points around the base of the inner cone (see Figure 15(d)). This was attributed to quenching effects due to the cold burner rim and has been discussed by Bonne et al. (1965). For less rich mixtures, between C/O = 0.95 and 1.1 (shielded flames) the mantle was whitish-grey in colour, emitting radiation mainly from C_2, C_3, and CH, although some continuous emission was also observed throughout the visible region.

For the purpose of calculating concentrations from the absorption data, it is necessary to know the effective path-length, L, of the probing light-beam through the luminous mantle. To this end, photographic measurements were made to determine the thickness of the mantle as a function of mixture strength and height above the burner top. Typical photographs are shown in Figure 15. The accuracy of the measurements was assessed by investigating the effect of exposure times on the apparent mantle thickness. For a single traversal, L was typically 3-4 mm. just above the tip of the reaction zone and the error in measurement was about $\pm$ 0.1 mm. At a mixture strength close to C/O = 1.0. the mantle was barely visible and less well defined, changing rapidly with slight variations in mixture strength; the error was thus higher (up to 0.5 mm.).

The remainder of this thesis is concerned with the

F I G U R E 15.

Photographs of fuel-rich C_2H_2 - O_2 flames showing luminous mantle.

a) C/O = 0.97, mantle just appearing.

b) C/O = 1.12, very light exposure to show reaction zone.

c) C/O = 1.12, normal exposure to show mantle.

d) C/O = 1.12, normal exposure, argon shielding.

Note the streak of carbon rising up the left of the flame.

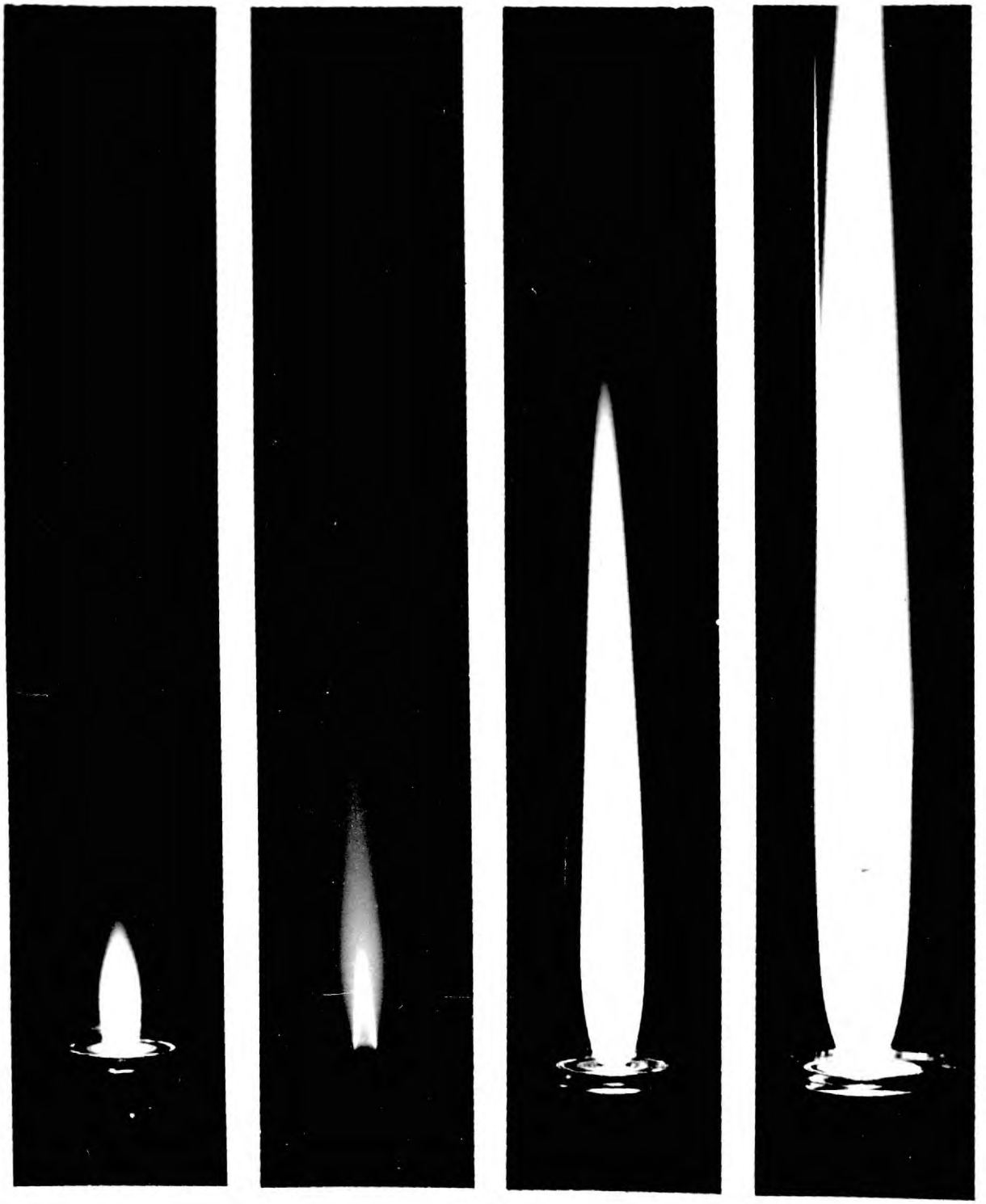
a
b
c
d

quantitative interpretation of the carbon radical spectra (Chapter 5) and a discussion of their relevance to the mechanism of soot formation in oxy-acetylene flames (Chapter 6).

CHAPTER 5.

DETERMINATION OF EFFECTIVE TEMPERATURES AND CONCENTRATIONS FROM C_2, C_3 AND CH SPECTRAL DATA.

I_t was shown in Chapter 2 that the concentration of absorbing molecules in specific rotational states can be calculated from the measured absorption in individual rotational lines. The total concentration can be derived from a knowledge of the population temperatures of the molecules over all possible rotational, vibrational and electronic energy states. This has been done for the C_2 radical where absorption could be measured in individual P and R branch lines of the (0,0) Swan band. The resolution of the spectrometer was insufficient to resolve the triplet structure of lines with K" values greater than about 20, and in the following analysis the spin splitting has been ignored. Justification for this and details of the approximations involved are given in Appendix 1.

5.1. C_2 temperature measurements.

Effective rotational and vibrational temperatures in both upper and lower electronic states were derived from emission and absorption measurements of the C_2 Swan bands, as follows:

a) Rotational temperatures.

The emission intensity, I_{em}, is related to the rotational temperature in the upper electronic state, $T_{R'}$, by the relation

$$I_{em} \propto S_{K'K''} \nu^4 \exp(-E_{K'}/kT_{R'}) \qquad (5.1)$$

where $S_{K'K''}$ is the line strength, ν the wavenumber of the transition, $E_{K'}$ the energy of the rotational level from which the transition originates, and k the Boltzmann constant.

A plot of $\ln (I_{em}/S_{K'K''} \nu^4)$ against $E_{K'}$ for various lines in the P branch or R branch of a band should give a straight line, the slope of which yields a value for $T_{R'}$.

A similar relationship holds for the absorption intensity and the lower rotational temperature, $T_{R''}$. It can be written as

$$[(I_o - I)/I_o]_{peak} \propto S_{K'K''} \nu \exp(-E_{K''}/kT_{R''}) \qquad (5.2)$$

where $[(I_o-I)/I_o]_{peak}$ is the peak fractional absorption, as defined in equation (2.7) and the other symbols have the same meaning as above except that the doubly primed letters refer to the lower electronic state of the transition.

$T_{R''}$ can be determined from the slope of the graph of $\ln [(I_o-I)/I_o \; S_{K'K''} \nu]_{peak}$ against $E_{K''}$.

Deviations from linearity can occur if there is appreciable self-absorption, but the concentration of C_2 molecules is too low for this effect to be important in flames. Implicit in the above equations is the assumption that local thermal equilibrium (L.T.E.) holds so that the Boltzmann distribution law is valid and can be characterised by the temperature parameter T.

The rotational structure of the (0,0) Swan band was analysed with the aid of the results of Callomon and Gilby (1963) and Johnson (1927). E_K values were given approximately by $B_oK(K + 1)$, where B_o is the rotational constant of the vibrational ground level. The dependence of eqs. (5.1) and (5.2) on ν^4 and ν, respectively, was neglected. The errors introduced by these approximations are negligible over the short wavelength interval covered in this work. Spectroscopic constants were taken from Ballick and Ramsay (1962). Line strengths for the transitions under consideration were derived from formulae given by Budo (1937) and were computed as described in Appendix 1.

Some lines are unsuitable for temperature measurements because they are perturbed or blended with neighbouring lines. Using a resolving power of 0.2 Å, only the P branch lines between K" = 25 and 32 and between K" = 40 and 46 were considered to be sufficiently free from

overlapping. Lines P(48) and R(46) appeared to be missing. However, closer examination under high resolution reveals that the expected triplets are replaced by six lines of equal intensity in two groups of 3 arranged symmetrically about the unperturbed position. (Calloman & Gilby, 1963). The perturbation arises through interaction with the $A^3\Pi_g$ state whose vibrational level, v = 11, coincides with the rotational level, K = 47, in the upper $A^3\Pi_g$ state. Another perturbation occurs in the (0,0) Swan band affecting the R(50) and P(52) lines. In this case, only one member of the triplet is affected. These perturbations appear to be localised and are easily recognisable. It is not thought that the line strengths of the other rotational lines are significantly altered and no experimental evidence for this was found.

Semi-logarithmic plots of the fractional peak absorption and emission intensity, divided by the line strength versus K(K+1), are given in Figures 16 - 19 for typical emission and absorption spectra from both the reaction zone and luminous mantle. The data used is set out in tables A.1 to A.6 and presented in Appendix 2.

The graphs gave reasonable straight lines and there were no indications to suggest a breakdown of L.T.E. For emission, the results were consistent with those of previous workers (Gaydon, 1957; Marr, 1957). In the

DETERMINATION OF ROTATIONAL TEMPERATURES OF C_2 IN THE REACTION ZONE AND LUMINOUS MANTLE OF OXY-ACETYLENE FLAMES.

$T_{R'}$ = effective rotational temperature in the upper $A^3\Pi_g$ state.

$T_{R''}$ = effective rotational temperature in the lower $X^3\Pi_u$ state.

FIGURE 16. Luminous mantle, $T_{R'} = 3350^\circ K$.

FIGURE 17. Reaction Zone, $T_{R'} = 5000^\circ K$, $5150^\circ K$.

FIGURE 18. Reaction Zone, $T_{R''} = 4800^\circ K$.

FIGURE 19. Luminous mantle, $T_{R''} = 3550^\circ K$.

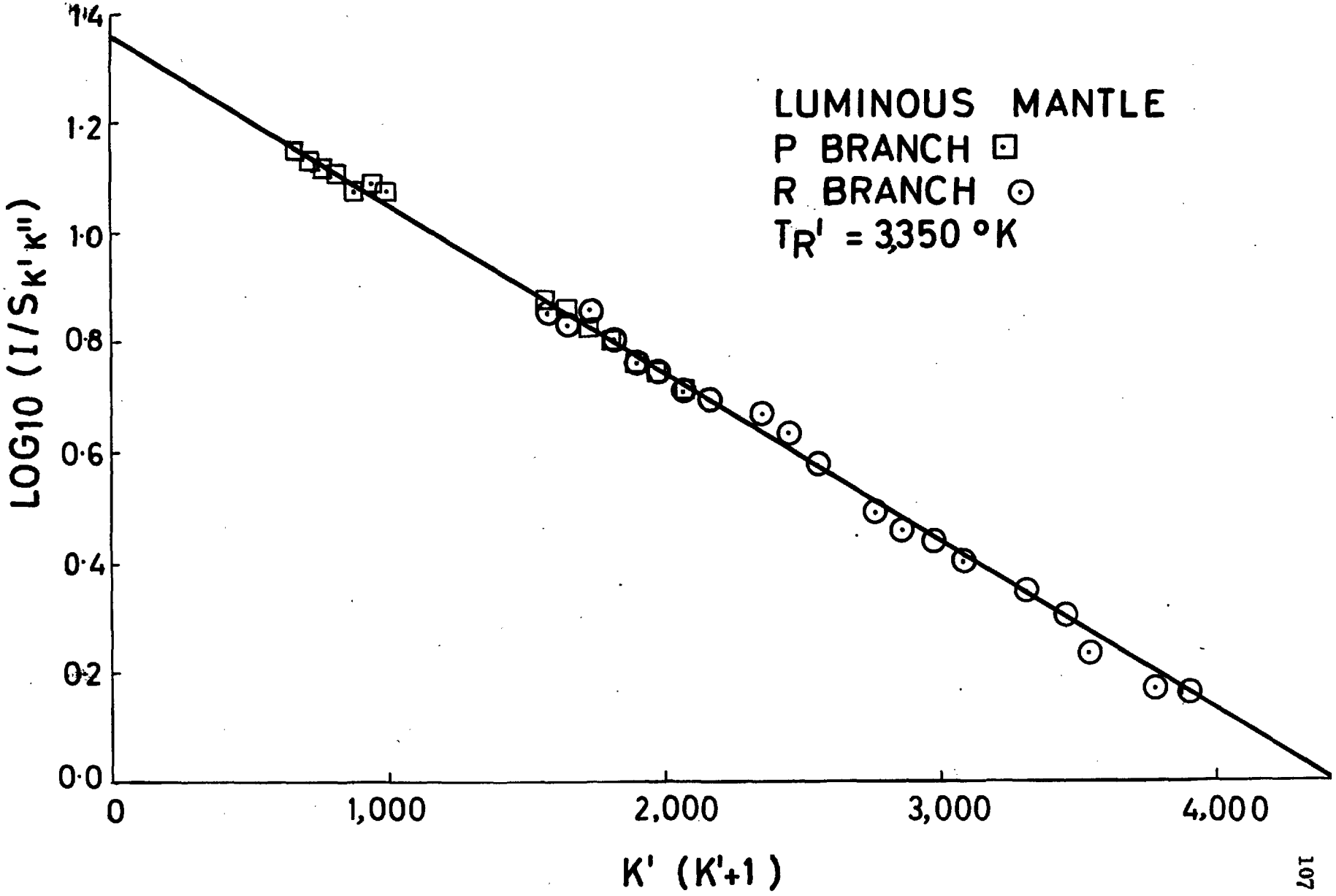
LUMINOUS MANTLE
P BRANCH ⊡
R BRANCH ⊙
$T_{R'}$ = 3,350 °K
LOG10 (I/$S_{K'K''}$)
1·4
1·2
1·0
0·8
0·6
0·4
0·2
0·0
0
1,000
2,000
3,000
4,000
K' (K'+1)

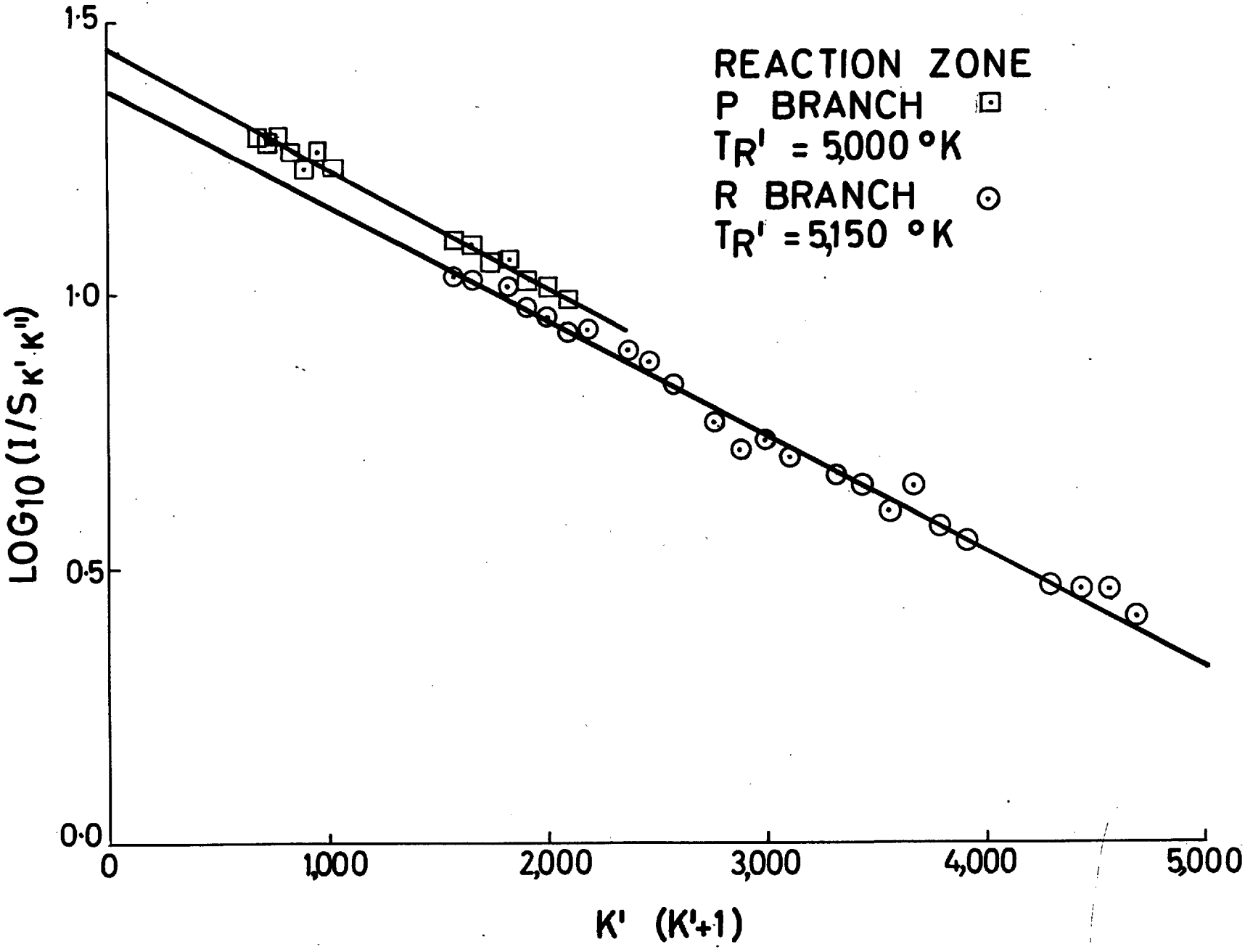
REACTION ZONE
P BRANCH
$T_{R'}$ = 5,000 °K
R BRANCH
$T_{R'}$ = 5,150 °K
LOG10 (I/S K' K'')
1·5
1·0
0·5
0·0
0
1,000
2,000
3,000
4,000
5,000
K' (K'+1)

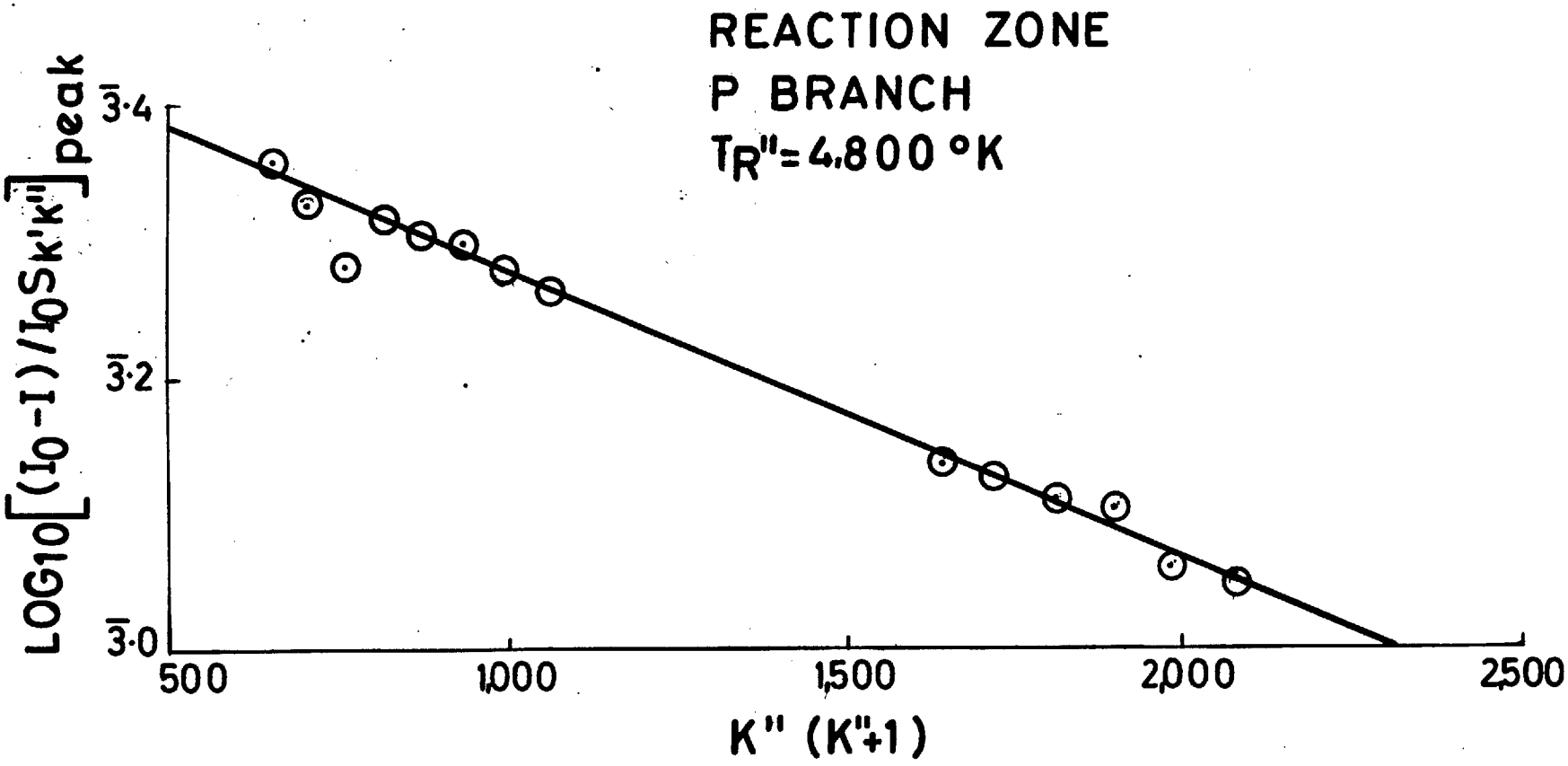
REACTION ZONE
P BRANCH
$T_R'' = 4,800\ °K$
$LOG_{10}[(I_0 - I)/I_0 S_{k'k''}]_{peak}$
$\bar{3}.4$
$\bar{3}.2$
$\bar{3}.0$
500
1,000
1,500
2,000
2,500
K'' (K''+1)

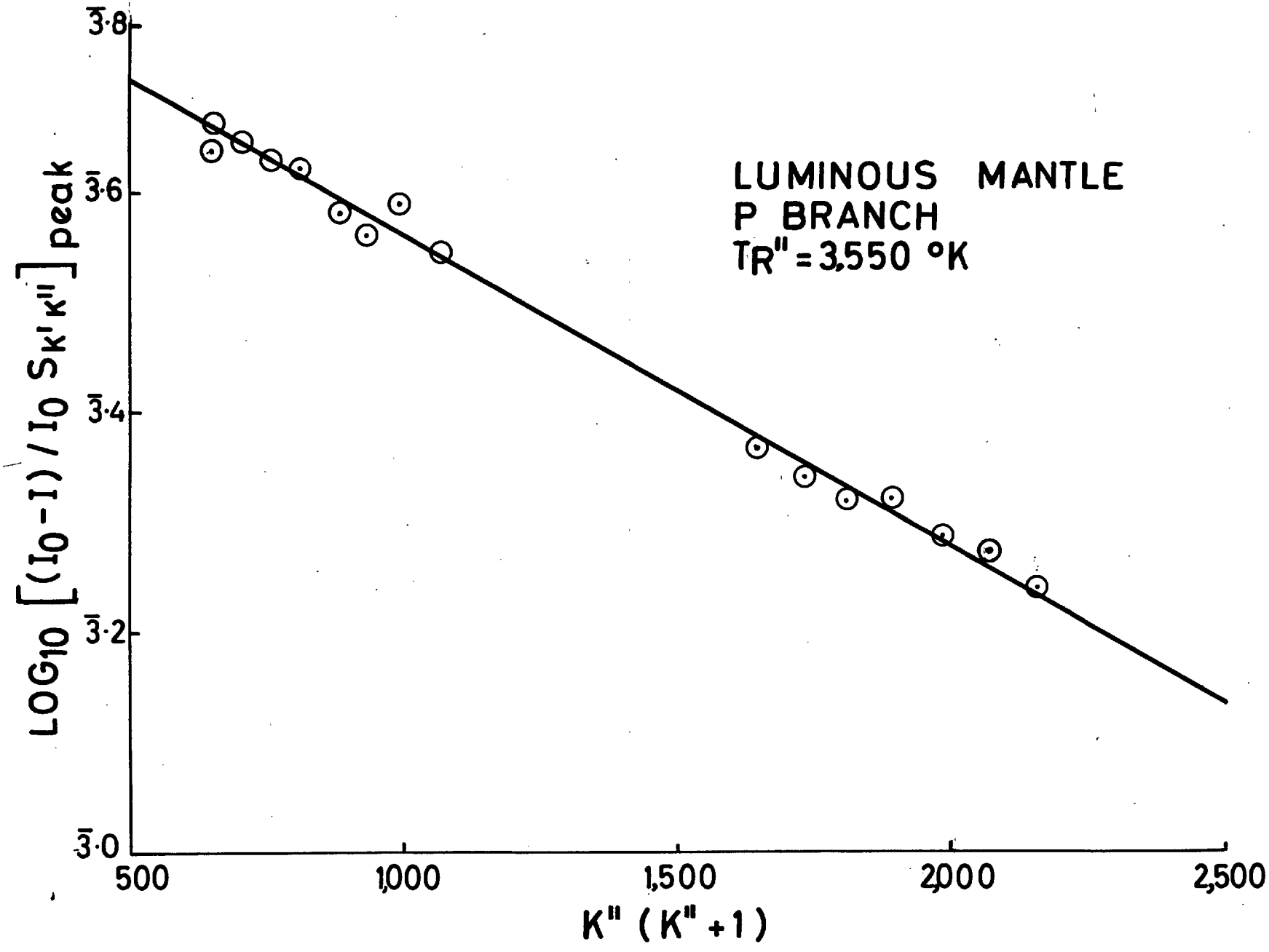
LUMINOUS MANTLE
P BRANCH
TR" = 3,550 °K
LOG10 [(I0 - I) / I0 SK'K"] peak
3̄·8
3̄·6
3̄·4
3̄·2
3̄·0
500
1,000
1,500
2,000
2,500
K" (K" + 1)

luminous mantle above the reaction zone, an average value of $T_{R'} = 3300 \pm 200^{o}K$ was obtained, which compares favourably with the calculated equilibrium temperature (see Chapter 6). The temperature in the reaction zone was much higher; a mean value of $T_{R'} = 5000 \pm 250^{o}K$ was derived from P and R branch measurements.

Absorption measurements showed a similar high rotational temperature in the reaction zone for the $X^{3}\Pi_{u}$ state of C_2.

The majority of the results were in the range $T_{R''} = 4500 \pm 500^{o}K$. Values of $T_{R''}$ in the mantle were lower, being in the range 3000 - 3600°K with more results at the upper end of the range than at the lower. The random error, as determined from the maximum and minimum slopes that could be drawn through the experimental points, was estimated to be $\pm 300^{o}K$. A possible systematic error arises in the absorption measurements concerning the position of the base line of the recorder trace corresponding to zero absorption (I_o). This may tend to give an overestimate for the rotational temperature, and would explain why the experimental results could well be 200 - 300°K higher than the adiabatic flame temperature. However, in view of the magnitude of the errors involved, no definite conclusions could be drawn regarding departures from thermal equilibrium.

The results were not sufficiently accurate to show whether there was a variation of the rotational temperature with mixture strength or distance above the burner; calculations of equilibrium temperatures (see section 6.1) predict a fall of about 200°K for C:O ratios in the range 1.0 - 2.0.

b) Vibrational temperatures.

Emission and absorption spectra of the 1-0 sequence around 4700 Å were used to estimate the vibrational excitation in $A^3\Pi_g$ and $X^3\Pi_u$ states of C_2. A typical emission spectrum is shown in Figure 20. Effective vibrational temperatures were derived from the relations:

$$I_{em} \propto A_{v'v''} \nu^4 \exp(-E_{v'}/kT_{v'}) \qquad (5.3)$$

$$[(I_o - I)/I_o]_{head} \propto A_{v'v''} \nu \exp(-E_{v''}/kT_{v''}) \qquad (5.4)$$

where $A_{v'v''}$ is the Franck-Condon factor of the vibrational transition $v' - v''$, E_v and T_v are the vibrational energy and temperature, respectively, and the other symbols have the same meaning as before.

The evaluation of vibrational temperatures from equations (5.3) and (5.4) is much less accurate than the corresponding determination of rotational temperatures. Whereas rotational transition probabilities or line

F I G U R E 20.

Low resolution scan of the 1-0 sequence of C_2 Swan bands.

Emission from luminous mantle of oxy-acetylene flame. 25 μ slits, 10Å/min. scan.

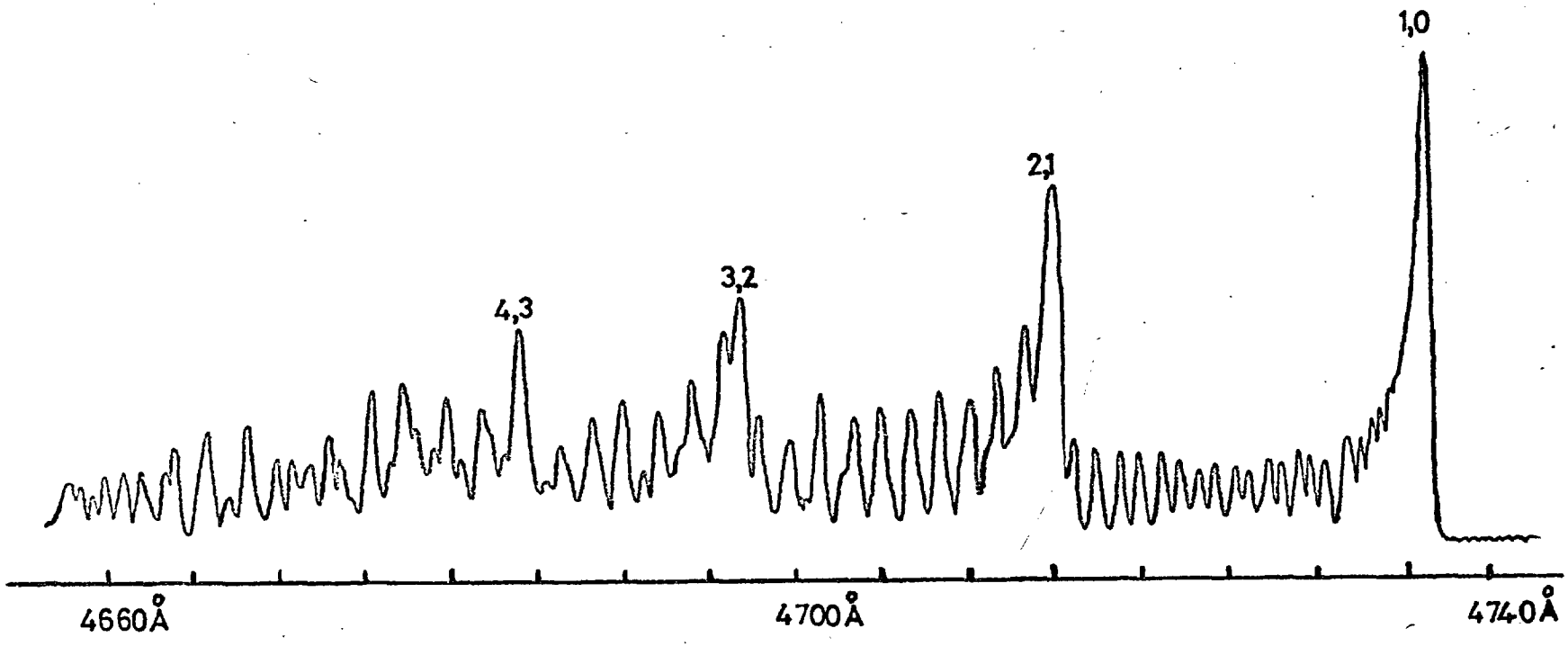

1,0 SEQUENCE OF C_2 SWAN BANDS

strengths can be calculated without difficulty from known constants, vibrational transition probabilities can only be evaluated by integration of vibrational wavefunctions. It is necessary to make approximations in the correction of these from parabolic to actual potential-energy curves and there is usually some lack of knowledge of the variation of the dipole moment of the molecule with internuclear distance. However, Franck-Condon factors are now available for many diatomic molecules, and these are proportional to the vibrational transition probabilities if the electronic transition moment does not vary appreciably with vibrational quantum number, v (Nicholls et al, 1957). The $A_{v'v''}$ values used in this chapter were taken from the calculations of Jain (1964).

Some approximation is also involved in taking the band-head peak intensities to represent the true relative band intensities. Rotational structure complicates the intensity distribution of each band and makes measurement of overall intensity difficult. The intensity distribution varies from band to band within the system and also with the effective rotational temperature. The shape of a band head is mainly determined by the quantity $|B_{v'} - B_{v''}|$ and will vary for different $v' - v''$ combinations since the rotational constant B_v depends on v. For the 1-0 sequence of C_2 (Swan), this variation is small

and a low-resolution scan of the (1,0), (2,1), (3,2), and (4,3) heads may be expected to provide a fair representation of the overall band intensities.

Semi-logarithmic plots of $I_{em}/A_{v'v''}$ and $[(I_o - I)/I_o A_{v'v''}]_{head}$ against vibrational energy are presented in Figures 21-23. The experimental data from which the vibrational temperatures were derived is given in Appendix 2. Also included on the graphs are similar straight-line plots, using experimentally determined relative transition probabilities (designated $A'_{v'v''}$) in place of the calculated Franck-Condon factors. They were taken from the work of King (1948). He derived the $A'_{v'v''}$ values from relative intensity measurements of bandheads appearing in carbon-furnace emission spectra under conditions of thermodynamic equilibrium. Temperatures were of the order of 3000°K and the spectral resolution appears to have been similar to that employed here.

The use of these experimental transition probabilities might, therefore, be expected to yield better straight-line plots than the calculated Franck-Condon factors, and this was generally found to be the case. In particular, the $A_{v'v''}$ value for the (4,3) band showed the greatest discrepancy between Jain's calculations and King's result.

DETERMINATION OF VIBRATIONAL TEMPERATURES OF C_2 IN THE REACTION ZONE AND LUMINOUS MANTLE OF OXY-ACETYLENE FLAMES.

FIGURE 21. Luminous mantle, $T_{v''}$ = 3300°K, 3400°K.

FIGURE 22. Luminous mantle, $T_{v'}$ = 3600°K 3800°K

FIGURE 23. Reaction zone, $T_{v'}$ = 6500°K 7800°K.

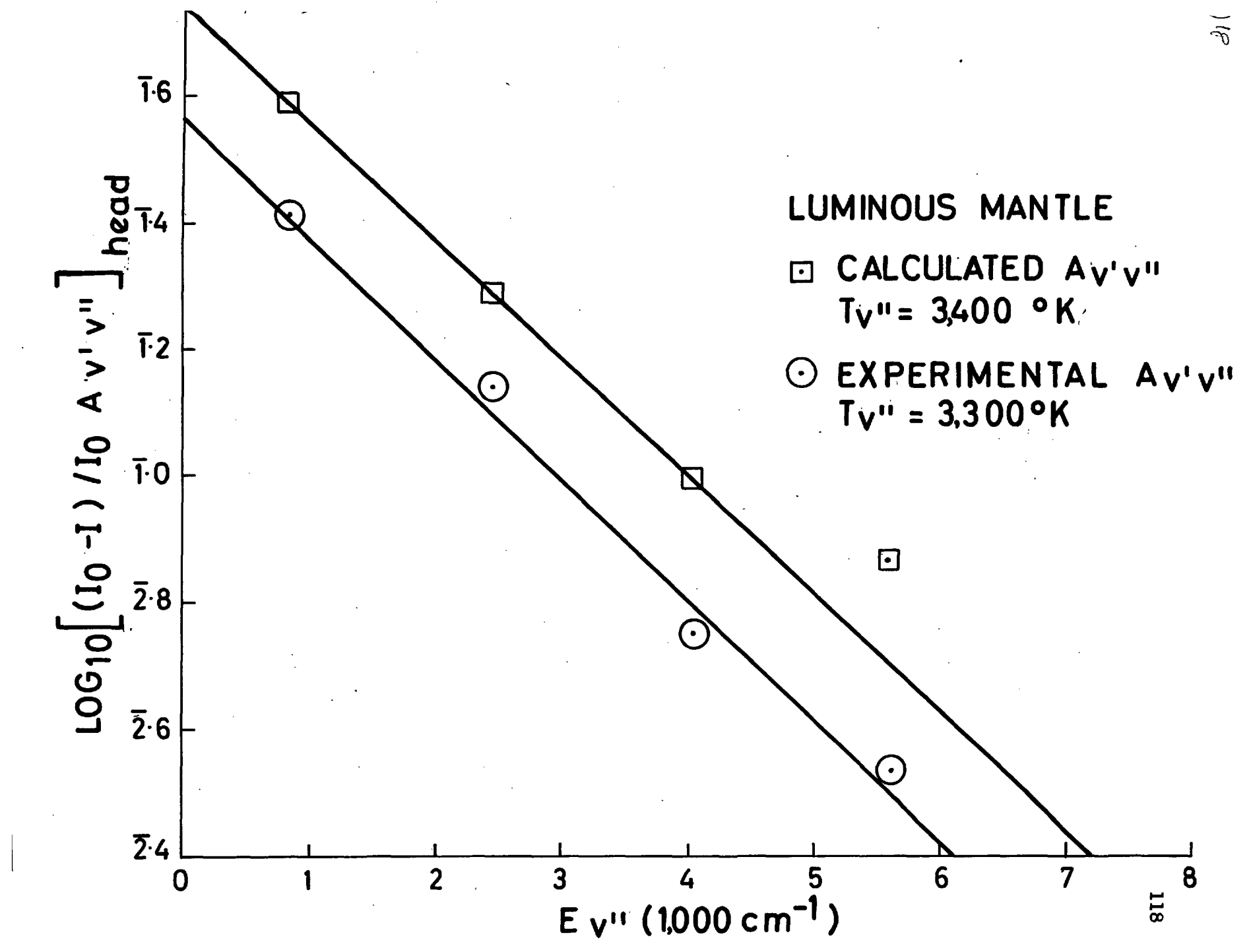
LUMINOUS MANTLE
CALCULATED Av'v''
Tv'' = 3,400 °K
EXPERIMENTAL Av'v''
Tv'' = 3,300°K
LOG10[(I0 -I) /I0 Av'v'']head
Ī·6
Ī·4
Ī·2
Ī·0
2̄·8
2̄·6
2̄·4
0
1
2
3
4
5
6
7
8
E v'' (1,000 cm-1)

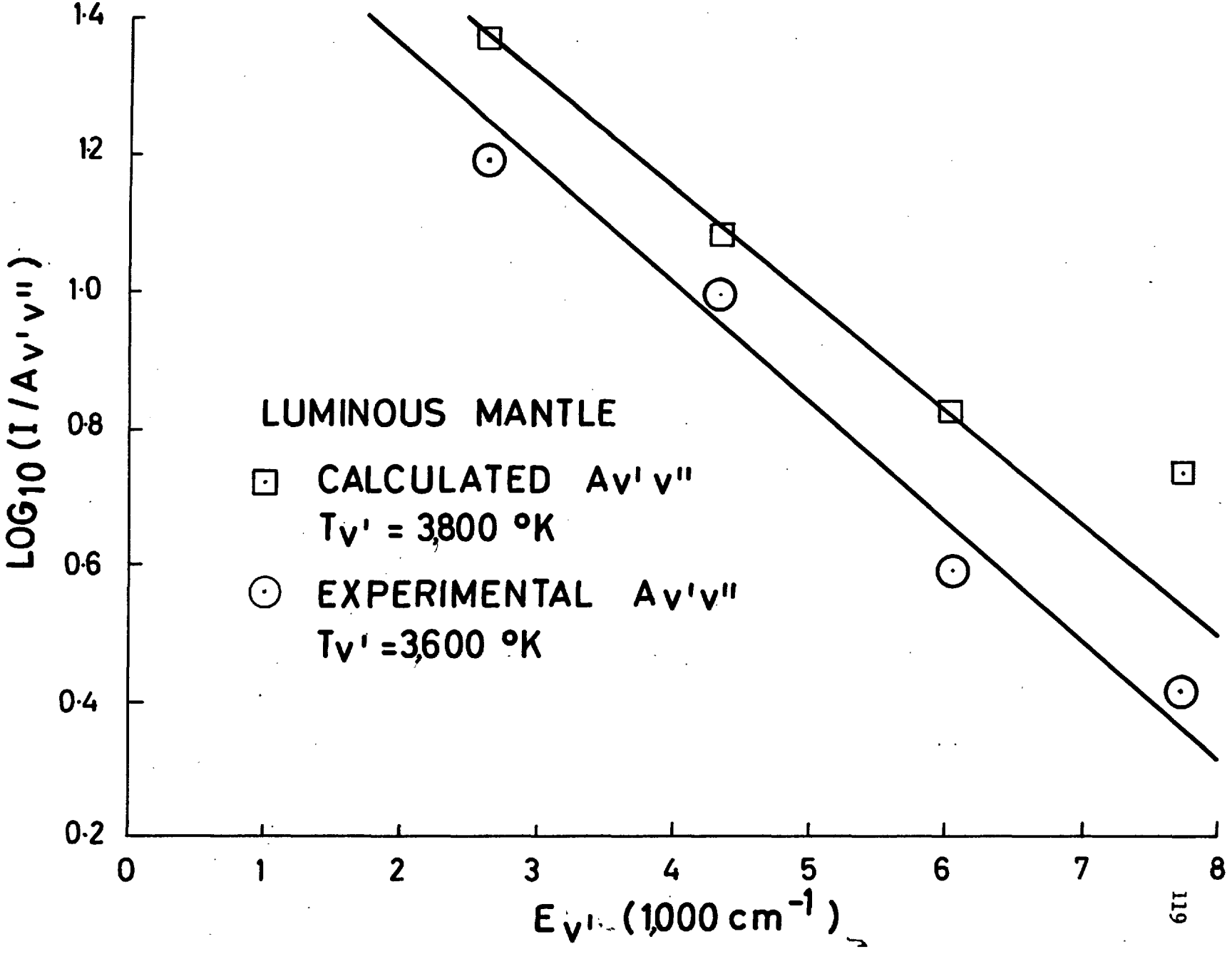
1·4
1·2
1·0
0·8
0·6
0·4
0·2
LOG10 (I / Av'v'')
LUMINOUS MANTLE
CALCULATED Av'v''
Tv' = 3,800 °K
EXPERIMENTAL Av'v''
Tv' = 3,600 °K
0
1
2
3
4
5
6
7
8
Ev' (1,000 cm-1)

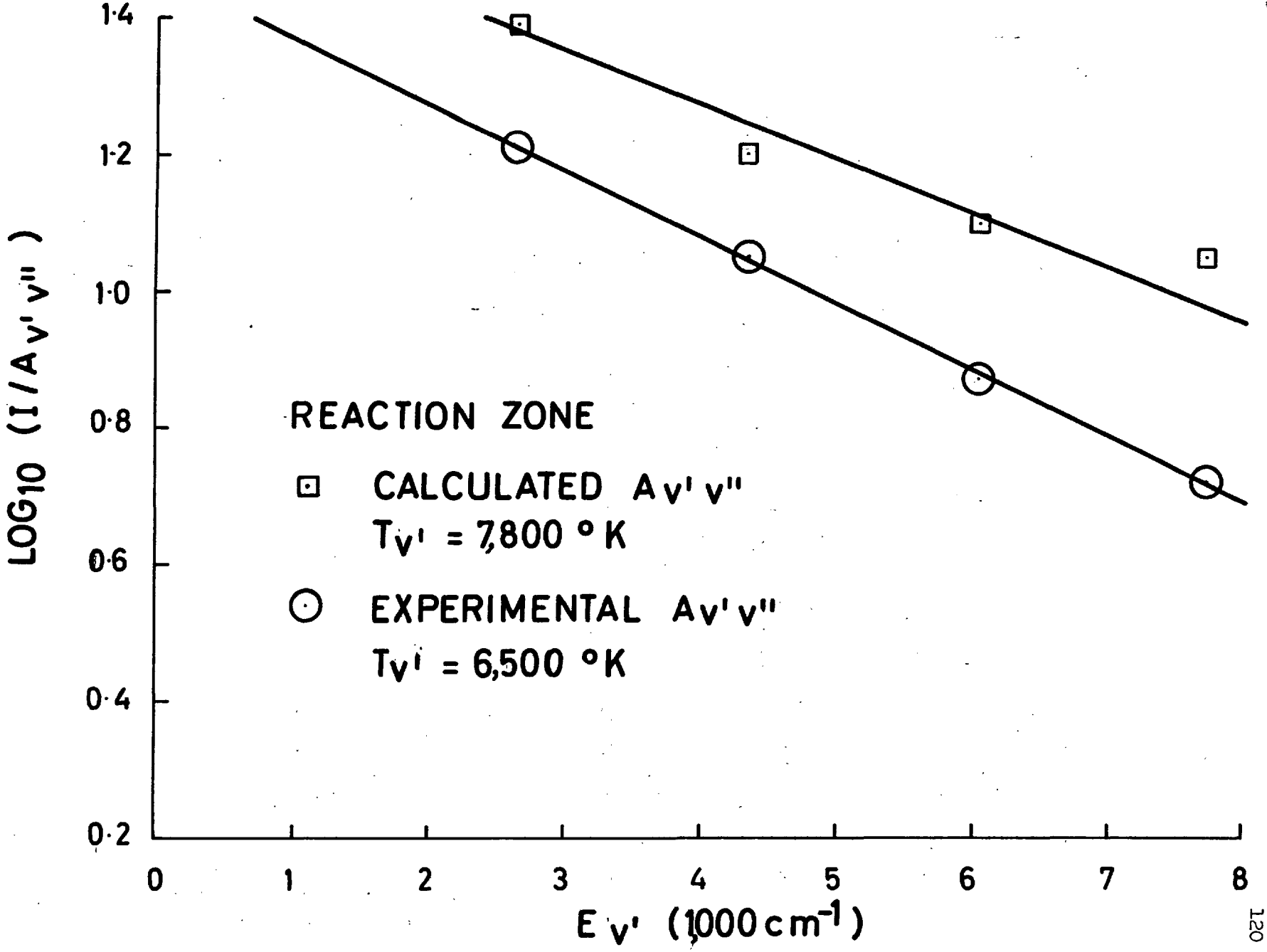
1·4
1·2
1·0
0·8
0·6
0·4
0·2
LOG10 (I / Av' v'')
REACTION ZONE
CALCULATED Av' v''
Tv' = 7,800 °K
EXPERIMENTAL Av' v''
Tv' = 6,500 °K
0
1
2
3
4
5
6
7
8
E v' (1000 cm-1)

The calculated transition probabilities gave slightly higher vibrational temperatures than those obtained by using King's values. For the luminous mantle, the temperature in the $X^3\Pi_u$ state was estimated to be 3400°K and 3300°K respectively, and the upper state vibrational temperatures, $T_{v''}$, were 3800°K and 3600°K. Temperatures in the reaction zone were much higher; values of $T_{v'}$ were in the range 6000 - 8000°K and a high value for $T_{v''}$ was also indicated, although the weakness of the absorption prevented quantitative measurements being made.

Marr (1957) obtained a temperature of $T_{v'}$ = 3900°K from emission measurements in the mantle of oxy-acetylene flames. He suggested that self-absorption might at least partly account for the apparent thermal disequilibrium in the mantle but the present absorption measurements indicate that the corrections are small.

5.2. Concentration measurements.

a) C_2 concentration.

The total concentration of C_2 molecules in the $X^3\Pi_u$ state was determined with the aid of the relationships introduced in Chapter 2. The concentration of molecules in the K"th rotational level of the (0,0) band is given by equation (2.12)

$$N_{K''} = \frac{mc^2}{\pi e^2} \frac{S}{L} \left[\frac{I_o - I}{I_o}\right]_{peak} \frac{2K''+1}{S_{K'K''}} \frac{1}{f_{oo}} \qquad (5.5)$$

where $[(I_o - I)/I_o]_{peak}$ = peak fractional absorption in the K"th line

$S_{K''K'} \simeq K''$; P branch

$\simeq K''+1$; R branch

and f_{oo} = oscillator strength of the (0,0) band of C_2 $(X^3\Pi_u \rightarrow A^3\Pi_g)$

There is some uncertainty in the literature as to the actual value of f_{oo}. Shock-tube methods (Fairbairn, 1966; Sviridov et al., 1966; Harrington et al., 1966) give a value in the region of 0.02 - 0.03, while measurements of C_2 emission from carbon-tube furnaces (see discussion by Porter et al., 1967) favour a lower value, ca. 0.005. An intermediate value, 0.016, was taken for this work, as given by Fink and Welge (1967) from lifetime measurements of C_2 $(A^3\Pi_g)$ by the phase-shift method.

The fractional absorption in the line P(31) was measured as a function of mixture strength and height above the reaction zone for fuel-rich acetylene-oxygen flames. An average peak fractional absorption of 4.1 x 10^{-2} per cm. of mantle was found in flames having C/O = 1.18, at a distance 2 mm. above the tip of the reaction zone. Substituting the following values in equation (5.5)

$mc^2/\pi e^2 = 1.13 \times 10^{12}$ cm.; $2K''+1 = 63$; $S_{K''} = 31$; $f_{oo} = 0.016$; $S = 0.72$ cm^{-1}; and $[(I_o-I)/I_oL]_{peak} = 4.1 \times 10^{-2}$ cm^{-1}, we get

$$N_{K''=31} = 4.24 \times 10^{12} \text{ cm}^{-3}.$$

The concentration of molecules in the $v'' = 0$ lower state was calculated by using equation (2.5). The rotational partition function, Q_{rot}, reduces to kT_R/B_v if $kT_R > B_v$, a condition which is satisfied for all cases considered here. Thus, substituting $B_o = 1.624$ cm^{-1}; $E_{K''} = 1610$ cm^{-1}; and $T_{R''} \simeq 3300^oK$ (section 5.1), we obtain

$$N(X^3\Pi_u, v'' = 0) = 1.92 \times 10^{14} \text{ cm}^{-3}.$$

Similarly, the total concentration of C_2 in the $X^3\Pi_u$ state may be calculated knowing the vibrational temperature, $T_{v''}$, and the partition function, Q_{vib}; $T_{v''} \simeq 3300^oK$ for the luminous mantle and Q_{vib} is given by

$$Q_{vib} = \exp(-E_{v''=0}/kT_{v''}) + \exp(-E_{v''=1}/kT_{v''}) + \exp(-E_{v''=2}/kT_{v''}) + \ldots\ldots$$
$$\simeq 1.3$$

Thus $N(X^3\Pi_u) \simeq 1.3 \exp(E_{v''=0}/kT_{v''})\ N_{v''=0}$
$$\simeq 2.0\ N_{v''=0}$$

Some C_2 molecules will also be present in the $^1\Sigma_g^+$ electronic ground state which lies 610 cm^{-1} below the $X^3\Pi_u$ state but has a multiplicity of only one sixth the

latter. When this contribution has been included, an overall concentration of 2.5 times the $X^3\Pi_u$, v" = 0 concentration was estimated.

Experimental errors amounted to 15-20%, but the total accuracy is limited by the value of the oscillator strength employed. A factor of two or three in the C_2 f value would not alter the general conclusions which have been drawn in Chapter 6.

An order-of-magnitude estimate of the concentration in the reaction zone could be made from a knowledge of its thickness. Gaydon (1957) gave a value of 0.02 mm. for stoichiometric oxy-acetylene flames at 1 atm., increasing to at least 0.1 mm. in fuel-rich flames. Taking the latter value as a lower limit for our flames, C_2 concentrations were estimated to be up to fifty times higher in the oxidation zone than in the mantle.

Relative concentrations of C_2 were studied as a function of mixture strength and height above the reaction zone by measuring the peak absorption in the unresolved (0,0) band-head. Here the absorption was about 3 times larger than in any of the individual rotational lines and therefore more easily measured. If the total width of the unresolvable head is large compared with the spectral band-width of the spectrometer and the Beer-Lambert Law holds, then the quantity $(1/L)\ \ln\ (I_o/I)_{peak}$ should be

proportional to the C_2 concentration. This was verified experimentally for up to 40% peak absorption, using a 10μ slit-width. The results are presented in Figures 24 and 25, and discussed in Chapter 6.

b) C_3 concentration.

Absorption of the 4050 Å band was too weak to measure accurately but was superposed on a fairly strong continuous absorption (see section 4.4 and Figure 13) from which quantitative concentration estimates were made. The resemblance between this continuum and that observed in a King furnace at the same temperature is fairly good, although the flame continuum appears to extend to shorter wavelengths. There is strong evidence to suggest that it is associated with C_3 (Phillips and Brewer, 1955; Marr and Nicholls, 1955), and is really a pseudo-continuum consisting of a large number of overlapping bands having the same bound states as the 4050 Å band system (Brewer and Engelke, 1962). The latter authors derived an f value of 0.13 for this transition from measurements of the integrated absorption in a carbon-tube furnace of known temperature. They neglected absorption below 3700 Å, which they estimated might add 30% to the total absorption. Our measurements indicate that nearly 60% of the total absorption is on the u.v. side of 3700 Å (see Figure 13) which would increase the f value from 0.13 to 0.32 if all

the absorption were due to the C_3 molecule.

It is possible that C_5 may contribute to the absorption, although its equilibrium concentration is much lower than that of C_3 at temperatures below 4000°K (see section 6.1). Recently, Echigo et al (1967) proposed that polymerised and decomposed hydrocarbon compounds emitted banded spectra in the near i.r. region in luminous flames, but there is no evidence to suggest that appreciable emission from these compounds occurs in the u.v. spectral region.

For the purpose of deriving a total C_3 concentration in the Σ^+_g ground state, the integrated absorption to the red of 3700 Å was measured and the value $f_{el} = 0.13$ substituted in the relation

$$f_{el}\, N\, (^1\Sigma^+_g) = \frac{mc^2}{\pi e^2} \int_{3700\,\text{Å}}^{5000\,\text{Å}} k_\nu \, d\nu$$

The maximum absorption, (560 cm^{-1}), occurred at a C/O ratio of 1.41 and yielded a C_3 concentration of 1.3×10^{15} molecules cm^{-3} for eleven traversals, 2 mm. above the reaction zone. Relative concentrations were studied as a function of mixture strength and height above the reaction zone by measuring the peak absorption at 3900Å. The absorption was independent of the spectral slit-width used and proportional to the total area under the curve of $(1/L) \ln (I_o/I)$ against wavenumber. The results have

been plotted in Figures 24 and 25 for comparison with data on C_2.

c) CH concentration.

An order-of-magnitude estimate of CH concentrations in the $X^2\Pi$ ground state was made from the absorption in the piled-up Q branch of the 3143 Å band system. Assuming a rectangular profile for the 3143 Å 'line' of width 20 cm^{-1}, and neglecting contributions from lines outside this bandwidth, the total integrated absorption of the band is readily estimated. An oscillator strength of $f = 6.2 \times 10^{-3}$, as suggested by Linevsky (1967), was used in equation (2.2) to convert the integrated absorption into CH concentration.

It was not possible to measure CH concentrations as a function of mixture strength or distance above the reaction zone because the absorption was always weak and the background noise level in this region was high. For 11 traversals through the luminous mantle the absorption in the (0,0) Q head was about 5% which yielded a concentration of around 10^{14} radicals cm^{-3}. Concentrations of CH in the reaction zone were estimated to be a factor of 50-100 higher, assuming a thickness of ca. 0.1 mm. for the reaction zone.

F I G U R E 24.

Variation of C_2 and C_3 concentrations with mixture strength.
Experimental results refer to traversals 2 mm. above the tip of the reaction zone of unshielded flames.

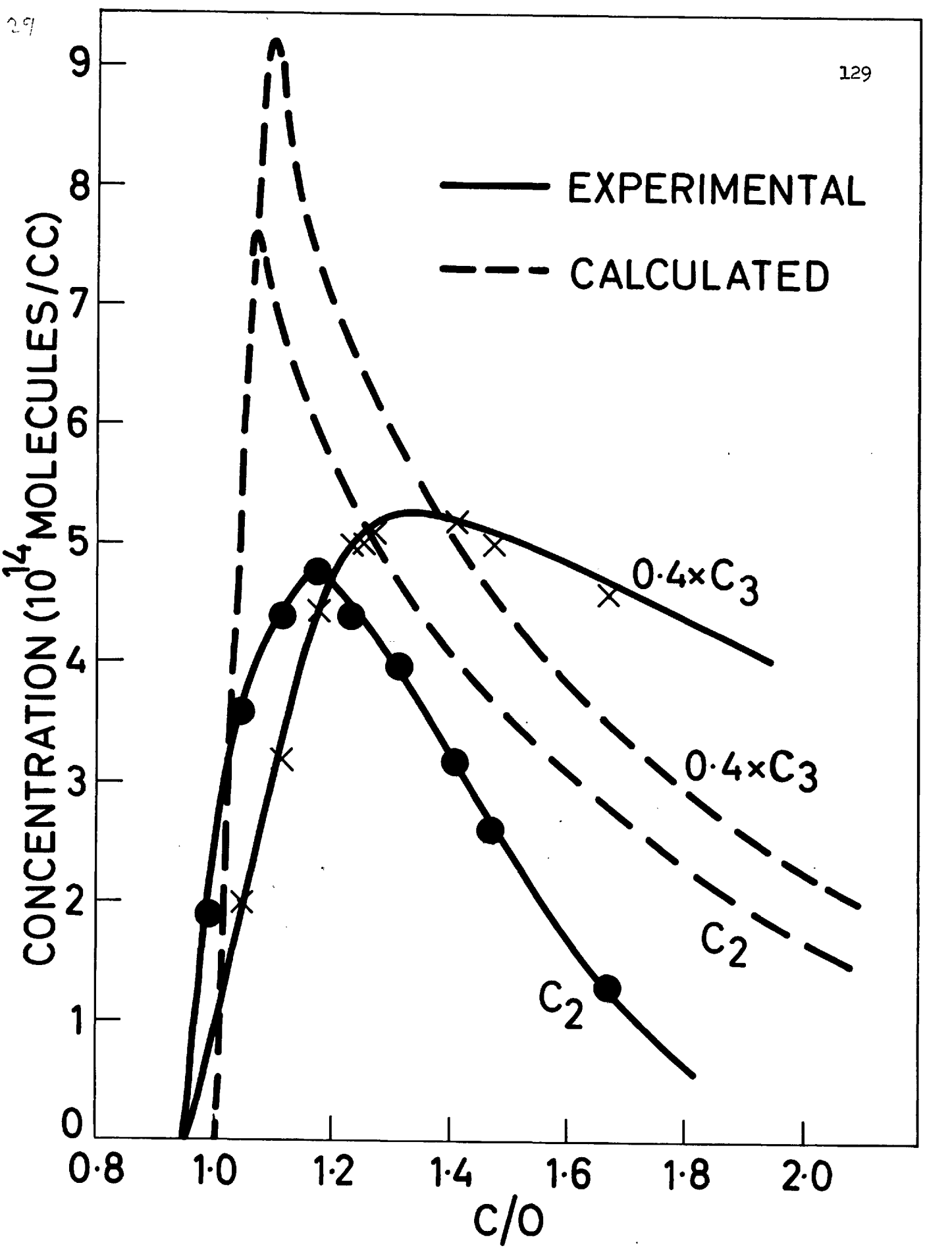
EXPERIMENTAL
CALCULATED
0·4×C3
0·4×C3
C2
C2
CONCENTRATION (10^14 MOLECULES/CC)
C/O
0
1
2
3
4
5
6
7
8
9
0·8
1·0
1·2
1·4
1·6
1·8
2·0

F I G U R E 25.

Variation of C_2 and C_3 concentrations with height above the reaction zone. Unshielded flames, C/O = 1.4.

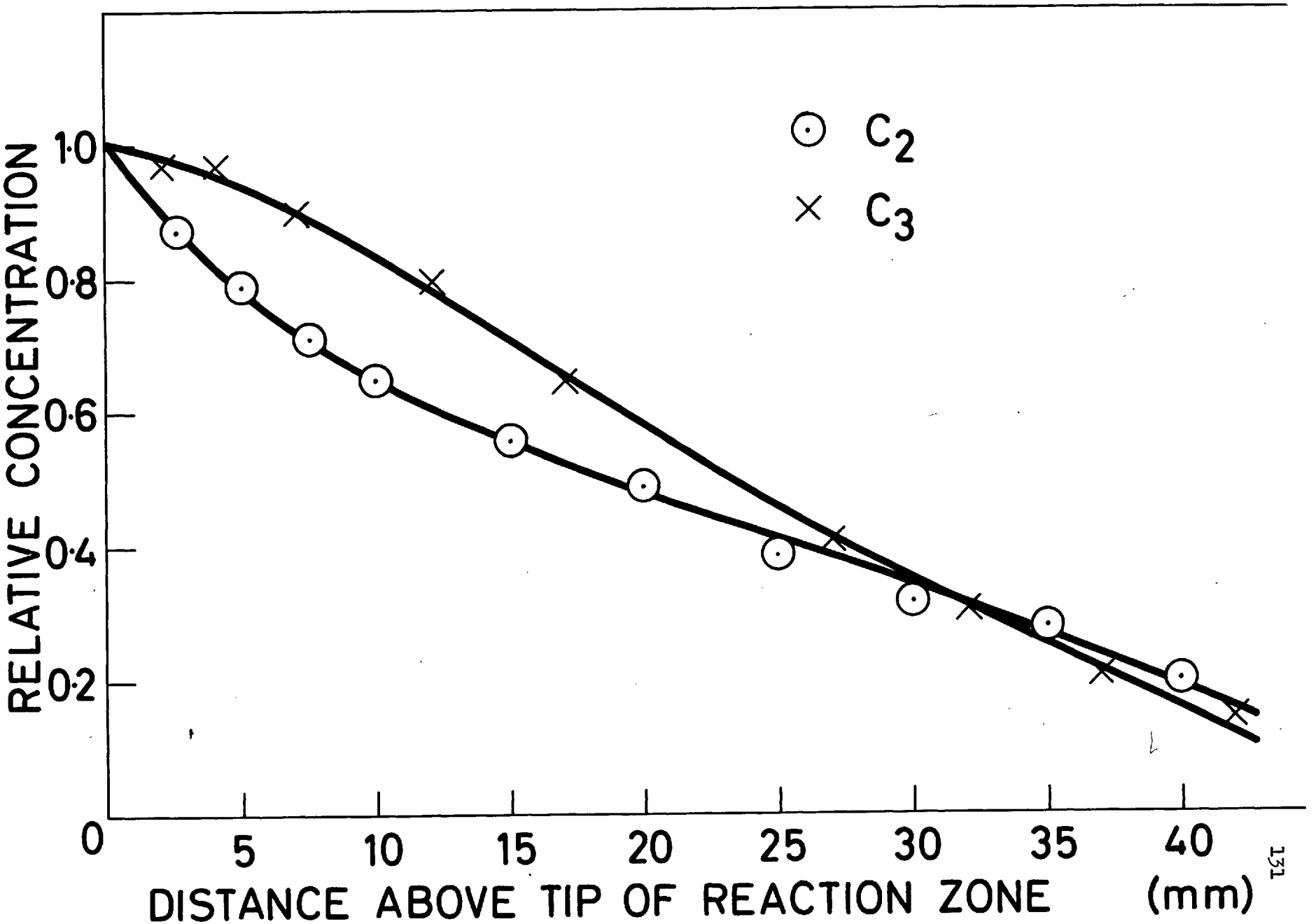
C2
C3
RELATIVE CONCENTRATION
1·0
0·8
0·6
0·4
0·2
0
5
10
15
20
25
30
35
40
DISTANCE ABOVE TIP OF REACTION ZONE
(mm)

CHAPTER 6.

EQUILIBRIUM CALCULATIONS OF CARBON RADICALS IN OXY-ACETYLENE FLAMES AND DISCUSSION OF CARBON FORMATION.

6.1. Equilibrium Calculations.

The results obtained in Chapter 5 are best discussed in the light of the expected equilibrium concentrations of carbon radicals in oxy-acetylene flames. The equilibrium composition and temperature of a flame can be calculated from thermochemical data for the reactants and products. Details of such calculations have been given in the book of Gaydon and Wolfhard (1960). The computations are laborious, relying on an iterative procedure to obtain the correct flame temperature, and are best handled by modern digital computers. All possible chemical species should be included but owing to a lack of thermochemical data for many of the minor constituents in hydrocarbon-oxygen flames, only the following products are usually considered: H_2O, O_2, H_2, CO_2, CO, OH, O, and H. This approximation is valid for near-stoichiometric flames but serious errors can occur for fuel-rich mixtures because appreciable concentrations of hydrocarbons are present in the burnt gas and solid carbon may be formed.

Gay et al. (1961) have calculated the temperature

and composition of acetylene-oxygen flames at various mixture strengths, taking into account the equilibrium between solid carbon and carbon vapour. They found that solid carbon should begin to be formed at a C:O ratio in the unburnt gas of 1.08 (corresponding to a flame temperature of 3275°K) when only monatomic and diatomic carbon vapour is considered. If higher polyatomic carbon molecules (C_3, C_4, C_5 etc.) are included in the calculations, the critical C:O ratio changes to 1.35 and the equilibrium flame temperature is reduced to 3095°K. The relevant thermochemical properties of the carbon molecules were taken from the theoretical calculations of Pitzer and Clementi (1959), who predicted that C_7 and C_9 should be the predominant species in equilibrium with solid carbon at 3000°K. This conclusion is not substantiated by mass-spectrometric studies of carbon vapour in equilibrium with graphite (Chupka and Inghram, 1955; Drowart et al. 1959). Experimentally, it appears that C_3 is the major constituent of carbon vapour at temperatures over 2000°K. Pitzer later revised his calculations (Strickler and Pitzer, 1964) and showed that no molecules larger than C_5 should contribute significantly to the vapour pressure of carbon except at temperatures well above 4000°K.

Equilibrium concentrations of C_2 and C_3 radicals were re-calculated from the results of Gay et al. using

TABLE 1

Equilibrium temperatures and partial pressures (atm.) of some carbon species in acetylene-oxygen flames at 1 atmosphere.

C/O	0.91	1.00	1.03	1.08	1.11	1.25	2.0
a) T(K)	3383	3325	3304	3275	3266	3233	3122
a) C_1(gas)	2.2×10^{-8}	1.9×10^{-5}	3.8×10^{-4}	4.8×10^{-4}	4.5×10^{-4}	3.5×10^{-4}	1.3×10^{-4}
C_2	3.8×10^{-13}	3.8×10^{-7}	1.8×10^{-4}	3.6×10^{-4}	3.2×10^{-4}	2.4×10^{-4}	8.2×10^{-5}
C_3	2.5×10^{-17}	3.1×10^{-8}	4.5×10^{-4}	9.5×10^{-4}	1.1×10^{-3}	7.4×10^{-4}	2.7×10^{-4}
a) CH	2.1×10^{-9}	2.1×10^{-6}	4.5×10^{-5}	6.1×10^{-5}	5.8×10^{-5}	4.9×10^{-5}	2.8×10^{-5}
a) C_2H_2	9×10^{-12}	1.6×10^{-5}	9×10^{-3}	0.0215	0.0226	0.0234	0.0257
a) * Csolid	0	0	0	0.0009	0.0197	0.0945	0.4139

* Moles per mole of gaseous products.

a) From table 7 of Gay et al. (1961)

their values of flame temperatures and atomic carbon concentrations (assuming only C_1 and C_2 are present) in conjunction with the equilibrium constants for the dissociation of C_2 and C_3 into carbon atoms. The dissociation energies of C_2 and C_3 were taken to be 143 k.cal/mole and 321 k.cal/mole, respectively (Gaydon, 1968). Results are listed in Table 1; Gay's values for CH, C_2H_2, and C_{solid} have also been included. Drowart's (1967) revised experimental results for the equilibrium vapour pressure of graphite have been extrapolated to 3250°K and are presented in Table 2. They give a convenient check on the calculations summarised in Table 1, and it is gratifying to note the satisfactory agreement between the two sets of results.

Table 2.

Equilibrium vapour pressures of carbon species in equilibrium with graphite at 3250°K.

Species	Pressure (atm.)
C_1	4.5×10^{-4}
C_2	4×10^{-4}
C_3	2.5×10^{-3}
C_5	6×10^{-6}
other species	$< 10^{-7}$

6.2. Comparison with actual carbon radical concentrations in flames.

In Figure 24, experimentally determined concentrations of C_2 and C_3 are compared with the calculated equilibrium values listed in Table 1. It is obvious that the measured concentration profiles are less steep than the calculated curves and the peaks occur at slightly richer mixtures. The absolute concentrations generally agree to within a factor of two but, whereas the calculated equilibrium concentration of carbon radicals is very low for mixture strengths of $C/O \leqslant 1.0$, experimentally one finds appreciable concentrations extending downstream of the reaction zone for $C/O > 0.95$. Results obtained with and without an outer flow of shielding gas are essentially the same. A decrease in total absorption occurs when no protective sheath is used, but this is due to the reduced size of the luminous mantle, as a result of reactions of carbon species with secondary combustion products, rather than to any change in concentration in the mantle itself.

For convenience, the experimental and calculated equilibrium concentrations of C_2, C_3 and CH in a typical rich flame ($C/O = 1.25$) are listed in Table 3.

Table 3.

Partial pressures (atm) of carbon radicals in a fuel-rich C_2H_2 - O_2 flame at 1 atm. (C/O = 1.25; T = 3233°K)

Species	C_2	C_3	CH
Calculated	2.4×10^{-4}	7.4×10^{-4}	4.9×10^{-5}
Experimental	2.1×10^{-4}	6.0×10^{-4}	5×10^{-5}

6.3. Discussion.

Differences between the calculated and experimental curves of concentration against mixture strength can be explained mainly in terms of the approximations involved in the equilibrium calculations and experimental measurements. Interpretation of quantitative spectroscopic measurements in flames, other than those with flat reaction zones, is complicated by the fact that the flame parameters will vary along the optical pathlength as defined by the associated optics. Thus, each experimental result represents some sort of mean quantity averaged over the pathlength through the flame. The C:O ratio may vary across the flame and be different locally from that in the original unburnt gas mixture. However, the carbon luminosity is fairly uniformly distributed around the inner cone, suggesting that the diffusion rates of oxidising species and acetylene molecules are not

appreciably different.

The onset of a mantle around the reaction zone for mixtures richer than C/O = 0.95, instead of the theoretical carbon point, C/O = 1.0, appeared to be a genuine effect and not due to inaccuracies in the calibration of gas flow rates. It is well-known that carbon formation in premixed flames is a non-equilibrium phenomenon and soot is frequently observed for mixtures with C/O < 1.0. Street and Thomas (1955) used the appearance and disappearance of the yellow carbon luminosity to measure the onset of sooting, and obtained a value of C/O = 0.83 for shielded acetylene-air flames. Homann et al. (1963) determined a critical C:O ratio of 0.91 for formation of carbon particles of diameters greater than about 40 Å in acetylene-oxygen flames at 10-30 mm. Hg pressure. On the other hand, Gay, Agnew, et al. (1961), using a small water-cooled metal plate positioned at various heights above the tip of the reaction zone, first found evidence of carbon deposition at a mixture strength of C/O = 1.16 in oxy-acetylene flames at 1 atm. From their published photographs and from the absence of change when nitrogen shielding was employed, it appears probable that their flames were turbulent.

In general, comparisons between different experimental observations are not very useful because

critical C:O ratios can be a function of flame structure, temperature, and quenching by the burner top, as well as being dependent on the criterion used to measure the onset of sooting. The luminous mantle of the shielded flames described in this thesis showed a yellowish colouration for mixture strengths greater than C/O$\sim$1.1. However weak, continuous emission was observed throughout the visible region for less-rich mixtures (C/O$\geqslant$0.95), suggesting that carbon particles were already present.

6.4. Equilibrium in the reaction zone and luminous mantle.

In common with earlier studies, large departures from thermal and chemical equilibrium were found to occur in the reaction zone. The temperature results obtained (section 5.1) show that C_2 is formed with excess rotational and vibrational energy and, during its lifetime in the reaction zone, the number of relaxing collisions is too small to redistribute the initial rotational and vibrational distribution to one corresponding to the equilibrium flame temperature. It is not clear how this non-thermal radiation arises. Gaydon et al. (1960) derived an electronic excitation temperature for C_2 in low pressure oxy-acetylene flames, and obtained a value 1000^{o}K in excess of the equilibrium temperature. The results strongly point to a chemiluminescent formation but the

actual mechanism is still obscure. Owing to the large heat of formation of C_2 (8.49 eV), it is difficult to postulate simple reactions which are sufficiently exothermic to explain the strong Swan band emission from flames. Gaydon and Wolfhard (1950) suggested that C_2 is formed in the $X^3\Pi_u$ state with excess rotational energy by the exothermic break-up of unsaturated hydrocarbon polymers. Subsequent excitation to the upper electronic state occurs by collision with a vibrationally excited molecule before the initial internal energy distribution has had time to equilibriate. This indirect chemiluminescent mechanism explained the effects of pressure and diluents on their C_2 ($A^3\Pi_g$) rotational temperature results but it is difficult to reconcile with absorption measurements of effective C_2 rotational and vibrational temperatures in the triplet ground state. Bleckrode and Nieuwpoort (1965) found that the population temperatures were too low to account for such an excitation mechanism and the present study at atmospheric pressure confirms that temperatures in the $X^3\Pi_u$ state tend to be lower than those in the $A^3\Pi_g$ state.

Although several reactions have been proposed for the direct formation of C_2 in the electronic excited state, it is not possible at present to test whether any of them do actually occur. Experimental evidence points to the

initial breakdown of the C-C bond in acetylene (section 1.6) rather than the successive stripping of hydrogen atoms from the carbon skeleton.

There is strong evidence pointing to the chemiluminescent production of CH radicals from C_2 via the reaction

$$C_2 + OH \longrightarrow CH^* + CO$$

although the reaction

$$C_2H + O \longrightarrow CH^* + CO$$

may also be important in certain circumstances (Ndaalio and Deckers, 1967).

Figure 25 shows the decay of C_2 and C_3 concentrations with height above the reaction zone. For less-rich mixtures, the gradients become steeper but the general form of both curves remains unchanged. It appears that the C_2 concentration does not fall to the steady equilibrium value until several millimetres beyond the reaction zone, whereas the C_3 concentration above the tip is slightly below the full equilibrium value. Curves of emission intensity were similar to the absorption results. Emission from C_2 was very much stronger in the reaction zone, but for C_3 the emission from the surrounding mantle region always masked that from the thin reaction zone, indicating that the radiation from the reaction zone itself was not abnormally strong and could well be absent.

There was little evidence for thermal disequilibrium in the mantle and the measured C_2 population temperatures were close to the maximum equilibrium flame temperature, i.e. 3300°K. Rather high vibrational temperatures for the $A^3\Pi_g$ state were recorded ($T_v' \simeq 3600°K$) and slightly high values were indicated for the $X^3\Pi_u$ state rotational temperature.

[illegible] responsible for the discrepancy.

The gradual fall in C_2 and C_3 concentrations is presumably due to cooling of the flame by radiation and other losses, and corresponds to a temperature drop of about 50°K per cm. height of mantle.

6.5. Connection between C_2, C_3 and carbon formation.

Some important aspects of soot formation in premixed flames were discussed in section 1.6 and various theories linking the radicals C_1, C_2, and C_3 with formation of solid carbon in flames were described in section 1.7.

No information has been obtained concerning atomic carbon concentrations, but measurements of C_2 and C_3 concentrations give some clues as to their relevance in the soot-forming processes occurring in high-temperature flames.

There are three possibilities:-

These results, if genuine, cannot be due to actual delayed relaxation of C_2 molecules chemically formed in the reaction zone, because the necessary relaxation times would have to be impossibly high, and the measured temperatures are independent of distance above the reaction zone. They could be caused by some continued reaction producing new excited molecules in the mantle but in view of the normal values obtained for $T_{v''}$ and $T_{R'}$ it is more likely that systematic errors are responsible for the discrepancy. The gradual fall in C_2 and C_3 concentrations is presumably due to cooling of the flame by radiation and other losses, and corresponds to a temperature drop of about $50^{\circ}K$ per cm. height of mantle.

6.5. Connection between C_2, C_3 and carbon formation.

Some important aspects of soot formation in premixed flames were discussed in section 1.6 and various theories linking the radicals C_1, C_2, and C_3 with formation of solid carbon in flames were described in section 1.7.

No information has been obtained concerning atomic carbon concentrations, but measurements of C_2 and C_3 concentrations give some clues as to their relevance in the soot-forming processes occurring in high-temperature flames.

There are three possibilities:-

1. They are important intermediates, i.e., carbon formation occurs via C_2 and C_3.
2. They are products, i.e., C_2 and C_3 are formed by evaporation of hot carbon particles or incipient particles.
3. The formation of solid carbon and C_2 and C_3 radicals occurs independently or by competing mechanisms.

The formation of solid carbon by direct condensation of carbon vapour can be ruled out. At temperatures of around 3000°C, the principal constituent of carbon vapour is C_3 (Table 2). However, the variation of C_3 condentration with mixture strength and height above the reaction zone indicates that it is a product from rather than precursor of solid carbon. C_3 is usually observed only in hot flames exhibiting a luminous mantle and its concentration immediately above the tip of the reaction zone appears to be slightly below the full equilibrium value, suggesting that it is formed by evaporation of hot carbon particles or incipient particles. The good agreement between calculated and experimental concentrations (Table 3) indicates that the equilibrium vapour pressure of soot particles is not appreciably different from that of pure graphite.

In lower-temperature flames, the vapour pressure of carbon is reduced and the continuous carbon particle radiation masks the C_2 and C_3 emission. Durie (1952)

observed the 4050 Å Comet-Head bands in hydrocarbon flames supported by fluorine. The flames were generally sooty, but gradual dilution of the fuel with hydrogen caused the luminosity to decrease and C_2 and C_3 bands began to appear through the continuous emission. The C_3 bands disappeared again together with the continuous emission from the carbon, leaving a blue-green flame emitting only C_2 and CH radiation.

Norrish, Porter, and Thrush (1955) detected the 4050 Å bands in the explosive oxidation of acetylene/oxygen mixtures studied by flash photolysis. They concluded that the C_3 molecules were formed from solid carbon particles and were in equilibrium with them. It is interesting to note that these authors also observed an absorption spectrum similar to that shown in figure 13, although they did not connect it with C_3 at that time.

C_2, on the other hand, is formed prior to solid carbon in the main oxidation zone. It has a very high concentration within the reaction zone (up to 10^{16} molecules cm^{-3}) and this does not fall to the steady equilibrium value until some mm. beyond the tip. In view of its close association with carbon formation in premixed flames and its relatively high initial concentration, reactions linking the two together deserve careful consideration.

The polymerization of C_2 molecules to form solid carbon as originally suggested by Smith (1940), can be ruled out even in very hot flames. Gaydon and Wolfhard (1950) showed by simple calculation that C_2 molecules collide with each other only once on average during their passage through the reaction zone. They assumed a normal gas-kinetic collision cross-section, and a C_2 concentration of about 10^{-3} atm. which is sufficiently close to the measured concentration to illustrate the unlikelihood of a direct polymerization mechanism. Also, cyanogen-oxygen flames, which have an equilibrium flame temperature of about 4800°K and show very strong C_2 emission, do not normally give any solid carbon.

An alternative suggestion, requiring lower C_2 concentrations and accounting for the relatively large hydrogen content in soot, is that C_2 radicals could act as nuclei for carbon formation from acetylene and unsaturated hydrocarbon fragments. The observation of Gaydon and Fairbairn (1955) that carbon is formed at low temperatures by reaction of acetylene with the products of a carbon monoxide after-glow (containing C_2 and atomic carbon) led them to conclude that the following reactions might be occurring:

$$C_2 + C_2H_2 \longrightarrow C_4 + H_2$$

$$C_4 + C_2H_2 \longrightarrow C_6 + H_2, \text{ etc.}$$

Tesner (1955) suggested that once carbon nuclei have been formed, surface decomposition of fuel or fuel fragments will be the most important route for carbon formation since dehydrogenation will be made easier by simultaneous carbon ring formation and release of energy. He studied the degree of dispersion of carbon particles formed by passing hydrocarbon vapour through a heated reaction tube and concluded that surface decomposition of the hydrocarbon proceeds at temperatures 150° to $200^{\circ}K$ lower than those necessary for the formation of carbon particle nuclei. Tesner estimated that a nucleus is four to five orders of magnitude smaller in volume than a particle and therefore only an insignificant proportion of the decomposing hydrocarbon goes to form the nuclei.

Conditions in actual flames will be different because flame temperatures are much higher and competing oxidation reactions are occurring which also help to break down the original fuel molecules. However, Tesner's results do not preclude the possibility of C_2 radicals initiating the growth of carbon particles in premixed flames.

Bonne, Homann, and Wagner (1965) made an extensive study of carbon formation in low-pressure flames and showed that polyacetylene compounds are formed and play an important part in the nucleation and growth stages

(see section 1.6). The polyacetylenes are assumed to have radical characteristics and be formed in the oxidation zone by radical reactions of the type:

$$C_2H_2 + O \longrightarrow CH_2 + CO$$
$$CH_2 + C_2H_2 \longrightarrow C_2H + CH_3$$
$$C_2H + C_2H_2 \longrightarrow C_4H_3$$
$$\longrightarrow C_4H_2 + H$$
$$C_4H_2 + C_2H_2 \longrightarrow C_6H_4$$
$$\longrightarrow C_6H_3 + H$$
$$\longrightarrow C_6H_2 + H_2$$
$$\text{etc.}$$

From the results of Gaydon and Fairbairn, it would appear that C_2 radicals could promote the formation of higher acetylenes by reactions of the type:

$$C_2 + C_2H_2 \longrightarrow C_2H + C_2H$$
$$C_2H + C_2H_2 \longrightarrow C_4H_3$$
$$C_4H_3 + C_2 \longrightarrow C_4H_2 + C_2H$$
$$C_4H_2 + C_2 \longrightarrow C_4H + C_2H$$
$$\text{etc.}$$

Unfortunately the radicals C_2H and CH_2 have not been observed spectroscopically in flames and present evidence does not allow their relevant importance to be assessed. In view of the high rate of production of C_2 radicals in the oxidation zone of high-temperature flames, reactions of the above type may be important and lead to

carbon formation along the lines suggested by Bonne, Homann, and Wagner.

6.6. Conclusions.

The general conclusions arrived at in this chapter are summarised below.

1. The concentrations of C_2 and C_3 in the mantle of oxy-acetylene flames, about 2×10^{14} and 1×10^{15} molecules cm^{-3}, respectively, are consistent with values expected for equilibrium with solid carbon.
2. There is little evidence for thermal disequilibrium in the luminous mantle.
3. Solid carbon is not formed by the direct condensation of carbon vapour.
4. C_3 is formed by evaporation of solid carbon and is not present in significant concentrations prior to the formation of incipient carbon particles.
5. C_2 radicals are chemically produced in the reaction zone before carbon formation begins. Their initial concentration, up to 10^{16} molecules cm^{-3}, is abnormally high and they may be important species in the nucleation stage of carbon formation.

6.7. Suggestions for future work.

It is thought to be worthwhile to mention some additional experiments which were considered but could not be carried out owing to lack of time.

Certain gases have been reported to have a marked effect on carbon formation and C_2 emission from flames. Addition of small amounts of chlorine containing compounds strongly increases the green C_2 emission from rich hydrocarbon-oxygen flames but only slightly increases the carbon luminosity. Sulphur trioxide causes a striking increase in carbon formation if as little as 0.1% is added to a premixed flame, whereas it has little effect when added to a diffusion flame (Gaydon and Wolfhard, 1960, p.187). Studies on the variation of C_2 concentration with addition of these gases would obviously be desirable in order to investigate the role of C_2 in the formation of carbon particles.

One of the outstanding problems in combustion today is the origin of chemi-ionization and chemi-excitation processes occurring in organic flames. A number of mechanisms has been proposed, but there is insufficient experimental evidence to check their validity because detailed radical concentration profiles are lacking. It would seem that the apparatus developed in this thesis is very suitable for such measurements on low-pressure flames where the reaction zones may be a few cms. thick.

Finally, a number of improvements to the apparatus are considered. The minimum amount of absorption that can be accurately measured is, in practice, determined by the stability of the background sources. Small movements of the arc between the electrodes cause fluctuations in the output intensity of a high-pressure arc lamp even though a stabilised power supply is used. It is possible to compensate for this effect by monitoring a fraction of the output intensity and using electronic circuits to vary the current passing through the lamp so the intensity remains effectively constant. A simple device was recently described by Schurer and Stoelhorst (1967) which should be adaptable to absorption studies.

Better signal-to-noise ratios can be achieved if high reflectivity mirrors are used for the multiple-reflection system. Since the advent of lasers, it has been possible to obtain reflectivities of over 98% at any specified wavelength in the visible or near u.v. regions. The disadvantage of high-reflection coatings is that they are applicable over only a narrow wavelength range and a set of different coated mirrors would be required to study widely separated spectra.

For many investigations, it should be possible to use tungsten-halogen filament lamps, which are inherently more stable than high-pressure arcs. With scale-expansion

facilities on the recorder output, it should be possible to measure absorption levels of about 0.1%.

REFERENCES.

1. Ballick, E.A. and Ramsay, D.A.; 1962, Astrophys.J., 137, 84.
2. Bleekrode, R.; Ph.D.Thesis, 1966, University of Amsterdam.
3. Bleekrode, R. and Nieuwpoort, W.C.; 1965, J.Chem.Phys., 43, 3680.
4. Bonne, U., Homann, K.H. and Wagner, H.Gg.; 1965, Tenth Symposium (International) on Combustion, p.503, The Combustion Institute.
5. Bradley, J.N. and Kistiakowsky, G.B.; 1961, J.Chem. Phys., 35, 264.
6. Brewer, L. and Engelke, J.L.; 1962, J.Chem.Phys., 36, 992.
7. Budo, A.; 1937, Z.Physik, 105, 579.
8. Cabannes, F.; 1956, J.Phys.Radium, 17, 492.
9. Calloman, J.H. and Gilby, A.C.; 1963, Can.J.Phys., 41, 995.
10. Drowart, J.; 1967, private communication.
11. Drowart, J., Burns, R.P, De Maria, G. and Inghram, M.G.; 1959, J.Chem.Phys., 31, 1131.
12. Durie, R.A.; 1952, Proc.Roy.Soc., A211, 110.
13. Echigo, R., Nishiwaki, N. and Hirata, M.; 1967, Eleventh Symposium (International)on Combustion, p.381, The Combustion Institute.
14. Fairbairn, A.R.; 1962, Eighth Symposium (International) on Combustion, p.304, Williams and Wilkins.
15. Fairbairn, A.R.; 1966, J.Quant.Spectr.Radiative Transfer, 6, 325.

16. Ferguson, R.E.; 1955, J.Chem.Phys., 23, 2085.

17. Ferguson, R.E.; 1957, Combust. and Flame, 1, 431.

18. Fink, E.H. and Welge, K.H.; 1967, J.Chem.Phys., 46, 4315.

19. Garton, W.R.S. and Rajaratnam, A.; 1957, Proc.Phys.Soc., A70, 815.

20. Garton, W.R.S., 1953, J.Sci.Instrum., 30, 119.

21. Gay, N.R., Agnew, J.T., Witzell, O.W. and Karabell, C.E.; 1961, Combust. and Flame, 5, 257.

22. Gaydon, A.G.; 1957, The Spectroscopy of Flames, Chapman and Hall.

23. Gaydon, A.G.; 1968, Dissociation Energies, Chapman and Hall, 3rd Edition.

24. Gaydon, A.G. and Wolfhard, H.G.; 1950, Proc.Roy.Soc., A201, 570.

25. Gaydon, A.G. and Fairbairn, A.R.; 1955, Fifth Symposium (International) on Combustion, p.324, Reinhold Publ.Co.

26. Gaydon, A.G. and Wolfhard, H.G.; 1960; Flames, their structure, radiation and temperature, Chapman and Hall, 2nd. Edition.

27. Gaydon, A.G., Spokes, G.N. and van Suchtelen, J.; 1960, Proc. Roy. Soc., A256, 323.

28. Harrington, J.A., Modica, A.P. and Libby, D.R.; 1966, J.Chem.Phys., 44, 3380.

29. Herzberg, G.; 1950, Spectra of Diatomic Molecules, Van Nostrand, 2nd Edition.

30. Homann, K.H., Mochizuki, M. and Wagner, H.Gg.; 1963, Z.Phys.Chem., N.F. 37, 299.

31. Homann, K.H. and Wagner, H.Gg.; 1967, Eleventh Symposium (International) on Combustion, p.371, The Combustion Institute.

32. Jain, D.C.; 1964, J.Quant.Spectr.Radiative Transfer, 4, 427.

33. Johnson, R.C.; 1927, Phil.Trans.Roy.Soc., A226, 157.

34. Kaskan, W.E.; 1958, Combust. and Flame, 2, 229.

35. King, R.B.; 1948, Astrophys. J., 108, 429.

36. Kostkowski, H.J. and Bass, A.M.; 1956, J.Opt.Soc.Amer., 46, 1060.

37. Marr, G.V.; 1957, Can.J.Phys., 35, 1265.

38. Marr, G.V. and Nicholls, R.W.; 1955, Can.J.Phys., 33,394.

39. Mitchell, A.C. and Zemansky, M.W.; 1961, Resonance Radiation and Excited Atoms, Cambridge Univ. Press, 2nd Edition.

40. Ndaalio, G. and Deckers, J.M.; 1967, Can.J.Chem., 45, 2441.

41. Nicholls, R.W., Frazer, P.A. and Jarmain, W.R.; 1959, Combust. and Flame, 3, 13.

42. Norrish, R.G.W., Porter, G. and Thrush, B.A.; 1953, Proc.Roy.Soc., A216, 165.

43. Norrish, R.G.W., Porter, G. and Thrush, B.A.; 1955, Proc.Roy.Soc., A227, 423.

44. Padley, P.J. and Sugden, T.M.; 1958, Proc.Roy.Soc., A248, 248.

45. Penner, S.S.; 1959, Quantitative Molecular Spectroscopy and Gas Emissivities, Addison Wesley.

46. Phillips, J.G. and Brewer, L.; 1955, Mem.Soc.Roy.Sci.Liege. Ser 4, 15, 341.

47. Place, E.R. and Weinberg, F.J.; 1967; Eleventh Symposium (International) on Combustion, p.324, The Combustion Institute.

48. Porter, R.P., Clark, A.H., Kaskan, W.E. and Browne, W.E.; Eleventh Symposium (Int.) on Combustion, p.907, The Combustion Institute.

49. Schurer, K. and Stoelhorst, J.; 1967, J.Sci.Instrum., 44, 952.

50. Silverman, S.; 1949, Third Symposium (International) on Combustion, p.498, Williams and Wilkins.

51. Smith, E.C.W.; 1940, Proc.Roy.Soc., A174, 110.

52. Snelleman, W.; Ph.D.Thesis, 1965, University of Utrecht.

53. Street, J.C. and Thomas, A.; 1955, Fuel, 34, 4.

54. Sviridov, A.G., Sobolev, N.N. and Novgorodev, M.Z.; 1966, J.Quant.Spectr.Radiative Transfer, 6, 337.

55. Tesner, P.A.; 1959, Seventh Symposium (Int.) on Combustion, p.546, Butterworths.

56. Walsh, A.; 1955, Spectrochim. Acta, 7, 108.

57. Welsh, H.L., Cumming, C. and Stansbury, E.J.; 1951, J.Opt.Soc.Amer., 41, 712.

58. Wheaton, J.E.G.; 1964, Appl.Optics, 3, 1247.

59. White, J.U.; 1942, J.Opt.Soc.Amer., 32, 285.

APPENDIX 1.

Rotational line strengths of C_2 Swan bands.

The Swan bands are due to $^3\Pi - {}^3\Pi$ transition and the bands show only P and R branches. Both electronic states approximate closely to Hund's case b coupling for J values greater than about 20. Owing to the small spin splitting each line is a close triplet and for the purposes of making temperature measurements from the rotational intensity distribution, a spectral resolution is employed which is insufficient to resolve the triplet structure.

In such cases where the multiplet structure is ignored and the lines are treated as singlets, it is more useful to describe the lines by the number K, the rotational quantum number apart from spin

$$K = \Lambda, \Lambda + 1, \Lambda + 2, \ldots$$

and the possible values of J for a given K are

$$J = K + S, K + S-1, K + S-2, \ldots |K-S|$$

At the same time the rotational line strength, $S_{K''K'}$, is generally assumed to be equal to the sum of the line strengths of the 2S + 1 components. It is difficult to find justifications for this assumption in order to check its general validity and therefore the following explanation is given.

Consider a rotational line (J", J') in an electronic band system e.g. C_2 $^3\Pi - {}^3\Pi$

The absorption intensity of the line $I^{abs}_{J"J'}$, may be written

$$I^{abs}_{J"J'} = C\, S_{J"J'} \exp\left[-B_{v"} J"(J+1)/kT_{R"} \right] \qquad (A.1)$$

where C is a constant for a given band (neglecting the slight ν dependence) and the D_v contribution to the rotational energy has been neglected.

For a P branch line, $\Delta J = J' - J" = -1$, and for an R branch line $\Delta J = +1$.

If the lines each consist of closely separated triplets the total absorption intensity may be written

$$I^{abs}_{K"K'} = {}^{R123}I^{abs}_{K"} = {}^{R1} I_{J"+1} + {}^{R2}I_{J"} + {}^{R3}I_{J"-1} \qquad (A.2)$$

for the unresolved line (R(K"), and

$$I^{abs}_{K"K'} = {}^{P123}I^{abs}_{K"} = {}^{P1} I_{J"+1} + {}^{P2}I_{J"} + {}^{P3}I_{J"-1} \qquad (A.3)$$

for the unresolved line P(K").

Using equations (A.1) and (A.2) we obtain

$${}^{R1}I^{abs}_{J"+1} = C\,{}^{R1}S_{J"+1} \exp\left[-B_{v"}(J"+1)(J"+2)/kT_{R"}\right]$$

$${}^{R2}I^{abs}_{J"} = C\,{}^{R2}S_{J"} \exp\left[-B_{v"} J" (J"+1)/kT_{R"}\right]$$

$${}^{R3}I^{abs}_{J"-1} = C\,{}^{R3}S_{J"-1} \exp\left[-B_{v"}(J"-1)\, J"/kT_{R"}\right]$$

and ${}^{R123} I^{abs}_{K"} /C$

$$= ({}^{R1}S_{J"+1} + {}^{R2}S_{J"} + {}^{R3}S_{J"-1}) \exp\left[-B_{v"}J"(J"+1)/kT_{R"}\right]$$

$$+ \frac{2J"B_{v"}}{kT_{R"}} ({}^{R3}S_{J"-1} - {}^{R1}S_{J"+1}) \exp\left[-B_{v"}J"(J"+1)/kT_{R"}\right]$$

$$+ (0) \left(\frac{J"B_{v"}}{kT_{R"}}\right)^2 + \cdots\cdots \qquad (A.4)$$

Assuming the 2nd term and higher terms are negligible we obtain

$$R123_{I_{K''}}^{abs} = {}^{R}I_{K''}^{abs} = C\,{}^{R}S_{K''} \exp\left[-B_{v''}K''(K''+1)/kT_{R''}\right] \quad (A.5)$$

where $${}^{R}S_{K''} = {}^{R1}S_{J''+1} + {}^{R2}S_{J''} + {}^{R3}S_{J''-1} \quad (A.6)$$

and K" equals the J" value of the R 2 line.

A similar result holds for the P branch lines. Thus equations (A.5) and (A.6) are valid if the 1st term in equation (A.4) predominates. This will always be the case at high temperatures as illustrated below.

Taking the R123 (K"=50) of the C_2 (0,0) Swan band as an example and assuming $T_{R''} = 3000^{\circ}K$ and $B_{0''} \simeq 1.6$, we find

$$\frac{2J''B_{v''}}{kT_{R''}} \simeq \frac{2 \times 50 \times 1.6}{0.7 \times 3000} \simeq 8 \times 10^{-2}$$

$${}^{R3}S_{J''-1} - {}^{R1}S_{J''+1} \simeq 48 - 52 = -4$$

$${}^{R1}S_{J''+1} + {}^{R2}S_{J''} + {}^{R3}S_{J''-1} \simeq 3 \times 51 = 153$$

(see below)

∴ 2nd term/1st term $\simeq 0.32/153 \simeq 2 \times 10^{-3}$

and higher terms are of the order $(0.08)^2$.

Budo (1937) has calculated line strengths for $^3\Pi - {}^3\Pi$ transitions and the relevant values for Hund's case b coupling are given below.

Line	Line strength $S_{J''J'}$
P1(J'')	$\frac{(J''-2)\ J''\ (2J''+1)}{(J''-1)\ (2J''-1)}$
P2(J'')	$\frac{(J''-1)^2\ (J''+1)^2}{J''^3}$
P3(J'')	$\frac{J''\ (J''+2)\ (2J''-1)}{(J''+1)\ (2J''+1)}$
R1(J'')	$\frac{(J''-1)\ (J''+1)\ (2J''+3)}{J''\ (2J''+1)}$
R2(J'')	$\frac{J''^2\ (J''+2)^2}{(J''+1)^3}$
R3(J'')	$\frac{(J''+1)\ (J''+3)\ (2J''+1)}{(J''+2)\ (2J''+3)}$

The line strengths ${}^{R}S_{K''}$ and ${}^{P}S_{K''}$ are calculated using equation (A.6) and we obtain

$$\begin{aligned} {}^{R}S_{K''} &\simeq 3K''\ (K''+2)/(K''+1) \\ {}^{P}S_{K''} &\simeq 3(K''-1)\ (K''+1)/K'' \end{aligned} \qquad \text{(A.7)}$$

For large values of K the line strengths reduce to

$$\begin{aligned} {}^{R}S_{K''} &\simeq 3(K''+1) \\ \text{and} \qquad {}^{P}S_{K''} &\simeq 3K'' \end{aligned} \qquad \text{(A.8)}$$

Budo defined his $S_{J''J'}$ values to be equal to the rotational transition probability times the statistical weight, and on this basis,

$$\sum_{J'} S_{J''J'} = 2J'' + 1$$

and $$\sum_{J''} S_{J'J''} = 2J' + 1 \qquad \text{(A.9)}$$

In the present work, it is more useful to normalise the line strengths over all possible K values, giving,

$$\sum_{K'} S_{K''K'} = 2K'' + 1$$

$$\sum_{K''} S_{K''K'} = 2K' + 1 \qquad \text{(A.10)}$$

Thus, it is necessary to divide the line strengths given by equations (A.7) and (A.8) by the factor 2S+1(=3) for them to be consistent with equation (A.10). This gives, for K values greater than 25,

$$R_{S_{K''}} = K'' + 1$$

$$P_{S_{K''}} = K'' \qquad \text{(A.11)}$$

the error being less than 1%.

N.B. the rotational partition function, Q_{rot}, is normalised in an analogous manner;

$$Q_{rot} = \sum_{K} (2K+1) \exp(-E_K/kT_R)$$

$$\simeq \frac{kT_R}{B_v}, \quad \text{not} \quad \frac{3kT_R}{B_v}.$$

APPENDIX 2.

DATA FOR DETERMINATION OF ROTATIONAL AND VIBRATIONAL TEMPERATURES OF C_2.

TABLE A.1. (Fig.16) P branch, $T_{R'} = 3350^{\circ}K$.

Experimental details: 2 Å/min. scan, 10 μ slits, C/O = 1.18, 2 mm. above tip of reaction zone.

transition P(K")	I arbitrary units	$S_{K'K"}$	$I/S_{K'K"}$ arbitrary units	$\log_{10}(I/S_{K'K"})$	K'(K'+1)
26	37.	26	1.42	1.15	650
27	36.5	27	1.35	1.13	702
28	40.5	28	1.45	1.16	756
29	36.5	29	1.26	1.10	812
30	36.	30	1.20	1.08	870
31	38.5	31	1.24	1.09	930
32	38	32	1.19	1.08	992
40	30.	40	7.5	0.88	1560
41	29.5	41	7.2	0.86	1640
42	28	42	6.7	0.82	1722
43	27	43	6.3	0.80	1806
44	25.5	44	5.8	0.76	1892
45	25.	45	5.5	0.74	1980
46	23.5	46	5.1	0.71	2070

TABLE A.2 (Fig.16). R branch, $T_{R'} = 3350^{\circ}K$.

Experimental details: As Table A.1.

transition R(K")	I arbitrary units	$S_{K'K"}$	$I/S_{K'K"}$ arbitrary units	$\log_{10}(I/S_{K'K"})$	K'(K'+1)
38	28.	39	7.2	0.86	1560
39	27.5	40	6.9	0.84	1640
40	30	41	7.3	0.86	1722
41	27	42	6.4	0.81	1806
42	25	43	5.8	0.77	1892
43	25	44	5.7	0.76	1980
44	23.5	45	5.2	0.72	2070
45	23.	47	5.0	0.70	2162
47	22.5	48	4.7	0.67	2352
48	21	49	4.3	0.64	2450
49	19	50	3.8	0.58	2550
51	16	52	3.1	0.49	2756
52	15	53	2.9	0.46	2862
53	15	54	2.8	0.44	2970
54	14.	55	2.6	0.41	3080
56	12.5	57	2.2	0.35	3306
57	11.5	58	2.0	0.30	3422
58	10	59	1.7	0.23	3540
59	11	60	1.8	0.26	3660
60	9	61	1.5	0.17	3782
61	9	62	1.4	0.16	3906

TABLE A.3. (Fig.17). P branch, $T_{R'} = 5000^{\circ}K$.

Experimental details: 2 Å/min. scan, 10 μ slits,

C/O = 0.90, Tip of reaction zone.

transition P(K")	I arbitrary units	$S_{K"K'}$	$I/S_{K"K'}$ arbitrary units	$\log_{10}(I/S_{K"K'})$	K'(K'+1)
26	5.1	26	19.4	1.29	650
27	5.1	27	18.9	1.28	702
28	5.5	28	19.6	1.29	756
29	5.4	29	18.8	1.27	812
30	5.3	30	17.5	1.24	870
31	5.7	31	18.4	1.26	930
32	5.6	32	17.4	1.24	992
40	5.1	40	12.8	1.11	1560
41	5.2	41	12.6	1.10	1640
42	4.9	42	11.6	1.06	1722
43	5.1	43	11.7	1.07	1806
44	4.8	44	10.8	1.03	1892
45	4.7	45	10.6	1.02	1980
46	4.6	46	9.9	1.00	2070

TABLE A.4. (Fig.17) R branch, $T_{R'} = 5150^{\circ}K$.

Experimental details: 5 Å/min. scan, otherwise as Table A.3.

transition R(K")	I arbitrary units	$S_{K'K"}$	$I/S_{K'K"}$	$\log_{10}(I/S_{K'K"})$	K'(K'+1)
38	42	39	10.8	1.04	1560
39	43	40	10.7	1.03	1640
41	44	42	10.5	1.02	1806
42	41	43	9.6	0.98	1892
43	40.5	44	9.2	0.97	1980
44	39	45	8.7	0.94	2070
45	40	46	8.7	0.94	2162
47	38.5	48	8.0	0.91	2352
48	37.5	49	7.7	0.89	2450
49	35	50	7.0	0.85	2550
51	31	52	6.0	0.78	2756
52	28	53	5.3	0.73	2862
53	30	54	5.6	0.75	2970
54	28	55	5.1	0.71	3080
56	27	57	4.8	0.68	3306
57	26	58	4.5	0.66	3422
58	24	59	4.1	0.61	3540
59	27	60	4.5	0.66	3660
60	23	61	3.8	0.58	3782
61	22.5	62	3.6	0.56	3906
64	19.5	65	3.0	0.48	4290
65	19.5	66	3.0	0.47	4420
66	20	67	3.0	0.47	4556
67	18	68	2.7	0.43	4692

TABLE A.5. (Fig.18). P branch, $T_{R''} = 4800^{\circ}K$.

Experimental details: 5 Å/min. scan, 10 μ slits,

C/O = 0.94, Tip of reaction zone.

transition P(K")	$\alpha \equiv [(I_o - I)/I_o]$ x10^2	$S_{K"K'}$	$\frac{\alpha}{S_{K"K'}}$ x10^3	$\log_{10}(\alpha/S_{K"K'})$	K"(K"+1)
25	5.7	25	2.28	$\bar{3}.36$	650
26	5.6	26	2.14	$\bar{3}.33$	702
27	5.2	27	1.93	$\bar{3}.28$	756
28	5.9	28	2.10	$\bar{3}.32$	812
29	5.9	29	2.03	$\bar{3}.31$	870
30	6.0	30	2.00	$\bar{3}.30$	930
31	5.9	31	1.90	$\bar{3}.28$	992
32	5.9	32	1.85	$\bar{3}.27$	1056
40	5.5	40	1.38	$\bar{3}.14$	1640
41	5.5	41	1.34	$\bar{3}.13$	1722
42	5.5	42	1.30	$\bar{3}.11$	1806
43	5.4	43	1.27	$\bar{3}.10$	1892
44	5.1	44	1.15	$\bar{3}.06$	1980
45	5.0	45	1.12	$\bar{3}.05$	2070

TABLE A.6. (Fig.19) P branch, $T_{R''} = 3550^{\circ}K$.

Experimental details: 2 Å/min. scan, 10 μ slits, C/O = 1.18, 2 mm. above tip of reaction zone.

transition P(K")	$\alpha \equiv [(I_o-I)/I_o]_p$ x10^2	$S_{K"K'}$	$\frac{\alpha}{S_{K"K'}}$ x10^3	$\log_{10}(\alpha/S_{K"K'})$	K"(K"+1)
25	11.5	25	4.60	$\bar{3}$.66	650
26	11.5	26	4.40	$\bar{3}$.64	702
27	11.4	27	4.25	$\bar{3}$.63	756
28	11.8	28	4.20	$\bar{3}$.62	812
29	11.1	29	3.81	$\bar{3}$.58	870
30	10.9	30	3.62	$\bar{3}$.56	930
31	12.0	31	3.87	$\bar{3}$.59	992
32	11.2	32	3.50	$\bar{3}$.54	1056
40	9.3	40	2.33	$\bar{3}$.37	1640
41	9.0	41	2.20	$\bar{3}$.34	1722
42	8.8	42	2.08	$\bar{3}$.32	1806
43	9.0	43	2.09	$\bar{3}$.32	1892
44	8.6	44	1.95	$\bar{3}$.29	1980
45	8.4	45	1.87	$\bar{3}$.27	2070
46	8.0	46	1.74	$\bar{3}$.24	2162

TABLE A.7. (Fig. 21)

Vibrational temperature $T_{v''}$ = 3400°K($A_{v'v''}$), 3300°K($A'_{v'v''}$)

Experimental details: 5Å/min scan, 30μ slits, C/O = 1.18

2mm. above tip of reaction zone

Transition (v', v")	1-0	2-1	3-2	4-3
$[(I_o - I/I_o)]_{head} \equiv \alpha$	9.25×10^{-2}	7.2×10^{-2}	4.0×10^{-2}	3.2×10^{-2}
$A_{v'v''}$	0.240	0.372	0.425	0.451
$A'_{v'v''}$	0.358	0.525	0.718	0.952
$\alpha/A_{v'v''}$	38.6×10^{-2}	19.3×10^{-2}	9.4×10^{-2}	7.2×10^{-2}
$\alpha/A'_{v'v''}$	25.8×10^{-2}	13.7×10^{-2}	5.6×10^{-2}	3.4×10^{-2}
$\log_{10}(\alpha/A_{v'v''})$	$\bar{1}.59$	$\bar{1}.29$	$\bar{2}.97$	$\bar{2}.86$
$\log_{10}(\alpha/A'_{v'v''})$	$\bar{1}.41$	$\bar{1}.14$	$\bar{2}.75$	$\bar{2}.53$
$E_{v''}$ (cm^{-1})	818	2436	4030	5600

TABLE A.8. (Fig. 22)

Vibrational temperature $T_{v'}$ = 3800°K($A_{v'v''}$), 3600°K($A'_{v'v''}$)

Experimental details: 10Å/min scan, 50μ slits, C/O = 1.18

2mm. above tip of reaction zone

Transition (v', v")	1-0	2-1	3-2	4-3
I_{head} arb. units	56	45	28	25
$A_{v'v''}$	0.240	0.372	0.425	0.451
$A'_{v'v''}$	0.358	0.525	0.718	0.952
$I_h/A_{v'v''}$	23.3	12.1	6.6	5.5
$I_h/A'_{v'v''}$	15.6	8.6	3.9	2.6
$\log_{10}(I_h/A_{v'v''})$	1.37	1.08	0.82	0.74
$\log_{10}(I_h/A'_{v'v''})$	1.19	0.93	0.59	0.41
$E_{v'}$ (cm^{-1})	2645	4348	6057	7715

TABLE A.9. (Fig. 23)

Vibrational temperature $T_{v'}$ = 7800°K($A_{v'v''}$), 6500°K($A'_{v'v''}$)

Experimental details: 10Å/min scan, 50μ slits, C/O = 0.90

2mm. below tip of reaction zone

Transition (v', v")	1-0	2-1	3-2	4-3
I_{head} arb. units	58	59	53	50
$A_{v'v''}$	0.240	0.372	0.425	0.451
$A'_{v'v''}$	0.358	0.525	0.718	0.952
$I_h/A_{v'v''}$	24.2	15.9	12.5	11.1
$I_h/A'_{v'v''}$	16.2	11.2	7.4	5.3
$\log_{10}(I_h/A_{v'v''})$	1.39	1.20	1.10	1.05
$\log_{10}(I_h/A'_{v'v''})$	1.21	1.05	0.87	0.72
$E_{v'}$ (cm^{-1})	2645	4348	6057	7715

STUDY OF THE ABSORPTION SPECTRA OF FREE RADICALS IN FLAMES

P. F. JESSEN AND A. G. GAYDON

Department of Chemical Engineering and Chemical Technology, Imperial College, London, S.W.7

A modified multiple reflection system in which the image of the source is focused into the flame instead of on to the mirror surfaces has been developed. It reduces troubles due to defocusing of the light beam by refractive index gradients in the flame and gives better spatial resolution. The Swan bands of C_2 and the 4050 Å C_3 band have been observed in the 'feather' of a rich oxy-acetylene flame, and all three systems of CH, as well as C_2 in the reaction zone.

Introduction

THE characteristic band spectra of the free radicals CH, OH and C_2 are prominent features in the emission spectrum of all hydrocarbon flames. Investigations of the occurrence of these spectra in flames under different conditions have led to a better understanding of the types of combustion occurring and the existence or otherwise of temperature equilibrium, but by themselves provide only limited information about the chemical kinetics of combustion. In emission, the intensity of a band system is determined by the temperature and conditions of chemiluminescent excitation as much as by the concentration of the radical itself, and is furthermore a summation over different stages of the reaction.

Absorption spectroscopy has the great advantage that it gives information about the concentrations of species in the lower electronic state. However, its obvious theoretical advantages are subject to severe experimental limitations which have greatly hampered the exploitation of this technique for the study of premixed flames. OH is the only radical which lends itself readily to investigation by absorption techniques because of its relatively high equilibrium concentration in flames and concentration profiles and studies of decay mechanisms have been made[1–3].

Many transient intermediate chemical species are found only in or near the primary reaction zone which is only a fraction of a millimetre thick in hot flames, and is often curved. Even if a flat reaction zone is achieved, by suitable burner design, it is still necessary to restrict the light to a narrow beam of very small angular aperture, and this pencil of light tends to be thrown out of the flame by refraction effects in the high temperature gradients existing in the reaction zone. Long pathlengths are necessary to obtain appreciable absorption because the concentrations of the absorbing species are generally very low. For photographic detection it is necessary to have a background source with a higher brightness temperature than the excitation temperature in the flame; this can be appreciably higher than the equilibrium flame temperature[4].

The difficulties have been discussed by Gaydon, Spokes and van Suchtelen[5]. They studied low pressure oxy-acetylene flames and were, for the first time in flames, able to detect weak absorption in the (0,0) band of C_2 at 5165 Å, and the 3143 Å band of CH. They employed a system of mirrors, first described by White[6], in which the light was reflected back and forth several times through the flame to increase the effective pathlength.

Although very compact and moderately easy to adjust, this multiple reflection system of White gives a wide light beam, and the consequent poor spatial resolution greatly limits its usefulness. Only thick reaction zones, such as those of low pressure flames or near-limit flames, can be studied, and even here the detailed flame

structure cannot be resolved. The reason is that the light beam is focused on the surface of one of the mirrors and a fairly wide beam actually passes through the flame. This nearly parallel beam is also very subject to schlieren-type deflections in the temperature gradients of the flame and these cause deterioration of the image formation, limiting the number of traversals which can be obtained.

We have employed a multiple reflection system which focuses the light into the flame and consequently has much better spatial resolution and is less affected by refractive index gradients than the White system.

Experimental

Apart from the burner and multiple reflection system, our apparatus is similar to that employed by Gaydon *et al.*[5]. The background source is a flashtube and the absorption spectra are recorded photographically with a 2 m grating spectrograph giving a reciprocal dispersion of 5 Å/mm. A synchronized rotating sector device ensures that the slit of the spectrograph is exposed only at the moment the flashtube is triggered. Figure 1 shows a diagram of the optical arrangement.

The multiple reflection system

The multiple reflection system consists essentially of two spherical concave mirrors of equal focal length, separated by a distance equal to twice their radius of curvature (see Figure 2). The centres of curvature of each mirror coincide at the point O. A narrow beam of light is brought to a focus at a point P which is laterally displaced from O by a small distance dependent on the number of traversals required. The beam is refocused after reflection from mirror B, at a point Q on the other side of the centre of curvature an equal distance away. Further images are formed at P and Q by successive reflections from mirrors A and B respectively; this results in the light beam moving round the arc of the circle defined by the mirrors. For a given angular aperture of the beam, the number of reflections possible is determined by the distance OP and the diameter of the mirrors. The minimum length of OP, corresponding to the maximum number of reflections, is set by the angular aperture of the beam. Obviously it is possible to increase the number of reflections by increasing the size of the mirrors, but it should be noted that the image formation deteriorates with increasing number of reflections. Since we are working slightly off the axis of the mirrors and rays strike them obliquely, the system is subject to all the aberrations associated with spherical mirrors. Thus, after several reflections, the images will become blurred and enlarged, and the points P and Q increasingly less clearly defined. We therefore have to make a com-

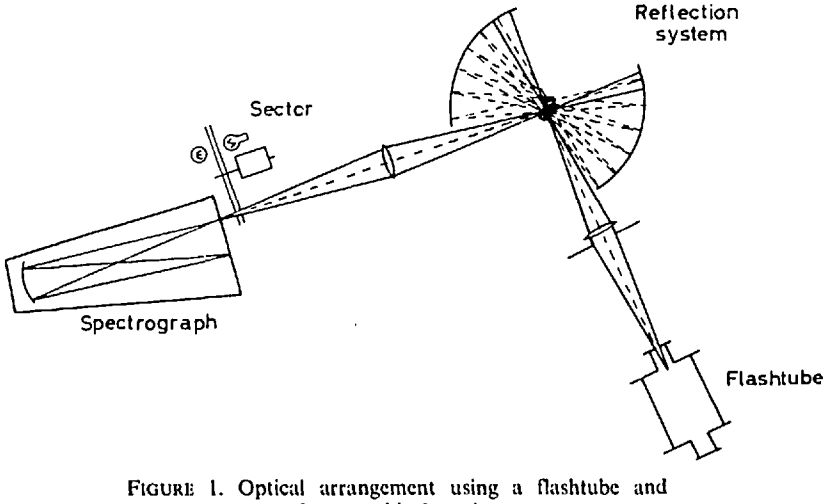

FIGURE 1. Optical arrangement using a flashtube and photographic detection

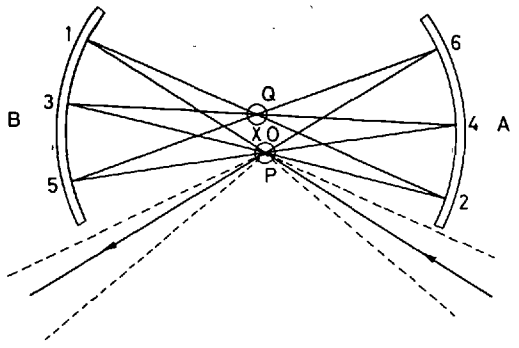

FIGURE 2. Multiple reflection system—seven traversals

promise between the number of traversals and the spatial resolution required when studying a particular flame.

Using four mirrors, each of 6 cm diameter and 10 cm radius of curvature, we found that up to twelve reflections were possible without adversely affecting the spatial resolution. With mirrors of longer focal length and by employing a light beam of still narrower aperture it should be possible to increase this number further.

The burner

To take full advantage of the increased absorbing pathlength offered by the system, two flames must be used, or alternatively a single burner can be employed having a diameter greater than the distance PQ, e.g. a flat flame burner.

We were particularly interested in investigating the luminous mantle or 'feather' surrounding the inner cone of a fuel-rich oxy-acetylene flame burning at atmospheric pressure, because appreciable concentrations of free radicals are known to exist there over a volume much larger than the reaction zone itself[7].

Several types of burner were tried. The most effective consisted of a pair of slot-type burners (3 mm × 3/4 mm) placed at the image points P and Q. The slot burners were built on to a modified commercial welding torch to prevent danger from flashback. The mirror system inverts the images of one flame on to the other. This prevents simultaneous study of an extended zone of the flame, but does not interfere with the step-by-step investigation of the absorption spectrum when a point source, such as a flashtube, is used as background.

The intensity of the background source is reduced after each traversal due to reflection losses. The resulting fall in brightness temperature can be calculated using Planck's law[5]; it is rather less serious at short wavelengths if a uniform reflection coefficient is assumed, but in practice the reflection coefficient of the mirrors decreases rapidly in the ultra-violet and the overall effect is a reduction of intensity at shorter wavelengths. Reasonable exposures could be obtained after twelve reflections with between twenty five and one hundred and fifty flashes depending on the type of plate and wavelength region examined.

Results

C_2

Weak C_2 absorption in the (0,0) band head at 5165 Å was detected with nine traversals, through the tip of the reaction zone of a fuel-rich flame. With thirteen traversals, the absorption was strong enough to show up most of the band heads and the rotational structure of the stronger bands. Figure 3 shows a microphotometer trace of the absorption spectrum in the 5165 Å region; an emission spectrum is also presented for comparison.

The C_2 absorption was strongest in the reaction zone, with mixture ratios of about three times stoichiometric, i.e. C_2H_2: O_2 = 6:5. It extended a few millimetres above the reaction zone into the luminous mantle although the intensity was reduced.

CH

CH absorption was observed in the reaction zone of slightly leaner flames with thirteen traversals. The three main band systems at 4315 Å, 3900 Å and 3143 Å were all detected although the absorption was very weak in the 4315 Å and 3900 Å systems. A microphotometer trace of the 4315 Å band is shown in Figure 4.

No absorption was detected in the luminous mantle above the inner cone.

C_3

We also detected weak absorption at 4050 Å just above the tip of the reaction zone, in flames

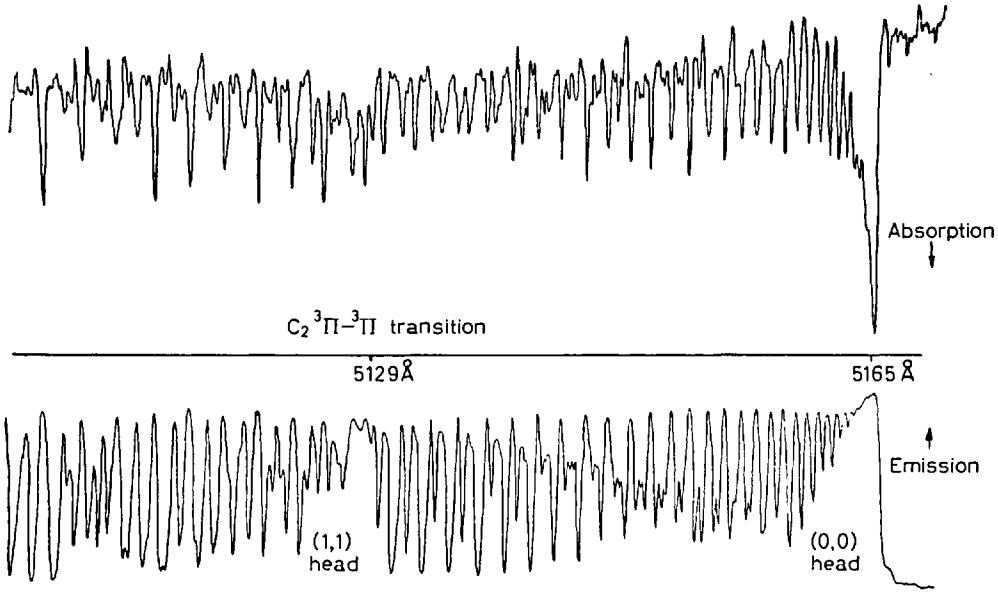

FIGURE 3. C_2 absorption spectrum

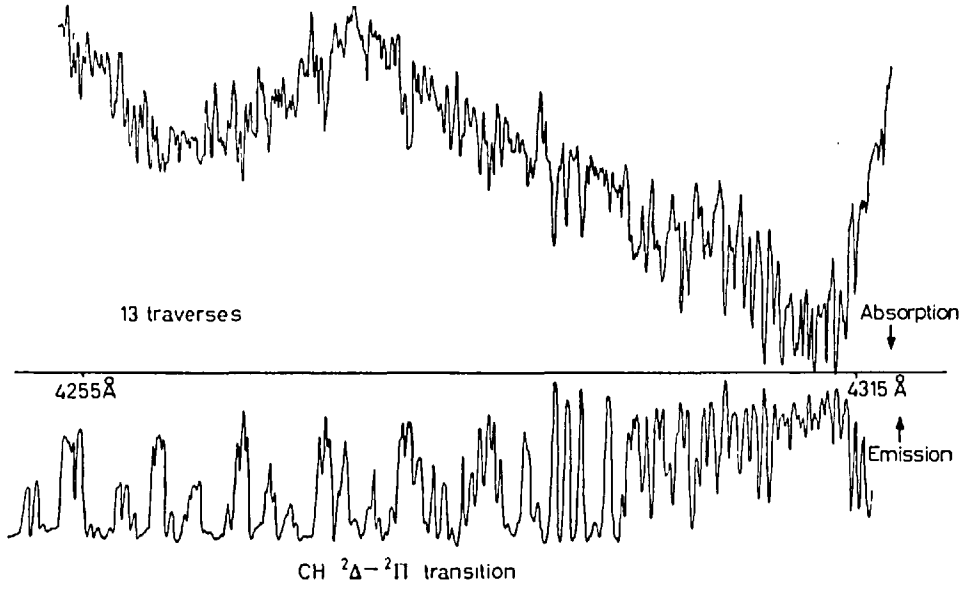

FIGURE 4. CH absorption spectrum

burning with mixture strengths between three and four times stoichiometric. The absorption is due to the C_3 radical which has a diffuse band system in this wavelength region and can also be observed in emission. Figure 5 shows a weak but reproducible peak at 4051·5 Å on top of the background noise.

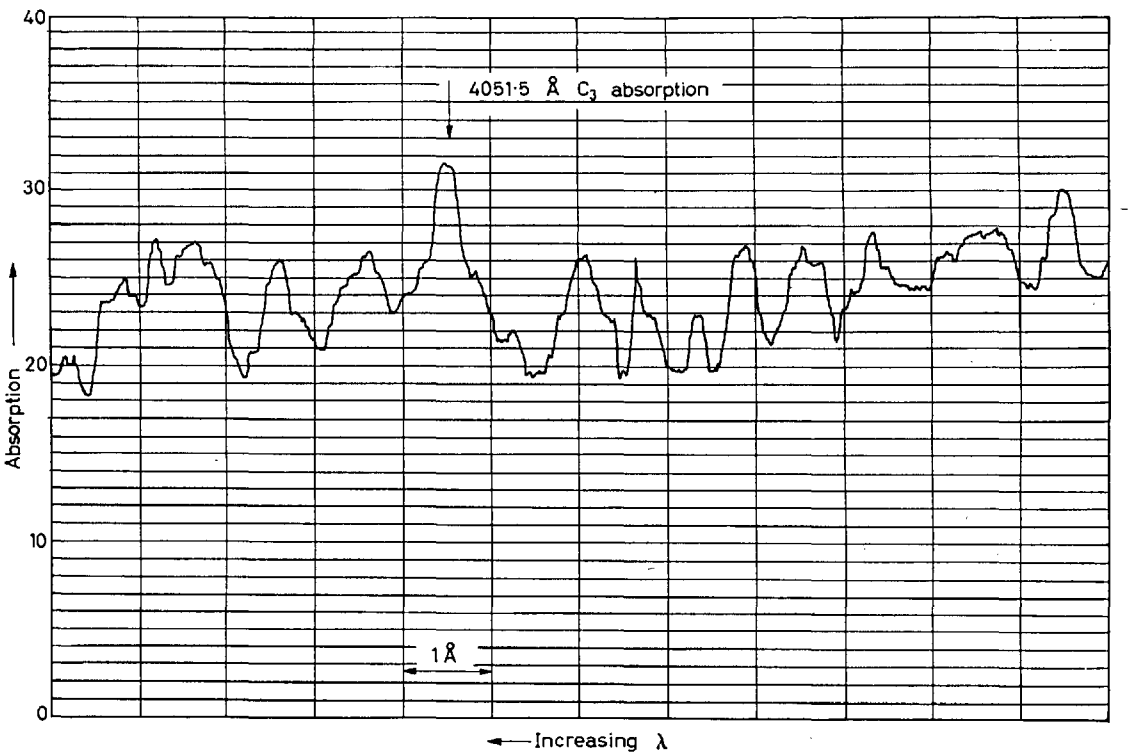

FIGURE 5. C_3 absorption

Discussion

Although several attempts have been made by a number of workers in the past, we are aware of only two previous reports of C_2 and CH absorption in flames. Gaydon *et al.*[5] studied an oxy-acetylene flame at low pressure using an effective pathlength of over 140 cm. They were able to detect C_2 and CH absorption in the reaction zone only at the (0,0) band head at 5165 Å and the piled up Q branch at 3143 Å respectively.

Bleekrode and Nieuwpoort[8] also studied the reaction zone of a low pressure oxy-acetylene flame using the White multiple reflection system. They employed photoelectric recording of the spectrum using phase-sensitive detection to discriminate between the background continuum and flame emission, and thus were able to use a background source of lower brightness temperature, namely a high pressure mercury lamp. The improved sensitivity gained in this way enabled them to detect the rotational structure in the Swan bands of C_2 and weak absorption in the 4315 Å and 3900 Å bands of CH. They also estimated the concentrations of the C_2 and CH radicals in the reaction zone to be 10^{13} cm^{-3} and 10^{12} cm^{-3} respectively.

There do not appear to be any previous reports of C_3 absorption in flames but it has been observed in absorption in the flash photolysis of oxy-acetylene mixtures[9], as also have C_2 and CH.

The presence of appreciable concentrations

of C_2 and C_3 radicals in the luminous mantle above the tip of the reaction zone of fuel-rich flames is of interest in connection with the mechanisms of carbon formation in flames. The mantle first becomes noticeable at mixture strengths greater than about twice stoichiometric, becoming whiter and extending farther up the flame as the fuel supply is increased, until it finally merges with the characteristic yellow carbon luminosity at mixture strengths greater than about four times stoichiometric.

Emission studies[7] have revealed that the region contains appreciable concentrations of free radicals but departures from equilibrium are not as great as in the reaction zone.

Free carbon atoms and the radicals C_2 and C_3 have been postulated to act as nuclei for the formation of soot particles in hot flames[10]. We are hoping to make some measurements of the concentrations of these radicals as a function of mixture strength and distance above the reaction zone. As yet we have only been able to detect the presence of carbon atoms by the emission line at 2478 Å. Improvements to the apparatus are being made which should increase the sensitivity of detection and facilitate quantitative measurements.

One of us (P.F.J.) is indebted to the Gas Council for financial support.

(Received April 1966; amended May 1966)

References

[1] OLDENBERG, O. and RIEKE, R. F. *J. chem. Phys.* **6**, 439 (1938)
[2] DWYER, R. J. and OLDENBERG, O. *J. chem. Phys.* **12**, 351 (1944)
[3] KASKAN, W. E. *Combustion & Flame*, **2**, 229 (1958)
[4] GAYDON, A. G. *The Spectroscopy of Flames*. Chapman and Hall: London (1957)
[5] GAYDON, A. G., SPOKES, G. N. and VAN SUCHTELEN, J. *Proc. Roy. Soc. A*, **256**, 323 (1960)
[6] WHITE, J. U. *J. opt. Soc. Amer.* **32**, 285 (1942)
[7] MARR, G. U. *Canad. J. Phys.* **35**, 1265 (1957)
[8] BLEEKRODE, R. and NIEUWPOORT, W. C. *J. chem. Phys.* **43**, 3680 (1965)
[9] NORRISH, R. G. W. *Disc. Faraday Soc.* **14**, 16 (1953)
[10] GAYDON, A. G. and WOLFHARD, H. G. *Flames*. Chapman and Hall: London (1960)

Reprinted from COMBUSTION AND FLAME
Quarterly Journal of the Combustion Institute
VOLUME 11 NO. 1 FEBRUARY 1967

Published by BUTTERWORTHS PUBLICATIONS LTD
88 KINGSWAY LONDON, W.C.2

Subscription: UNITED KINGDOM FIVE GUINEAS PER ANNUM
U.S.A. $16.00 „ „

Printed in Great Britain by Page Bros. (Nch.) Ltd., Mile Cross Lane, Norwich